NEGATIVE REGULATION OF PLANT STRESS SIGNALING BY THE EDR1 PROTEIN KINASE

Matthew Paul Neubauer

Submitted to the faculty of the University Graduate School
in partial fulfillment of the requirements
for the degree
Doctor of Philosophy
in the Department of Biology
Indiana University
March 2020

Accepted by the Graduate Faculty, Indiana University, in partial fulfillment of the requirements for the degree of Doctor of Philosophy

Doctoral Committee

_____

Roger W. Innes, Ph.D.

_____

Scott Michaels, Ph.D.

_____

Sidney Shaw, Ph.D.

_____

Nicholas Sokol, Ph.D.

February 21, 2020

Acknowledgements

I would like to thank my advisor, Roger Innes, for his support and guidance throughout my Ph.D. career. From the moment I arrived at IU, Roger has been welcoming and supportive of my research endeavors. Additionally, Roger has been a great resource of knowledge and experience. I would also like to acknowledge the help of my committee members throughout my Ph.D. studies. Scott Michaels, Sidney Shaw, and Nick Sokol provided helpful advice and guidance that influenced my experiments and helped me mature as a scientist.

I thank all members of the Innes lab, past and present, for their support and friendship over the years. I thank Irene Serrano for her mentorship as well as shaping my understanding of plant stress signaling. During my time at IU, I was fortunate to belong to a constructive and friendly community of scientists. I am especially thankful for the community of plant scientists at IU that has provided me with support, guidance, and endless materials.

While completing this work, I was supported by several fellowships including the Carlos O. Miller Fellowship, the Floyd Plant and Fungal Biology Summer Fellowship, and a training grant from the National Institute of General Medical Sciences. I thank all those involved in providing me the financial means to complete my studies.

I would also like to thank my friends and family. During my Ph.D. studies I have encountered many successes and difficulties, and my friends and family have supported me throughout. My parents, Tim and Mary, as well as my sister Katie have been critical in enabling me to pursue my Ph.D. I thank them for their love and support throughout

my life and my Ph.D. studies. I also thank my friends, old and new, who have been there for me through this time.

Matthew Paul Neubauer

NEGATIVE REGULATION OF PLANT STRESS SIGNALING BY THE EDR1 PROTEIN KINASE

In nature, plants endure a variety of stresses, ranging from pathogen infection to adverse environmental conditions. Although plants have evolved effective mechanisms for overcoming biotic and abiotic stress, these responses often come at the cost of growth and development. To maximize fitness, plants must carefully regulate stress signaling pathways so that they are active only when needed. The EDR1 protein kinase has been implicated as an important negative regulator of plant stress signaling. Loss-of-function *edr1* mutants display enhanced sensitivity to numerous biotic and abiotic stresses. Due to the variety of phenotypes displayed by *edr1* plants, EDR1 is believed to negatively regulate various plant stress signaling pathways. However, little is known about how EDR1 functions at the molecular level. My work has aimed to address some of these outstanding questions regarding EDR1 function. I have found that EDR1 directly interacts with and regulates the EDS1/PAD4 complex, which plays an important role in the regulation of plant stress responses and salicylic acid signaling. I have also shown that EDR1 physically interacts with the previously uncharacterized plant N-terminal acetyltransferase NAA50. I subsequently showed that NAA50 is essential for plant development as well as the repression of plant stress signaling. Importantly, loss of NAA50 results in a constitutive endoplasmic reticulum stress, which results in altered development and induced stress response signaling. Through the investigation of EDR1 function, I have uncovered a role for EDR1 in the negative regulation of EDS1/PAD4

signaling, as well as a link between EDR1, N-terminal acetylation, and the regulation of plant stress responses and development.

_____

Roger W. Innes, Ph.D.

_____

Scott Michaels, Ph.D.

_____

Sidney Shaw, Ph.D.

_____

Nicholas Sokol, Ph.D.

Table of Contents

List of Figures

List of Tables

Chapter 1: Literature Review

This dissertation describes experiments aimed at elucidating the functions of the Arabidopsis EDR1 protein, a negative regulator of plant stress response signaling. Chapter 2 details experiments demonstrating a role for EDR1 in the regulation of the EDS1 and PAD4 proteins, which have previously been shown to be central regulators of biotic stress responses. Chapter 3 describes experiments that uncovered an interaction between EDR1 and the N-terminal acetyltransferase NAA50. Additionally, the experiments in Chapter 3 demonstrate a role for NAA50 in regulating plant stress signaling and development. In this literature review, I will provide an overview of the molecular mechanisms that regulate plant stress signaling, as well as their complexity and crosstalk. Furthermore, the role of EDS1 and PAD4 in the regulation of plant stress signaling will be addressed. This chapter will also cover the current understanding of EDR1 and the mechanisms through which it regulates defense signaling. Finally, N-terminal acetylation and its various functions will be covered.

Plant Stress Responses are Mediated by Hormone Signaling

Plants face a variety of challenges from the environment as well as other organisms. As sessile organisms, plants must be able to adapt to and confront these challenges. The variety of stresses that plants endure necessitate an equally complex and varied set of stress responses and signaling pathways. These pathways are essential for plant survival, and a greater understanding of how they function is critical for the development of improved crops and agricultural methods (Csukasi et al., 2009). Here, I

describe some of the hormone signaling pathways utilized by plants to regulate growth and defense, and the ways these pathways interact.

Plant stress responses rely heavily upon hormone signaling pathways regulated by small molecules such as abscisic acid (ABA), ethylene (ET), jasmonic acid (JA), and salicylic acid (SA) (Figure 1-1). Hormones play unique roles in responding to different stresses. SA is associated with responses to biotrophic pathogens, whereas JA and ET promote responses to necrotrophic pathogens, insects, and wounding (Pieterse et al., 2009; Glazebrook, 2005; Zhang and Li, 2019; Howe, 2004; Wasternack, 2007). ABA is primarily associated with abiotic stress responses and promotes tolerance to osmotic and cold stress (Finkelstein et al., 2002; Yamaguchi-Shinozaki and Shinozaki 2006; Nakashima et al., 2009).

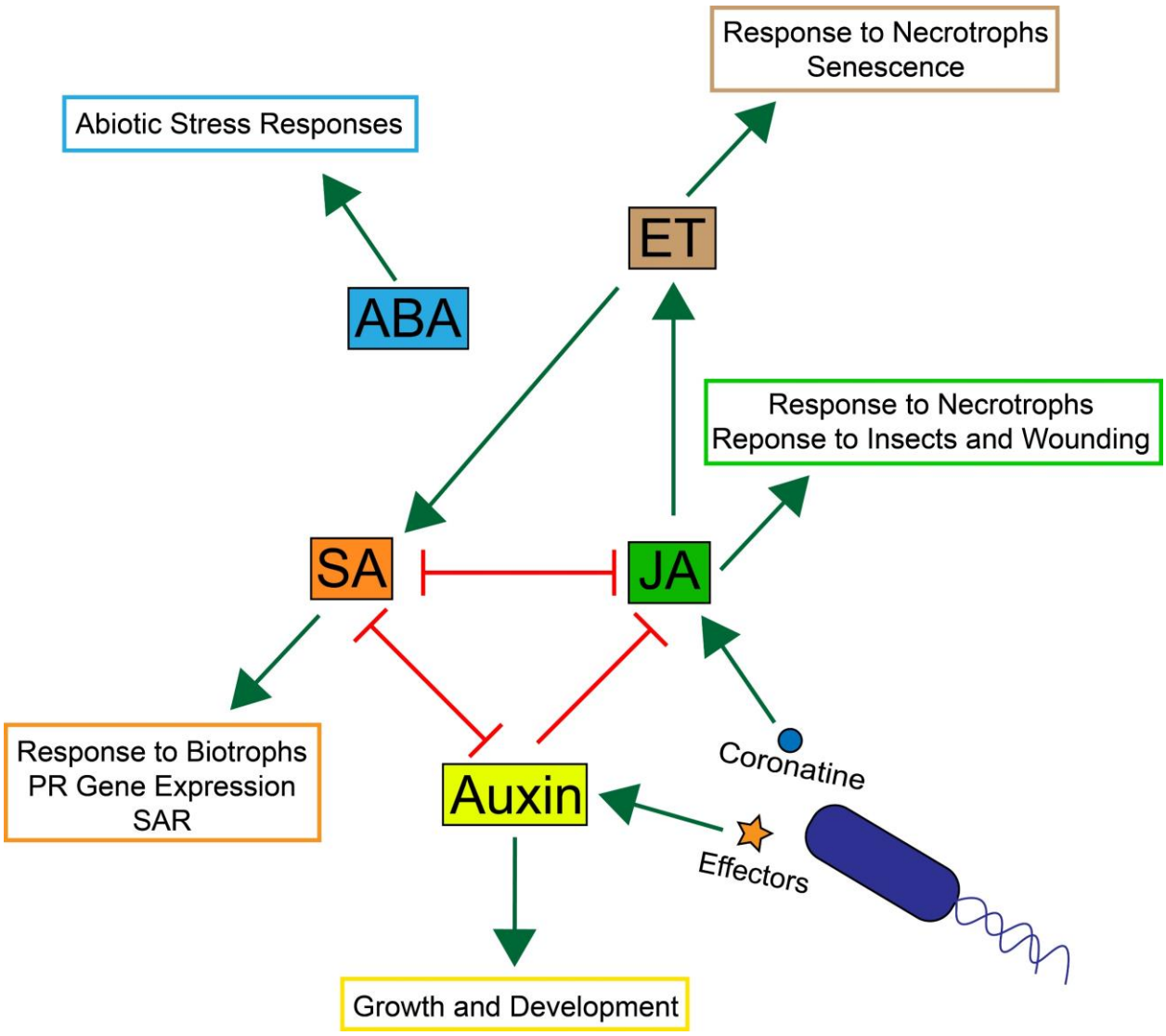

Figure 1-1. Plant hormones regulate stress signaling. The plant hormones ABA, SA, ET, and JA promote plant stress signaling. ABA is primarily involved in responses to abiotic stress, such as drought and cold stress. JA and ET are associated with responses to necrotrophic pathogens and insects. SA mediates plant responses against biotrophic pathogens, stimulates the expression of PR genes, and is required for SAR. ET and JA signaling pathways generally promote one another, whereas the relationship between JA and SA is largely antagonistic. The growth-promoting hormone auxin interferes with plant defense signaling pathways, particularly those mediated by SA and JA. Pathogens such as *P. syringae* exploit hormone crosstalk by promoting JA and auxin signaling through the secretion of coronatine and effector proteins, thereby repressing SA signaling.

Plant hormone signaling pathways produce various changes to plant physiology that enable plant stress tolerance (Verma et al., 2016; Pieterse et al., 2012). SA, alongside other signaling molecules such as N-Hydroxypipecolic acid, promotes a phenomenon known as systemic acquired resistance (SAR) through which distal plant tissues become stress tolerant following pathogen detection (Fu and Dong, 2013; Huang et al., 2019). Additionally, SA accumulation promotes expression of Pathogenesis Related (PR) genes, which encode proteins with antimicrobial activity (van Loon et al., 2006). JA promotes resistance to herbivorous insects by eliciting defense gene expression, altering development, and triggering the production of protease inhibitors and secondary metabolites that inhibit insect feeding (Howe and Jander, 2008). During drought stress conditions, ABA promotes stomatal closure (Zhang et al., 1987), as well as gene expression changes that promote drought tolerance (Zhu, 2002; Fujita et al., 2005; Finkelstein et al., 2002). The molecular and genetic pathways activated by plant hormones are essential for plant stress tolerance.

A significant degree of crosstalk exists between plant hormone signaling pathways. There is a well-established antagonistic relationship between SA and JA. Work in tomato demonstrated that SA can repress JA-mediated wound responses (Doherty et al., 1988). During infection by the hemibiotroph *P. syringae*, SA-mediated defenses are upregulated and JA signaling is repressed, ultimately enhancing host susceptibility to necrotrophs (Spoel et al., 2007). JA signaling is known to antagonize SA-based defense responses (Pieterse et al., 2009; Zheng et al., 2012; Van der Does et al., 2013). This antagonistic relationship is taken advantage of by pathogens through the use of coronatine, a small molecule that mimics JA. Coronatine secretion from pathogens inhibits host SA signaling,

thereby enhancing host susceptibility (Brooks et al., 2005; Zheng et al., 2012). On the other hand, JA and ET generally promote each other. JA and ET act synergistically in promoting expression of numerous stress response genes (Penninckx et al., 1998; Lorenzo et al., 2003; Pré et al., 2008). ET can also act to promote SA signaling. ET was found to be essential for the onset of SAR in tobacco (Verberne et al., 2003). Many SA-regulated transcripts also require an intact ET signaling pathway to be properly activated during a defense response (Glazebrook et al., 2003). The ability for stress hormone pathways to regulate one another is believed to enable plants to tailor their responses according to the specific stresses they encounter (Pieterse et al., 2009).

Stress signaling in plants must be carefully regulated to maintain proper development. There is a well-established growth-defense tradeoff in plants (Huot et al., 2014). Plant stress responses require a significant amount of energy, often coming at the cost of plant development (Walters and Heil, 2007). That many plant biotic stress responses result in cell death (Greenberg and Yao, 2004), illustrates the significant impact defense signaling can have on development. Crosstalk between plant hormone pathways encourages a commitment to either defense or development signaling. Growth-promoting hormones such as auxin negatively impact defense signaling. Auxin has been shown to have a largely negative impact on the expression of genes involved in JA signaling (Liu and Wang, 2006). Auxin similarly has a negative impact on SA-based defenses. Auxin signaling represses plant resistance to *P. syringae*, which is largely SA-based (Navarro et al., 2006; Chen et al., 2007). Many plant pathogens take advantage of this relationship by producing auxin and secreting effector proteins that alter plant auxin signaling (Spaepen et al., 2007; Chen et al., 2007). Conversely, SA promotes plant

defenses through the repression of auxin signaling (Wang et al., 2007). The mutually negative crosstalk that exists between growth- and defense-promoting hormone pathways ensures that finite resources are conserved for those processes which are most relevant to the plant at any given time (Huot et al., 2014).

EDS1 and PAD4 are Important Regulators of Plant Stress Signaling

ENHANCED DISEASE SUSCEPTIBILITY1 (*EDS1*) and *PHYTOALEXIN DEFICIENT4* (*PAD4*) play important roles in the regulation of plant stress signaling. *PAD4* was first identified in an Arabidopsis forward genetic screen for plants displaying enhanced susceptibility to *Pseudomonas syringae* pv. *maculicola* (Glazebrook et al., 1996). *EDS1* was identified in a screen for mutants with defective *RPP1*- and *RPP5*-mediated resistance to *Peronospora parasitica* (Parker et al., 1996). Loss of *EDS1* was also found to abolish *RPS4*-mediated resistance to *Pseudomonas syringae* carrying the avirulence gene *avrRps4* (Aarts et al., 1998). Thus, *EDS1* is required for defense mediated by *RPP1, RPP5*, and *RPS4*, all of which belong to the TIR-NB-LRR (TNL) class of plant disease resistance (*R*) genes (Botella et al., 1998; Parker et al., 1997; Gassmann et al., 1999). TNL complexes play an important role in effector-triggered immunity (ETI), which relies upon a host being able to detect the presence of pathogen effectors and induce transcriptional reprogramming (Cui et al., 2015; Tsuda and Somssich, 2015). *EDS1* is essential for TNL-based ETI, making it an important regulator of plant defense signaling (Wiermer et al., 2005).

A major function of *EDS1* and *PAD4* is the promotion of SA signaling during both basal and TNL-mediated resistance. Loss of function *eds1* and *pad4* mutants are

hypersusceptible to pathogens and display lower SA accumulation during infection (Zhou et al., 1998; Feys et al., 2001). Thus, *EDS1* and *PAD4* are generally viewed as promoters of SA signaling (Wiermer et al., 2005). In fact, overexpression of *EDS1* and *PAD4* increases basal levels of SA and boosts SA signaling during a defense response (Cui et al., 2017). Not only do *EDS1* and *PAD4* promote SA accumulation during a defense response, but they function in a positive feedback loop with SA (Vlot et al., 2009). Expression of *EDS1* and *PAD4* is enhanced by SA accumulation (Jirage et al., 1999; Feys et al., 2001). Given that *EDS1* and *PAD4* function within a positive feedback loop with SA, the negative regulation of *EDS1* and *PAD4* is likely an important point of control in plant defense signaling.

EDS1 and PAD4 physically interact and function as signaling partners. Both *EDS1* and *PAD4* are required for the induction of SA during a defense response (Jirage et al., 1999; Feys et al., 2001). Enhanced *PAD4* expression during a defense response is *EDS1*-dependent, while *EDS1* expression is partially *PAD4*-dependent (Feys et al., 2001). Although overexpression of both *EDS1* and *PAD4* together promotes SA accumulation and resistance, overexpression of either alone does not (Cui et al., 2017). This demonstrates that *EDS1* and *PAD4* function together to promote defense signaling. The physical association between EDS1 and PAD4 is essential for proper downstream signaling. EDS1 and PAD4 both contain an N-terminal lipase-like domain, as well as a C-terminal ‘EP’ domain, consisting of an alpha-helical bundle (Feys et al., 2005; Wagner et al., 2013). EDS1/PAD4 complexes are formed through an interaction between the N-terminal lipase-like domains. Mutations that inhibit the interaction between EDS1 and PAD4 reduce EDS1/PAD4 signaling (Wagner et al., 2013). This may be explained by the

instability of PAD4 when it is not complexed with EDS1, as disrupting the association of PAD4 with EDS1 significantly reduces PAD4 accumulation (Rietz et al., 2011).

Recent evidence suggests that EDS1- and PAD4-mediated regulation of defense signaling may occur through transcriptional regulation. Both EDS1 and PAD4 display nucleo-cytoplasmic localization (Feys et al., 2005). EDS1 nuclear localization is required for transcriptional reprogramming during ETI (García et al., 2010). EDS1 and PAD4 have been shown to physically associate with a number of nuclear TNLs (Bhattacharjee et al., 2011; Heidrich et al., 2011; Kim et al., 2012; Huh et al., 2017). These observations indicate that EDS1 and PAD4 may play a role in the regulation of defense signaling through direct interactions with nuclear proteins.

Recent work has shown that EDS1 and PAD4 negatively regulate the JA regulator, MYC2. The MYC2 transcription factor plays a major role in the transcriptional regulation of JA- and coronatine-induced defenses (Kazan and Manners, 2013). EDS1 and PAD4 have been found to inhibit coronatine-induced inhibition of SA signaling through the regulation of MYC2 (Cui et al., 2018). Interestingly, formation of the EDS1/PAD4 complex was found to be essential for this process. The negative regulation of MYC2 by EDS1/PAD4 heteromers demonstrates that in addition to promoting SA signaling, EDS1 and PAD4 may regulate crosstalk between hormone signaling pathways.

EDS1 and PAD4 play important roles in plant biotic stress responses. The physical interaction between both proteins is important for their accumulation, as well as their ability to regulate various aspects of stress signaling. Thus, inhibition of EDS1/PAD4 complex formation is one potential way for plants to fine-tune stress signaling. However,

very little is known about how EDS1 and PAD4 are regulated, and whether EDS1/PAD4 complex formation can be inhibited.

EDR1 is a Negative Regulator of Defense Signaling

The tradeoff between growth and defense encourages plants to carefully regulate their defense responses in order to protect growth and fitness. Negative regulation of defense signaling enables plants to conserve energy by shutting down unnecessary defense processes. One such negative regulator is ENHANCED DISEASE RESISTANCE1 (EDR1).

EDR1 was identified in a mutant screen for plants displaying enhanced resistance to *Pseudomonas syringae* (Frye and Innes, 1998). Loss-of-function *edr1* mutants were also found to have enhanced resistance to *Golovinomyces cichoracearum*, the causal agent of powdery mildew. This resistance phenotype was associated with increased necrosis at sites of fungal penetration (Frye and Innes, 1998). However, unlike other enhanced resistance mutants such as *cpr1* or *mpk4*, *edr1* mutants do not display severe dwarfism (Bowling et al., 1994; Petersen et al., 2000). Furthermore, *edr1* plants do not display constitutively active defense signaling or senescence. Expression of defense markers such as *PR-1* or *BGL2* is not significantly higher in uninfected *edr1* plants (Frye and Innes, 1998). This indicates that EDR1 acts to repress defense signaling after a stress event has occurred, rather than before.

Loss of *EDR1* results in enhanced defense signaling during stress responses (Christiansen et al., 2011; Frye and Innes, 1998). Transcriptome analysis of *edr1* mutants during powdery mildew infection revealed a significant increase in a variety of stress

signaling genes (Christiansen et al., 2011). *edr1* mutants display earlier induction of genes associated with the endomembrane trafficking system, reactive oxygen species (ROS) signaling, and protein kinase signaling relative to wildtype. *edr1*-induced resistance and cell death appear to result from an increase in defense gene expression during infection.

In addition to displaying enhanced resistance to biotrophic pathogens, *edr1* plants display a range of other stress signaling phenotypes. Loss of *EDR1* results in enhanced ethylene sensitivity and enhanced growth inhibition and senescence during drought (Frye et al., 2001; Tang et al., 2005). Loss of *EDR1* also results in hypersensitivity to ABA treatment (Wawrzynska et al., 2008). The variety of *edr1* phenotypes demonstrates that EDR1 regulates numerous signaling pathways.

Genetic evidence indicates that EDR1-mediated regulation of defense signaling occurs primarily through the SA and ET signaling pathways (Figure 1-2). *edr1*-mediated enhanced resistance to powdery mildew is suppressed by loss-of-function mutations that affect SA signaling, such as *npr1-1* (Cao et al., 1997)*, sid2-1* (Wildermuth et al., 2001), *pad4-1* (Zhou 1998), and *eds1-1* (Falk et al., 1999; Frye et al., 2001). However, the *ein2* (Alonso et al., 1999) and *coi1* (Xie et al., 1998) mutations, which affect ET and JA signaling respectively, do not suppress *edr1*-mediated resistance to powdery mildew (Frye et al., 2001). Mutations in SA regulators also suppress drought-induced lesions and growth inhibition in *edr1* plants (Tang et al., 2005). This indicates that some *edr1* phenotypes result from an increase in SA signaling. Loss of the ET regulator ORE9 was found to suppress the ET sensitivity and drought-induced growth inhibition of *edr1* mutants (Tang et al., 2005). Interestingly, mutations affecting SA signaling have no effect

on *edr1* ethylene hypersensitivity. This demonstrates that EDR1 regulates two distinct SA- and ET-based signaling pathways (Tang et al., 2005).

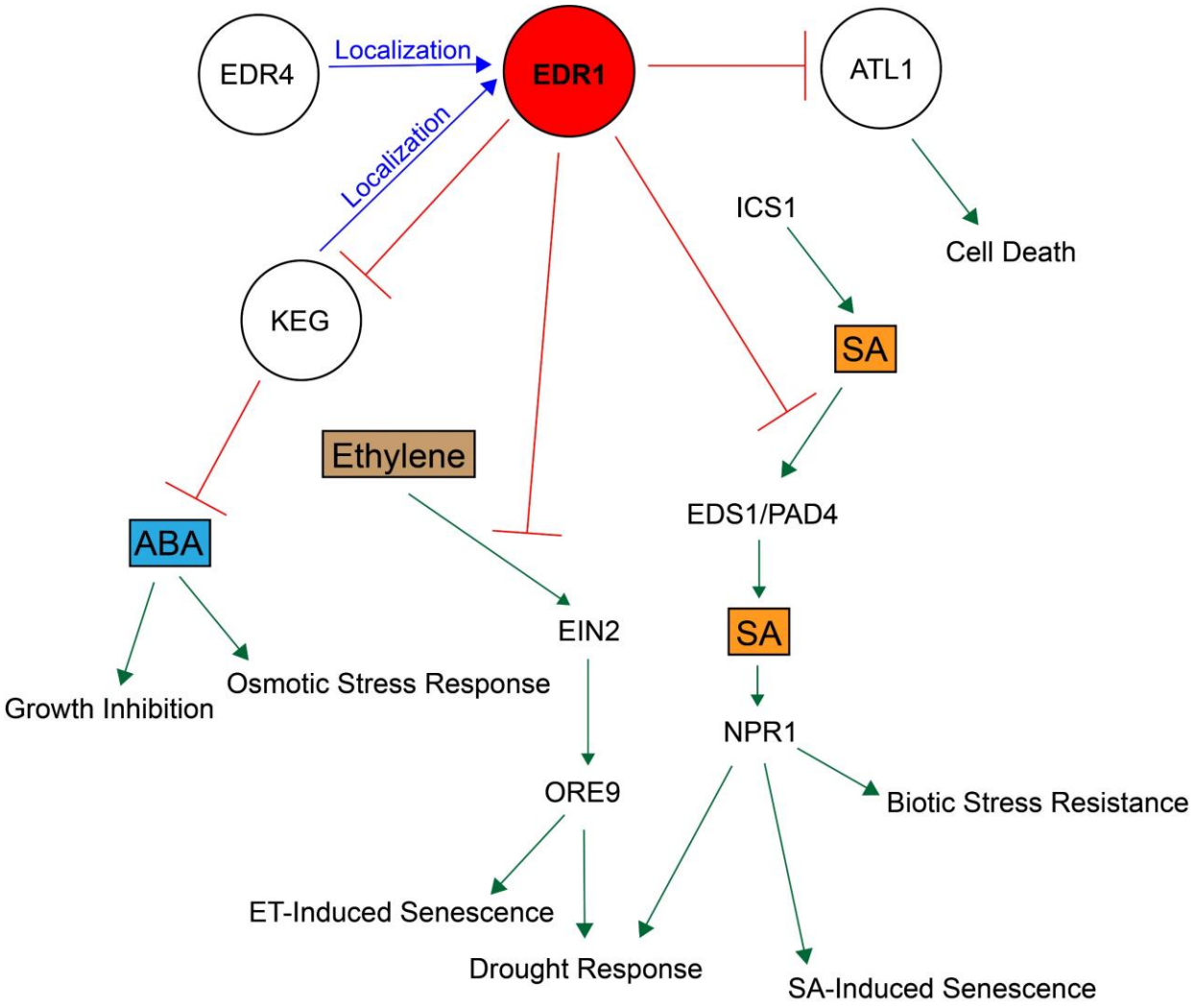

Figure 1-2. EDR1 negatively regulates plant stress signaling. EDR1 is a negative regulator of ET and SA signaling. Mutations in SA regulators *EDS1*, *PAD4*, *NPR1,* and *ICS1* suppress *edr1*-mediated resistance, cell death, and drought hypersensitivity. Mutations in the ET regulators *EIN2* and *ORE9* suppress *edr1*-mediated ET-induced senescence. Loss of *EIN2* but not *ORE9* suppresses *edr1*-mediated drought-induced growth inhibition. A mutation in KEG, a negative regulator of ABA, suppresses all *edr1* phenotypes. *EDR4* appears to belong to the same genetic pathway as *EDR1* and *KEG*. EDR1 localization is altered by mutations in KEG and EDR4. EDR1 is a negative regulator of ATL1, which positively regulates cell death.

Although loss-of-function mutations in defense regulators can suppress some *edr1* phenotypes, only the *keg-4* mutation has been demonstrated to suppress all *edr1* phenotypes. In a mutant screen for suppressors of *edr1*-mediated ABA sensitivity and disease resistance, a missense mutation in *KEEP ON GOING* (*KEG*) was identified. This mutation, denoted as *keg-4,* suppresses the enhanced resistance and ABA hypersensitivity of *edr1* mutants. Furthermore, *keg-4* also suppresses drought-induced growth inhibition and ethylene sensitivity in *edr1* mutants (Wawrzynska et al., 2008). This suggests that KEG may operate in the same signaling pathway as EDR1.

KEG has been implicated in the regulation of ABA signaling and plant development. KEG was originally identified in a screen for Arabidopsis mutants displaying enhanced ABA sensitivity (Stone et al., 2006). In addition to causing enhanced sensitivity to ABA treatment, loss of *KEG* inhibits plant development. *keg* seedling development is severely impaired, demonstrating a role for *KEG* in post-germinative seedling development (Stone et al., 2006). KEG, which contains an active E3 ubiquitin ligase domain, has been demonstrated to play a direct role in the regulation of ABA signaling by targeting ABA-responsive transcription factors for degradation (Stone et al., 2006). KEG ubiquitination activity results in the degradation of ABI5, ABF1, ABF3, and CIPK26, all known activators of ABA signaling (Liu and Stone, 2010; Liu and Stone, 2013; Chen et al., 2013; Lyzenga et al., 2013).

In addition to its role in regulating plant development and ABA signaling, KEG has been implicated in the regulation of endomembrane trafficking and vacuole development. KEG localizes to early endosomes (Gu and Innes, 2011). Loss of *KEG* results in fragmented vacuoles and impairs the secretion of apoplastic defense proteins and the

transport of plasma membrane-localized proteins to the vacuole (Gu and Innes, 2012). This suggests that a major function of KEG may be the regulation of protein trafficking.

In addition to regulating KEG, EDR1 has also been implicated in the negative regulation of another E3 ubiquitin ligase, ARABIDOPSIS TOXICOS EN LEVADURA1 (ATL1). Like KEG, ATL1 localizes to endomembrane structures and physically associates with EDR1. ATL1 positively regulates cell death and senescence. Overexpression of *ATL1* induces cell death in Arabidopsis and *N. benthamiana*. In transgenic Arabidopsis, overexpression of *ATL1* results in spontaneous cell death and dwarfism. Interestingly, EDR1 expression can inhibit *ATL1*-induced senescence in *N. benthamiana*, demonstrating a role for *EDR1* in repressing cell death. Knockdown of *ATL1* reduces *edr1*-induced powdery mildew resistance and cell death, suggesting that ATL1 overactivity contributes to the *edr1* resistance phenotype (Serrano et al., 2014).

Enhanced Disease Resistance 4 (*EDR4*) was identified in the same genetic screen that identified *EDR1*. As with *edr1* plants*, edr4* plants display enhanced resistance to powdery mildew and enhanced expression of defense genes during infection. As with *EDR1*, loss of *EDR4* does not result in constitutive defense gene induction or dwarfism. EDR4 is made up of a coiled-coil domain, four low-complexity regions, and a duf3133 domain, but has no known enzymatic domains. EDR4 primarily localizes to the plasma membrane and endosomal compartments. Evidence suggests that EDR4 may regulate endomembrane trafficking. EDR4 physically associates with CLATHRIN HEAVY CHAIN2, and *edr4* mutants display reduced rates of endocytosis. *EDR1* and *EDR4* appear to belong to the same genetic pathway, as loss of *EDR4* does not enhance *edr1* phenotypes. Intriguingly, the *keg-4* mutation also suppresses *edr4*-mediated enhanced

resistance, indicating that KEG, EDR1, and EDR4 operate in the same pathway (Wu et al., 2015).

A major role of the EDR1-interacting proteins KEG and EDR4 may be the regulation of EDR1 localization. Transient expression experiments have demonstrated that EDR1 localizes primarily to the endoplasmic reticulum (ER) and the nucleus (Christiansen et al., 2011). However, evidence suggests that EDR1 localization may be more complex. Co-expression with KEG results in EDR1 localizing to early endosomes. The *keg-4* mutation prevents KEG-mediated re-localization of EDR1 (Gu and Innes, 2011). Like KEG, EDR4 may regulate EDR1 localization. Both EDR4 and EDR1 localize to fungal penetration sites. The localization of EDR1 to these sites is EDR4-dependent (Wu et al., 2015). This suggests that a major function of EDR1 may be the regulation of defense signaling at penetration sites, and that EDR4 and KEG may be responsible for this re-localization.

EDR1-mediated negative regulation of defense signaling may occur through phosphorylation. *EDR1* encodes a predicted protein composed of 933 amino acids, of which the C-terminal 276 encode a kinase domain (Tang and Innes, 2002). The EDR1 kinase domain bears similarity to the CTR1 protein kinase, a well-known regulator of ethylene signaling, as well as Raf-like mitogen-activated protein kinase kinase kinases (MAPKKKs) (Frye et al., 2001; Kieber et al., 1993; Ichimura et al., 2002). EDR1 displays both intra- and inter-molecular phosphorylation activity *in vitro* (Tang and Innes, 2002). EDR1-mediated regulation of defense signaling may be kinase-dependent. Transgenic plants expressing a kinase inactive EDR1 display a dominant-negative phenotype, having *edr1*-like powdery mildew resistance and ethylene sensitivity (Tang and Innes, 2002). The

negative regulation of ATL1 by EDR1 appears to be through phosphorylation. Mimicking phosphorylation of S312 of ATL1 inhibits its ubiquitination activity and prevents ATL1-induced cell death in *N. benthamiana* (Serrano et al., 2014). Blocking phosphorylation of $ATL1^{S312}$ inhibits EDR1-mediated suppression of ATL1-induced cell death (Serrano et al., 2014). This indicates that EDR1 may negatively regulate ATL1 by phosphorylation of $ATL1^{S312}$. However, direct phosphorylation of ATL1 by EDR1 has not been shown.

Despite the evidence that EDR1 may act as a MAPKKK, a true *in vivo* phosphorylation target for EDR1 has not been reliably shown. Although the EDR1 kinase domain resembles that of a MAPKKK, the N-terminal non-kinase portion of EDR1 does not bear resemblance to other known proteins. In fact, EDR1 may repress phosphorylation of the MAP kinases (MAPKs) MPK3 and MPK6. Loss of *edr1* enhances MPK3 and MPK6 phosphorylation. It has been suggested that EDR1 may negatively regulate MAPK signaling by interfering with the interaction between MAP kinase kinases and MAPKs (Zhao et al., 2014).

Despite many years of work, we lack a clear understanding of how EDR1 functions. The *edr1* mutation results in a wide range of phenotypes, suggesting that EDR1 regulates various aspects of plant stress signaling. The identification of additional EDR1 regulatory targets may shed light on the mechanisms by which EDR1 exerts control over plant defense signaling. This dissertation describes experiments designed to address the outstanding questions regarding EDR1 function. A suppressor mutant screen uncovered a role for EDR1 in the regulation of EDS1 and PAD4. Additionally, a yeast two-hybrid screen identified an EDR1-interacting protein that is required for the regulation of plant stress signaling and development.

N-terminal Acetylation May Impact Plant Stress Signaling

Chapter 3 describes the characterization of NAA50, an N-terminal acetyltransferase that interacts with EDR1. Here, I review the current knowledge surrounding N-terminal acetylation and its role in regulating protein function in animals, yeast, and plants.

Recent evidence indicates that N-terminal acetylation (NTA), a co-translational protein modification, plays an important role in the regulation of plant stress signaling and development. It has long been appreciated that post-translational modification (PTM) of proteins plays an important role in the regulation of plant stress signaling (Hunter, 2007). Although less studied than PTM, co-translational modification of proteins also plays an important role in the regulation of protein function.

NTA is a widespread protein modification. The majority of eukaryotic proteins, including roughly 80% of human proteins, are N-terminally acetylated (Brown and Roberts, 1976; Driesen et al., 1985; Polevoda and Sherman, 2003; Arnesen et al., 2009). NTA was first detected over 60 years ago (Narita, 1958), and was initially thought to primarily protect proteins from degradation (Jornvall, 1975). However, recent work has implicated NTA in a variety of regulatory functions (Ree et al., 2018).

NTA is mediated by multiple N-terminal acetyltransferase (NAT) complexes. There are six NAT complexes in humans, designated NatA-F (Polevoda et al., 2009; Aksnes et al., 2016). These complexes contain unique catalytic components, and in some situations, auxiliary subunits (Polevoda et al., 2009; Aksnes et al., 2016). For instance, the NatA complex includes the Naa10, Naa15, Naa50, and HYPK subunits, with Naa10 acting as the catalytic component (Mullen et al., 1989; Park and Szostak, 1992; Gautschi et al.,

2003; Arnesen et al., 2006; Arnesen et al., 2010). Although it associates with the NatA complex, Naa50 serves as the catalytic component of the NatE complex (Arnesen et al., 2006). The auxiliary subunit Naa15 likely plays a role in substrate binding and the tethering of Naa10 and Naa50 to the ribosome (Gautschi et al., 2003). These complexes are highly conserved throughout eukaryotes, including Drosophila, yeast, and humans (Arnesen et al., 2009; Goetze et al., 2009; Polevoda, 1999; Polevoda and Sherman, 2003). The high level of conservation of NAT complexes suggests that NTA is an essential process in eukaryotes.

NAT complexes display specificity toward their target substrates. In particular, the two most N-terminal residues determine which NAT complexes modify a given peptide (Polevoda et al., 2009). The NatA complex targets peptides that have lost their N-terminal methionine residue following cleavage by methionine aminopeptidases (Arnesen et al., 2009; Polevoda and Sherman, 2003). The other Nat complexes target peptides that have retained their N-terminal methionine (Polevoda et al., 2009; Arnesen, 2011). The NatB complex acetylates N-termini composed of acidic or hydrophilic residues at the second position (Starheim et al., 2008; Van Damme et al., 2012). The NatC, NatE, and NatF complexes target proteins with hydrophobic and amphipathic N-termini (Starheim et al., 2009; Van Damme et al., 2016; Evjenth et al., 2009; Van Damme et al., 2015; Van Damme et al., 2011; Aksnes et al., 2015a).

There is evidence that NAT complexes are involved in the regulation of protein folding. Loss of NatA in yeast results in the accumulation of misfolded proteins, an increase in chaperone accumulation, and a stress response (Holmes et al., 2014). The NatA-associated Huntingtin Yeast Two-Hybrid Protein K (HYPK) has also been implicated

in the regulation of protein folding (Raychaudhuri et al., 2008; Arnesen et al., 2010). HYPK has chaperone-like activity, and its expression can impede the formation of Huntingtin (Htt) aggregates (Raychaudhuri et al., 2008). Knockdown of HYPK as well as Naa10 or Naa15 leads to increased aggregation of Htt (Arnesen et al., 2010). NatB-mediated NTA plays a role in preventing α-synuclein aggregation, a process associated with Parkinson's disease. NTA of α-synuclein stabilizes the N-terminal α-helix, which inhibits protein aggregation (Bartels et al., 2011; Bartels et al., 2014).

That loss of NAT complex components can result in protein misfolding indicates that NTA plays a role in the regulation of protein folding. If NTA is indeed required for proper protein folding, loss of NAT complex components may trigger ER stress. ER stress can result from the accumulation of misfolded proteins in the secretory pathway and is often triggered when increased demands are placed on the translational machinery, such as during development or stress responses (Bao and Howell, 2017; Vitale and Boston, 2008). Cells attempt to alleviate ER stress through the Unfolded Protein Response (UPR), which is characterized by an increase in the expression of chaperones, the removal of misfolded proteins from the ER, and a reduction in translation (Williams et al., 2014; Liu and Howell, 2010). If prolonged ER stress is not properly managed, the UPR transitions into a pro-apoptotic phase (Woehlbier and Hetz, 2011; Walter and Ron, 2011).

The Human Naa60 protein has been shown to play a unique role in the regulation of transmembrane proteins (Aksnes et al., 2015a). Naa60 localizes to the Golgi and is specifically involved in the NTA of the cytosolic N-termini of transmembrane proteins. The loss of Naa60 induces fragmentation of the Golgi, indicating that Naa60-mediated NTA may regulate Golgi topology (Aksnes et al., 2015a).

NTA, particularly that mediated by NatC, has also been shown to affect protein localization. Arl3p is a Golgi-localized GTPase required for the recruitment of other GTPases to the Golgi (Setty et al., 2003; Panic et al., 2003). In yeast, NatC N-terminally acetylates Arl3p, resulting in its localization to the Golgi via an interaction with the Golgi membrane protein Sys1p (Behnia et al., 2004; Setty et al., 2004). In the absence of NatC, Arl3p is not properly recruited to the Golgi and is unable to recruit Arl1p (Behnia et al., 2004; Setty et al., 2004). Another yeast protein, Trm1-II, requires NatC for proper localization. Loss of NatC, but not NatA or NatB, results in the mislocalization of Trm1-II to the nucleoplasm rather than the inner nuclear membrane (Murthi and Hopper, 2005). Although NatC-mediated NTA is important for the localization of Arl3p and Trm1-II, it does not always have this effect. Loss of NatC was found to have no effect on the localization of 13 yeast NatC substrates (Aksnes et al., 2013). This demonstrates that NTA, even that mediated by the same complex, affects proteins uniquely.

NTA can also target proteins for degradation through the Ac/N-end rule pathway (Lee et al., 2016). NTA was first shown to act as a degradation signal in yeast, where the E3 ubiquitin ligase Doa10 was found to target N-terminally acetylated proteins for degradation (Hwang et al., 2010). NTA also acts as a degradation signal on the yeast Cog1 protein. NTA of Cog1 is recognized by the E3 ubiquitin ligase Not4, which subsequently targets Cog1 for degradation. Although NTA of Cog1 acts as a degradation signal, N-terminally acetylated Cog1 can be protected from degradation by association with other COG complex components. In this way, the Ac/N-end rule may act to ensure that COG subunits accumulate at the proper stoichiometry (Shemorry et al., 2013). The Ac/N-end rule has been demonstrated to function in mammals as well. NTA of the human

Rgs2 protein is recognized by the Teb4 E3 ligase, the mammalian orthologue of Doa10 (Park et al., 2015). Rgs2 is an important regulator of blood pressure (Heximer et al., 2003) and mutations that alter N-terminal Rgs2 residues decrease protein accumulation and are associated with hypertension (Bodenstein et al., 2007; Yang et al., 2005). Interestingly, such Rgs2 mutants were found to be targets of Teb4, however, the short-lived ML-RGS2 variant is also targeted by the Arg/N-end rule pathway (Park et al., 2015). Taken together, the regulation of Rgs2 by the Ac/N-end rule pathway implicates NTA as an important regulator of human hypertension (Aksnes et al., 2015b). Contrary to the view that NTA stabilizes proteins, this work highlights that NTA can act as a degradation signal.

Recent evidence suggests that NTA may play a vital role in regulating plant development and stress responses. Studies of the Arabidopsis NatA and NatB complexes have demonstrated that NTA is required for plant development and the regulation of stress signaling. Arabidopsis *NAA10* and *NAA15* are essential for embryonic development (Feng et al., 2016). Additionally, knockdown of either *NAA10* or *NAA15* results in morphological defects and drought resistance (Linster et al., 2015). Interestingly, NAA10 and NAA15 accumulation was found to be negatively impacted by ABA treatment (Linster et al., 2015).

Arabidopsis NatA and NatB have been implicated in the regulation of the SNC1 receptor. Differential NTA mediated by either complex regulates SNC1 stability, thereby influencing plant defense signaling (Xu et al., 2015). In Arabidopsis, loss of NAA30, the catalytic component of NatC, results in dwarfism and reduced photosystem II efficiency (Pesaresi et al., 2003). Thus, NTA appears to play a vital role in plant development, as well as biotic and abiotic stress signaling. However, the characterization of plant NAT

complexes is incomplete, and it is unknown whether other NAT complexes serve important functions in plants.

Summary and Significance of Research

Although much is known about the signaling pathways involved in plant stress signaling, we still lack a clear understanding of how various aspects of defense signaling are regulated. EDS1 and PAD4 play a critical role in the promotion of SA signaling during biotic stress, yet little is known about how EDS1 and PAD4 are regulated. Recent evidence indicates that NTA may play an important role in regulating plant stress signaling, however, some plant NAT complexes have yet to be characterized. Although *EDR1* has been well-established as a negative regulator of defense signaling, there is a lack of evidence for the direct involvement of EDR1 in regulating defense signaling. My work has aimed to address the questions surrounding the involvement of EDR1 in plant stress signaling, uncovering a role for EDR1 in the direct regulation of EDS1 and PAD4 as well as the previously uncharacterized N-terminal acetyltransferase NAA50.

In Chapter 2, I describe a genetic screen for second site mutations that either enhanced or suppressed *edr1* mutant phenotypes. This screen led to the discovery of a mutation in *PAD4* that enhances some, but not all, *edr1* phenotypes. The identification of this mutation, which results in a change of amino acid Ser135 to Phe135 (*pad4*^{S135F}) (*pad4-13*), prompted us to investigate the role of EDR1 in the regulation of EDS1 and PAD4. The *pad4-13* mutation was found to enhance plant resistance and cell death during powdery mildew infection. Investigation of PAD4^{S135F} showed that the S135F amino acid substitution does not significantly impact PAD4 accumulation, localization, or interaction

with EDS1, suggesting that it may enhance PAD4 activity through a yet-unknown mechanism. *pad4-13* was found to enhance cell death in *edr1* plants during powdery mildew infection, but did not enhance *edr1*-mediated resistance to powdery mildew, indicating that *EDR1* and *PAD4* may regulate similar processes. EDR1 was found to physically interact with both EDS1 and PAD4, demonstrating that EDR1 may directly regulate these proteins. Interestingly, EDR1 was shown to inhibit the formation of the EDS1/PAD4 complex. Analysis of previously generated transcriptome data established that *EDR1* negatively regulates a significant proportion of EDS1/PAD4-promoted transcripts. This work establishes that EDR1 negatively regulates PAD4 and EDS1 directly by preventing their interaction.

In Chapter 3, I describe my work on a previously uncharacterized EDR1-interacting protein, the N-terminal acetyltransferase NAA50, that was first identified in a yeast two-hybrid screen. This work uncovered a potential link between EDR1, NTA, and the regulation of plant development and stress responses. Genetic analysis of mutants lacking *NAA50* demonstrated an essential role for NAA50 in plant growth and development. Loss of *NAA50* results in dwarfism and altered stem and root growth. Furthermore, loss of *NAA50* was found to trigger cell death and senescence, indicating that, like *EDR1*, *NAA50* may negatively regulate cell death signaling. Indeed, transcriptome analysis demonstrated that loss of *NAA50* triggers a significant reduction in growth signaling, and an increase in defense signaling. NAA50 enzymatic activity was found to be essential for root development and fertility. Interestingly, loss of *NAA50* results in a constitutive ER stress phenotype, suggesting that NAA50-mediated NTA may be required to prevent ER stress. This work establishes NAA50 as an important regulator of

plant development and stress responses. Furthermore, this work reveals a potential role for EDR1 in the regulation of NTA and the suppression of ER stress.

Literature Cited

Aarts, N., Metz, M., Holub, E., Staskawicz, B.J., Daniels, M.J. and Parker, J.E. (1998) Different requirements for EDS1 and NDR1 by disease resistance genes define at least two R gene-mediated signaling pathways in Arabidopsis. Proceedings of the National Academy of Sciences **95:** 10306-10311.

Aksnes, H., Osberg, C. and Arnesen, T. (2013) N-terminal acetylation by NatC is not a general determinant for substrate subcellular localization in *Saccharomyces cerevisiae*. PLOS ONE **8:** e61012.

Aksnes, H., Van Damme, P., Goris, M., Starheim, Kristian K., Marie, M., Støve, Svein I., Hoel, C., Kalvik, Thomas V., Hole, K., Glomnes, N., Furnes, C., Ljostveit, S., Ziegler, M., Niere, M., Gevaert, K. and Arnesen, T. (2015a) An organellar N-acetyltransferase, Naa60, acetylates cytosolic n termini of transmembrane proteins and maintains Golgi integrity. Cell Reports **10:** 1362-1374.

Aksnes, H., Drazic, A. and Arnesen, T. (2015b) (Hyper)tension release by N-terminal acetylation. Trends in Biochemical Sciences **40:** 422-424.

Aksnes, H., Drazic, A., Marie, M. and Arnesen, T. (2016) First things first: vital protein marks by N-terminal acetyltransferases. Trends in Biochemical Sciences **41:** 746-760.

Alonso, J.M., Hirayama, T., Roman, G., Nourizadeh, S. and Ecker, J.R. (1999) EIN2, a bifunctional transducer of ethylene and stress responses in Arabidopsis. Science **284:** 2148-2152.

Arnesen, T., Anderson, D., Torsvik, J., Halseth, H.B., Varhaug, J.E. and Lillehaug, J.R. (2006) Cloning and characterization of hNat5/hSan: an evolutionarily conserved component of the NatA protein N-α-acetyltransferase complex. Gene **371:** 291-295.

Arnesen, T., Van Damme, P., Polevoda, B., Helsens, K., Evjenth, R., Colaert, N., Varhaug, J.E., Vandekerckhove, J., Lillehaug, J.R., Sherman, F. and Gevaert, K. (2009) Proteomics analyses reveal the evolutionary conservation and divergence of N-terminal acetyltransferases from yeast and humans. Proceedings of the National Academy of Sciences **106:** 8157.

Arnesen, T., Starheim, K.K., Van Damme, P., Evjenth, R., Dinh, H., Betts, M.J., Ryningen, A., Vandekerckhove, J., Gevaert, K. and Anderson, D. (2010) The chaperone-like protein Hypk acts together with NatA in cotranslational N-terminal acetylation and prevention of Huntingtin aggregation. Molecular and Cellular Biology **30:** 1898-1909.

Arnesen, T. (2011) Towards a functional understanding of protein N-terminal acetylation. PLOS Biology **9:** e1001074.

Bao, Y. and Howell, S.H. (2017) The unfolded protein response supports plant development and defense as well as responses to abiotic stress. Frontiers in Plant Science **8**.

Bartels, T., Choi, J.G. and Selkoe, D.J. (2011) α-Synuclein occurs physiologically as a helically folded tetramer that resists aggregation. Nature **477:** 107-110.

Bartels, T., Kim, N.C., Luth, E.S. and Selkoe, D.J. (2014) N-alpha-acetylation of α-Synuclein increases its helical folding propensity, Gm1 binding specificity and resistance to aggregation. PLOS ONE **9:** e103727.

Behnia, R., Panic, B., Whyte, J.R.C. and Munro, S. (2004) Targeting of the Arf-like GTPase Arl3p to the Golgi requires N-terminal acetylation and the membrane protein Sys1p. Nature Cell Biology **6:** 405-413.

Bhattacharjee, S., Halane, M.K., Kim, S.H. and Gassmann, W. (2011) Pathogen effectors target Arabidopsis EDS1 and alter its interactions with immune regulators. Science **334:** 1405-1408.

Bodenstein, J., Sunahara, R.K. and Neubig, R.R. (2007) N-terminal residues control proteasomal degradation of Rgs2, Rgs4, and Rgs5 in human embryonic kidney 293 cells. Molecular Pharmacology **71:** 1040-1050.

Botella, M.A., Parker, J.E., Frost, L.N., Bittner-Eddy, P.D., Beynon, J.L., Daniels, M.J., Holub, E.B. and Jones, J.D.G. (1998) Three genes of the Arabidopsis Rpp1 complex resistance locus recognize distinct *Peronospora parasitica* avirulence determinants. The Plant Cell **10:** 1847-1860.

Bowling, S.A., Guo, A., Cao, H., Gordon, A.S., Klessig, D.F. and Dong, X. (1994) A mutation in Arabidopsis that leads to constitutive expression of systemic acquired resistance. The Plant Cell **6:** 1845-1857.

Brooks, D.M., Bender, C.L. and Kunkel, B.N. (2005) The *Pseudomonas syringae* phytotoxin coronatine promotes virulence by overcoming salicylic acid-dependent defences in *Arabidopsis thaliana*. Molecular Plant Pathology **6:** 629-639.

Brown, J.L. and Roberts, W.K. (1976) Evidence that approximately eighty per cent of the soluble proteins from Ehrlich ascites cells are Nalpha-acetylated. Journal of Biological Chemistry **251:** 1009-1014.

Cao, H., Glazebrook, J., Clarke, J.D., Volko, S. and Dong, X. (1997) The Arabidopsis NPR1 gene that controls systemic acquired resistance encodes a novel protein containing ankyrin repeats. Cell **88:** 57-63.

Chen, Z., Agnew, J.L., Cohen, J.D., He, P., Shan, L., Sheen, J. and Kunkel, B.N. (2007) *Pseudomonas syringae* type III effector AvrRpt2 alters *Arabidopsis thaliana* auxin physiology. Proceedings of the National Academy of Sciences **104:** 20131-20136.

Chen, Y.-T., Liu, H., Stone, S. and Callis, J. (2013) ABA and the ubiquitin E3 Ligase KEEP ON GOING affect proteolysis of the *Arabidopsis thaliana* transcription factors ABF1 and ABF3. The Plant Journal **75:** 965-976.

Christiansen, K.M., Gu, Y., Rodibaugh, N. and Innes, R.W. (2011) Negative regulation of defence signalling pathways by the EDR1 protein kinase. Molecular Plant Pathology **12:** 746-758.

Csukasi, F., Merchante, C. and Valpuesta, V. (2009) Modification of plant hormone levels and signaling as a tool in plant biotechnology. Biotechnology Journal **4:** 1293-1304.

Cui, H., Tsuda, K. and Parker, J.E. (2015) Effector-triggered immunity: from pathogen perception to robust defense. Annual Review of Plant Biology **66:** 487-511.

Cui, H., Gobbato, E., Kracher, B., Qiu, J., Bautor, J. and Parker, J.E. (2017) A core function of EDS1 with PAD4 is to protect the salicylic acid defense sector in Arabidopsis immunity. New Phytologist **213:** 1802-1817.

Cui, H., Qiu, J., Zhou, Y., Bhandari, D.D., Zhao, C., Bautor, J. and Parker, J.E. (2018) Antagonism of transcription factor MYC2 by EDS1/PAD4 complexes bolsters salicylic acid defense in Arabidopsis effector-triggered immunity. Molecular Plant **11:** 1053-1066.

Doherty, H.M., Selvendran, R.R. and Bowles, D.J. (1988) The wound response of tomato plants can be inhibited by aspirin and related hydroxy-benzoic acids. Physiological and Molecular Plant Pathology **33:** 377-384.

Driessen, H.P.C., De Jong, W.W., Tesser, G.I. and Bloemendal, H. (1985) The mechanism of N-terminal acetylation of protein. Critical Reviews in Biochemistry **18:** 281-325.

Evjenth, R., Hole, K., Karlsen, O.A., Ziegler, M., Arnesen, T. and Lillehaug, J.R. (2009) Human Naa50p (Nat5/San) displays both protein Nα- and Nε-acetyltransferase activity. Journal of Biological Chemistry **284:** 31122-31129.

Falk, A., Feys, B.J., Frost, L.N., Jones, J.D.G., Daniels, M.J. and Parker, J.E. (1999) EDS1, an essential component of R gene-mediated disease resistance in Arabidopsis has homology to eukaryotic lipases. Proceedings of the National Academy of Sciences **96:** 3292-3297.

Feng, J., Li, R., Yu, J., Ma, S., Wu, C., Li, Y., Cao, Y. and Ma, L. (2016) Protein N-terminal acetylation is required for embryogenesis in Arabidopsis. Journal of Experimental Botany **67:** 4779-4789.

Feys, B.J., Moisan, L.J., Newman, M.-A. and Parker, J.E. (2001) Direct interaction between the Arabidopsis disease resistance signaling proteins, EDS1 and PAD4. The EMBO Journal **20:** 5400-5411.

Feys, B.J., Wiermer, M., Bhat, R.A., Moisan, L.J., Medina-Escobar, N., Neu, C., Cabral, A. and Parker, J.E. (2005) Arabidopsis SENESCENCE-ASSOCIATED GENE101 stabilizes and signals within an ENHANCED DISEASE SUSCEPTIBILITY1 complex in plant innate immunity. The Plant Cell **17:** 2601-2613.

Finkelstein, R.R., Gampala, S.S.L. and Rock, C.D. (2002) Abscisic acid signaling in seeds and seedlings. The Plant Cell **14:** S15-S45.

Frye, C.A. and Innes, R.W. (1998) An Arabidopsis mutant with enhanced resistance to powdery mildew. The Plant Cell **10:** 947-956.

Frye, C.A., Tang, D. and Innes, R.W. (2001) Negative regulation of defense responses in plants by a conserved MAPKK kinase. Proceedings of the National Academy of Sciences **98:** 373-378.

Fu, Z.Q. and Dong, X. (2013) Systemic acquired resistance: turning local infection into global defense. Annual Review of Plant Biology **64:** 839-863.

Fujita, Y., Fujita, M., Satoh, R., Maruyama, K., Parvez, M.M., Seki, M., Hiratsu, K., Ohme-Takagi, M., Shinozaki, K. and Yamaguchi-Shinozaki, K. (2005) AREB1 is a transcription activator of novel ABRE-dependent ABA signaling that enhances drought stress tolerance in Arabidopsis. The Plant Cell **17:** 3470-3488.

García, A.V., Blanvillain-Baufumé, S., Huibers, R.P., Wiermer, M., Li, G., Gobbato, E., Rietz, S. and Parker, J.E. (2010) Balanced nuclear and cytoplasmic activities of EDS1 are required for a complete plant innate immune response. PLOS Pathogens **6:** e1000970.

Gassmann, W., Hinsch, M.E. and Staskawicz, B.J. (1999) The Arabidopsis RPS4 bacterial-resistance gene is a member of the TIR-NBS-LRR family of disease-resistance genes. The Plant Journal **20:** 265-277.

Gautschi, M., Just, S., Mun, A., Ross, S., Rücknagel, P., Dubaquié, Y., Ehrenhofer-Murray, A. and Rospert, S. (2003) The yeast Nα-acetyltransferase NatA is quantitatively anchored to the ribosome and interacts with nascent polypeptides. Molecular and Cellular Biology **23:** 7403-7414.

Glazebrook, J., Rogers, E.E. and Ausubel, F.M. (1996) Isolation of Arabidopsis mutants with enhanced disease susceptibility by direct screening. Genetics **143:** 973-982.

Glazebrook, J., Chen, W., Estes, B., Chang, H.-S., Nawrath, C., Métraux, J.-P., Zhu, T. and Katagiri, F. (2003) Topology of the network integrating salicylate and jasmonate signal transduction derived from global expression phenotyping. The Plant Journal **34:** 217-228.

Glazebrook, J. (2005) Contrasting mechanisms of defense against biotrophic and necrotrophic pathogens. Annual Review of Phytopathology **43:** 205-227.

Goetze, S., Qeli, E., Mosimann, C., Staes, A., Gerrits, B., Roschitzki, B., Mohanty, S., Niederer, E.M., Laczko, E., Timmerman, E., Lange, V., Hafen, E., Aebersold, R., Vandekerckhove, J., Basler, K., Ahrens, C.H., Gevaert, K. and Brunner, E. (2009) Identification and functional characterization of N-terminally acetylated proteins in *Drosophila melanogaster*. PLOS Biology **7:** e1000236.

Greenberg, J.T. and Yao, N. (2004) The role and regulation of programmed cell death in plant–pathogen interactions. Cellular Microbiology **6:** 201-211.

Gu, Y. and Innes, R.W. (2011) The KEEP ON GOING protein of Arabidopsis recruits the ENHANCED DISEASE RESISTANCE1 protein to trans-Golgi network/early endosome vesicles. Plant Physiology **155:** 1827-1838.

Gu, Y. and Innes, R.W. (2012) The KEEP ON GOING protein of Arabidopsis regulates intracellular protein trafficking and is degraded during fungal infection. The Plant Cell **24:** 4717-4730.

Heidrich, K., Wirthmueller, L., Tasset, C., Pouzet, C., Deslandes, L. and Parker, J.E. (2011) Arabidopsis EDS1 connects pathogen effector recognition to cell compartment–specific immune responses. Science **334:** 1401-1404.

Heximer, S.P., Knutsen, R.H., Sun, X., Kaltenbronn, K.M., Rhee, M.-H., Peng, N., Oliveira-dos-Santos, A., Penninger, J.M., Muslin, A.J., Steinberg, T.H., Wyss, J.M., Mecham, R.P. and Blumer, K.J. (2003) Hypertension and prolonged vasoconstrictor signaling in Rgs2-deficient mice. The Journal of Clinical Investigation **111:** 445-452.

Holmes, W.M., Mannakee, B.K., Gutenkunst, R.N. and Serio, T.R. (2014) Loss of amino-terminal acetylation suppresses a prion phenotype by modulating global protein folding. Nature Communications **5:** 4383.

Howe, G.A. (2004) Jasmonates as signals in the wound response. Journal of Plant Growth Regulation **23:** 223-237.

Howe, G.A. and Jander, G. (2008) Plant immunity to insect herbivores. Annual Review of Plant Biology **59:** 41-66.

Huang, W., Wang, Y., Li, X. and Zhang, Y. (2020) Biosynthesis and regulation of salicylic acid and N-hydroxypipecolic acid in plant immunity. Molecular Plant **13:** 31-41.

Huh, S.U., Cevik, V., Ding, P., Duxbury, Z., Ma, Y., Tomlinson, L., Sarris, P.F. and Jones, J.D.G. (2017) Protein-protein interactions in the RPS4/RRS1 immune receptor complex. PLOS Pathogens **13:** e1006376.

Hunter, T. (2007) The age of crosstalk: phosphorylation, ubiquitination, and beyond. Molecular Cell **28:** 730-738.

Huot, B., Yao, J., Montgomery, B.L. and He, S.Y. (2014) Growth–defense tradeoffs in plants: a balancing act to optimize fitness. Molecular Plant **7:** 1267-1287.

Hwang, C.-S., Shemorry, A. and Varshavsky, A. (2010) N-terminal acetylation of cellular proteins creates specific degradation signals. Science **327:** 973-977.

Ichimura, K., Shinozaki, K., Tena, G., Sheen, J., Henry, Y., Champion, A., Kreis, M., Zhang, S., Hirt, H., Wilson, C., Heberle-Bors, E., Ellis, B.E., Morris, P.C., Innes, R.W., Ecker, J.R., Scheel, D., Klessig, D.F., Machida, Y., Mundy, J., Ohashi, Y. and Walker, J.C. (2002) Mitogen-activated protein kinase cascades in plants: a new nomenclature. Trends in Plant Science **7:** 301-308.

Jirage, D., Tootle, T.L., Reuber, T.L., Frost, L.N., Feys, B.J., Parker, J.E., Ausubel, F.M. and Glazebrook, J. (1999) *Arabidopsis thaliana* PAD4 encodes a lipase-like gene that is important for salicylic acid signaling. Proceedings of the National Academy of Sciences **96:** 13583-13588.

Jörnvall, H. (1975) Acetylation of protein N-terminal amino groups structural observations on α-amino acetylated proteins. Journal of Theoretical Biology **55:** 1-12.

Kazan, K. and Manners, J.M. (2013) MYC2: the master in action. Molecular Plant **6:** 686-703.

Kieber, J.J., Rothenberg, M., Roman, G., Feldmann, K.A. and Ecker, J.R. (1993) CTR1, a negative regulator of the ethylene response pathway in Arabidopsis, encodes a member of the RAF family of protein kinases. Cell **72:** 427-441.

Kim, T.-H., Kunz, H.-H., Bhattacharjee, S., Hauser, F., Park, J., Engineer, C., Liu, A., Ha, T., Parker, J.E., Gassmann, W. and Schroeder, J.I. (2012) Natural variation in small molecule–induced TIR-NB-LRR signaling induces root growth arrest via EDS1- and PAD4-complexed R protein VICTR in Arabidopsis. The Plant Cell **24:** 5177-5192.

Lee, K.-E., Heo, J.-E., Kim, J.-M. and Hwang, C.-S. (2016) N-terminal acetylation-targeted N-end rule proteolytic system: The Ac/N-end rule pathway. Molecules and cells **39:** 169-178.

Linster, E., Stephan, I., Bienvenut, W.V., Maple-Grødem, J., Myklebust, L.M., Huber, M., Reichelt, M., Sticht, C., Geir Møller, S., Meinnel, T., Arnesen, T., Giglione, C., Hell, R. and Wirtz, M. (2015) Downregulation of N-terminal acetylation triggers ABA-mediated drought responses in Arabidopsis. Nature Communications **6:** 7640.

Liu, J. and Wang, X.-J. (2006) An integrative analysis of the effects of auxin on jasmonic acid biosynthesis in *Arabidopsis thaliana*. Journal of Integrative Plant Biology **48:** 99-103.

Liu, J.-X. and Howell, S.H. (2010) Endoplasmic reticulum protein quality control and its relationship to environmental stress responses in plants. The Plant Cell **22:** 2930-2942.

Liu, H. and Stone, S.L. (2010) Abscisic acid increases Arabidopsis ABI5 transcription factor levels by promoting KEG E3 Ligase self-ubiquitination and proteasomal degradation. The Plant Cell **22:** 2630-2641.

Liu, H. and Stone, S.L. (2013) Cytoplasmic degradation of the Arabidopsis transcription factor ABSCISIC ACID INSENSITIVE 5 is mediated by the RING-type E3 Ligase KEEP ON GOING. Journal of Biological Chemistry **288:** 20267-20279.

Lorenzo, O., Piqueras, R., Sánchez-Serrano, J.J. and Solano, R. (2003) ETHYLENE RESPONSE FACTOR1 integrates signals from ethylene and jasmonate pathways in plant defense. The Plant Cell **15:** 165-178.

Lyzenga, W.J., Liu, H., Schofield, A., Muise-Hennessey, A. and Stone, S.L. (2013) Arabidopsis CIPK26 interacts with KEG, components of the ABA signalling network and is degraded by the ubiquitin–proteasome system. Journal of Experimental Botany **64:** 2779-2791.

Mullen, J.R., Kayne, P.S., Moerschell, R.P., Tsunasawa, S., Gribskov, M., Colavito-Shepanski, M., Grunstein, M., Sherman, F. and Sternglanz, R. (1989) Identification and characterization of genes and mutants for an N-terminal acetyltransferase from yeast. The EMBO Journal **8:** 2067-2075.

Murthi, A. and Hopper, A.K. (2005) Genome-wide screen for inner nuclear membrane protein targeting in *Saccharomyces cerevisiae*. Roles for N-acetylation and an integral membrane protein **170:** 1553-1560.

Nakashima, K., Ito, Y. and Yamaguchi-Shinozaki, K. (2009) Transcriptional regulatory networks in response to abiotic stresses in Arabidopsis and grasses. Plant Physiology **149:** 88-95.

Narita, K. (1958) Isolation of acetylpeptide from enzymic digests of TMV-protein. Biochimica et Biophysica Acta **28:** 184-191.

Navarro, L., Dunoyer, P., Jay, F., Arnold, B., Dharmasiri, N., Estelle, M., Voinnet, O. and Jones, J.D.G. (2006) A plant miRNA contributes to antibacterial resistance by repressing auxin signaling. Science **312:** 436-439.

Panic, B., Whyte, J.R.C. and Munro, S. (2003) The Arf-like GTPases Arl1p and Arl3p act in a pathway that interacts with vesicle-tethering factors at the Golgi apparatus. Current Biology **13:** 405-410.

Park, E.C. and Szostak, J.W. (1992) Ard1 and Nat1 proteins form a complex that has N-terminal acetyltransferase activity. The EMBO Journal **11:** 2087-2093.

Park, S.-E., Kim, J.-M., Seok, O.-H., Cho, H., Wadas, B., Kim, S.-Y., Varshavsky, A. and Hwang, C.-S. (2015) Control of mammalian G protein signaling by N-terminal acetylation and the N-end rule pathway. Science **347:** 1249-1252.

Parker, J.E., Holub, E.B., Frost, L.N., Falk, A., Gunn, N.D. and Daniels, M.J. (1996) Characterization of *eds1*, a mutation in Arabidopsis suppressing resistance to *Peronospora parasitica* specified by several different RPP genes. The Plant Cell **8:** 2033-2046.

Parker, J.E., Coleman, M.J., Szabò, V., Frost, L.N., Schmidt, R., van der Biezen, E.A., Moores, T., Dean, C., Daniels, M.J. and Jones, J.D. (1997) The Arabidopsis downy mildew resistance gene RPP5 shares similarity to the toll and interleukin-1 receptors with N and L6. The Plant Cell **9:** 879-894.

Penninckx, I.A.M.A., Thomma, B.P.H.J., Buchala, A., Métraux, J.-P. and Broekaert, W.F. (1998) Concomitant activation of jasmonate and ethylene response pathways is required for induction of a plant defensin gene in Arabidopsis. The Plant Cell **10:** 2103-2113.

Pesaresi, P., Gardner, N.A., Masiero, S., Dietzmann, A., Eichacker, L., Wickner, R., Salamini, F. and Leister, D. (2003) Cytoplasmic N-terminal protein acetylation is required for efficient photosynthesis in Arabidopsis. The Plant Cell **15:** 1817.

Petersen, M., Brodersen, P., Naested, H., Andreasson, E., Lindhart, U., Johansen, B., Nielsen, H.B., Lacy, M., Austin, M.J., Parker, J.E., Sharma, S.B., Klessig, D.F., Martienssen, R., Mattsson, O., Jensen, A.B. and Mundy, J. (2000) Arabidopsis MAP KINASE 4 negatively regulates systemic acquired resistance. Cell **103:** 1111-1120.

Pieterse, C.M.J., Leon-Reyes, A., Van der Ent, S. and Van Wees, S.C.M. (2009) Networking by small-molecule hormones in plant immunity. Nature Chemical Biology **5:** 308-316.

Pieterse, C.M.J., Van der Does, D., Zamioudis, C., Leon-Reyes, A. and Van Wees, S.C.M. (2012) Hormonal modulation of plant immunity. Annual Review of Cell and Developmental Biology **28:** 489-521.

Polevoda, B., Norbeck, J., Takakura, H., Blomberg, A. and Sherman, F. (1999) Identification and specificities of N-terminal acetyltransferases from *Saccharomyces cerevisiae*. The EMBO Journal **18:** 6155-6168.

Polevoda, B. and Sherman, F. (2003) Composition and function of the eukaryotic N-terminal acetyltransferase subunits. Biochemical and Biophysical Research Communications **308:** 1-11.

Polevoda, B., Arnesen, T. and Sherman, F. (2009) A synopsis of eukaryotic Nα-terminal acetyltransferases: Nomenclature, subunits and substrates. BMC Proceedings **3:** S2.

Pré, M., Atallah, M., Champion, A., De Vos, M., Pieterse, C.M.J. and Memelink, J. (2008) The Ap2/Erf domain transcription factor ORA59 integrates jasmonic acid and ethylene signals in plant defense. Plant Physiology **147:** 1347-1357.

Raychaudhuri, S., Majumder, P., Sarkar, S., Giri, K., Mukhopadhyay, D. and Bhattacharyya, N.P. (2008) Huntingtin interacting protein Hypk is intrinsically unstructured. Proteins: Structure, Function, and Bioinformatics **71:** 1686-1698.

Ree, R., Varland, S. and Arnesen, T. (2018) Spotlight on protein N-terminal acetylation. Experimental & Molecular Medicine **50:** 90.

Rietz, S., Stamm, A., Malonek, S., Wagner, S., Becker, D., Medina-Escobar, N., Corina Vlot, A., Feys, B.J., Niefind, K. and Parker, J.E. (2011) Different roles of ENHANCED DISEASE SUSCEPTIBILITY1 (EDS1) bound to and dissociated from PHYTOALEXIN DEFICIENT4 (PAD4) in Arabidopsis immunity. New Phytologist **191:** 107-119.

Serrano, I., Gu, Y., Qi, D., Dubiella, U. and Innes, R.W. (2014) The Arabidopsis EDR1 protein kinase negatively regulates the ATL1 E3 ubiquitin Ligase to suppress cell death. The Plant Cell **26:** 4532.

Setty, S.R.G., Shin, M.E., Yoshino, A., Marks, M.S. and Burd, C.G. (2003) Golgi recruitment of grip domain proteins by Arf-like GTPase 1 is regulated by Arf-like GTPase 3. Current Biology **13:** 401-404.

Setty, S.R.G., Strochlic, T.I., Tong, A.H.Y., Boone, C. and Burd, C.G. (2004) Golgi targeting of Arf-like GTPase Arl3p requires its Nα-acetylation and the integral membrane protein Sys1p. Nature Cell Biology **6:** 414-419.

Shemorry, A., Hwang, C.-S. and Varshavsky, A. (2013) Control of protein quality and stoichiometries by N-terminal acetylation and the N-end rule pathway. Molecular Cell **50:** 540-551.

Spaepen, S., Vanderleyden, J. and Remans, R. (2007) Indole-3-acetic acid in microbial and microorganism-plant signaling. FEMS Microbiology Reviews **31:** 425-448.

Spoel, S.H., Johnson, J.S. and Dong, X. (2007) Regulation of tradeoffs between plant defenses against pathogens with different lifestyles. Proceedings of the National Academy of Sciences **104:** 18842-18847.

Starheim, Kristian K., Arnesen, T., Gromyko, D., Ryningen, A., Varhaug, Jan E. and Lillehaug, Johan R. (2008) Identification of the human Nα-acetyltransferase complex b (hNatB): a complex important for cell-cycle progression. Biochemical Journal **415:** 325-331.

Starheim, K.K., Gromyko, D., Evjenth, R., Ryningen, A., Varhaug, J.E., Lillehaug, J.R. and Arnesen, T. (2009) Knockdown of human Nα-terminal acetyltransferase complex c leads to p53-dependent apoptosis and aberrant human Arl8b localization. Molecular and Cellular Biology **29:** 3569-3581.

Stone, S.L., Williams, L.A., Farmer, L.M., Vierstra, R.D. and Callis, J. (2006) KEEP ON GOING, a RING E3 Ligase essential for Arabidopsis growth and development, is involved in abscisic acid signaling. The Plant Cell **18:** 3415-3428.

Tang, D. and Innes, R.W. (2002) Overexpression of a kinase-deficient form of the EDR1 gene enhances powdery mildew resistance and ethylene-induced senescence in Arabidopsis. The Plant Journal **32:** 975-983.

Tang, D., Christiansen, K.M. and Innes, R.W. (2005) Regulation of plant disease resistance, stress responses, cell death, and ethylene signaling in Arabidopsis by the EDR1 protein kinase. Plant Physiology **138.**

Tsuda, K. and Somssich, I.E. (2015) Transcriptional networks in plant immunity. New Phytologist **206:** 932-947.

Van Damme, P., Evjenth, R., Foyn, H., Demeyer, K., De Bock, P.-J., Lillehaug, J.R., Vandekerckhove, J., Arnesen, T. and Gevaert, K. (2011) Proteome-derived peptide libraries allow detailed analysis of the substrate specificities of Nα-acetyltransferases and point to hNaa10p as the post-translational actin Nα-acetyltransferase. Molecular & Cellular Proteomics **10:** M110.004580.

Van Damme, P., Lasa, M., Polevoda, B., Gazquez, C., Elosegui-Artola, A., Kim, D.S., De Juan-Pardo, E., Demeyer, K., Hole, K., Larrea, E., Timmerman, E., Prieto, J., Arnesen, T., Sherman, F., Gevaert, K. and Aldabe, R. (2012) N-terminal acetylome analyses and functional insights of the N-terminal acetyltransferase NatB. Proceedings of the National Academy of Sciences **109:** 12449-12454.

Van Damme, P., Hole, K., Gevaert, K. and Arnesen, T. (2015) N-terminal acetylome analysis reveals the specificity of Naa50 (Nat5) and suggests a kinetic competition between N-terminal acetyltransferases and methionine aminopeptidases. PROTEOMICS **15:** 2436-2446.

Van Damme, P., Kalvik, T.V., Starheim, K.K., Jonckheere, V., Myklebust, L.M., Menschaert, G., Varhaug, J.E., Gevaert, K. and Arnesen, T. (2016) A role for human N-alpha acetyltransferase 30 (Naa30) in maintaining mitochondrial integrity. Molecular & Cellular Proteomics **15:** 3361-3372.

Van der Does, D., Leon-Reyes, A., Koornneef, A., Van Verk, M.C., Rodenburg, N., Pauwels, L., Goossens, A., Körbes, A.P., Memelink, J., Ritsema, T., Van Wees, S.C.M. and Pieterse, C.M.J. (2013) Salicylic acid suppresses jasmonic acid signaling downstream of SCFCOI1-JAZ by targeting GCC promoter motifs via transcription factor ORA59. The Plant Cell **25:** 744-761.

van Loon, L.C., Rep, M. and Pieterse, C.M.J. (2006) Significance of inducible defense-related proteins in infected plants. Annual Review of Phytopathology **44:** 135-162.

Verberne, M.C., Hoekstra, J., Bol, J.F. and Linthorst, H.J.M. (2003) Signaling of systemic acquired resistance in tobacco depends on ethylene perception. The Plant Journal **35:** 27-32.

Verma, V., Ravindran, P. and Kumar, P.P. (2016) Plant hormone-mediated regulation of stress responses. BMC Plant Biology **16:** 86.

Vitale, A. and Boston, R.S. (2008) Endoplasmic reticulum quality control and the unfolded protein response: Insights from plants. Traffic **9:** 1581-1588.

Vlot, A.C., Dempsey, D.M. and Klessig, D.F. (2009) Salicylic acid, a multifaceted hormone to combat disease. Annual Review of Phytopathology **47:** 177-206.

Wagner, S., Stuttmann, J., Rietz, S., Guerois, R., Brunstein, E., Bautor, J., Niefind, K. and Parker, Jane E. (2013) Structural basis for signaling by exclusive EDS1 heteromeric complexes with SAG101 or PAD4 in plant innate immunity. Cell Host & Microbe **14:** 619-630.

Walter, P. and Ron, D. (2011) The unfolded protein response: from stress pathway to homeostatic regulation. Science **334:** 1081.

Walters, D. and Heil, M. (2007) Costs and trade-offs associated with induced resistance. Physiological and Molecular Plant Pathology **71:** 3-17.

Wang, D., Pajerowska-Mukhtar, K., Culler, A.H. and Dong, X. (2007) Salicylic acid inhibits pathogen growth in plants through repression of the auxin signaling pathway. Current Biology **17:** 1784-1790.

Wasternack, C. (2007) Jasmonates: an update on biosynthesis, signal transduction and action in plant stress response, growth and development. Annals of Botany **100:** 681-697.

Wawrzynska, A., Christiansen, K.M., Lan, Y., Rodibaugh, N.L. and Innes, R.W. (2008) Powdery mildew resistance conferred by loss of the ENHANCED DISEASE RESISTANCE1 protein kinase is suppressed by a missense mutation in KEEP ON GOING, a regulator of abscisic acid signaling. Plant Physiology **148:** 1510-1522.

Wiermer, M., Feys, B.J. and Parker, J.E. (2005) Plant immunity: the EDS1 regulatory node. Current Opinion in Plant Biology **8:** 383-389.

Wildermuth, M.C., Dewdney, J., Wu, G. and Ausubel, F.M. (2001) Isochorismate synthase is required to synthesize salicylic acid for plant defence. Nature **414:** 562-565.

Williams, B., Verchot, J. and Dickman, M.B. (2014) When supply does not meet demand-ER stress and plant programmed cell death. Frontiers in Plant Science **5:** 211-211.

Woehlbier, U. and Hetz, C. (2011) Modulating stress responses by the UPRosome: a matter of life and death. Trends in Biochemical Sciences **36:** 329-337.

Wu, G., Liu, S., Zhao, Y., Wang, W., Kong, Z. and Tang, D. (2015) ENHANCED DISEASE RESISTANCE4 associates with CLATHRIN HEAVY CHAIN2 and modulates plant immunity by regulating relocation of EDR1 in Arabidopsis. The Plant Cell **27:** 857-873.

Xie, D.-X., Feys, B.F., James, S., Nieto-Rostro, M. and Turner, J.G. (1998) COI1: an Arabidopsis gene required for jasmonate-regulated defense and fertility. Science **280:** 1091-1094.

Xu, F., Huang, Y., Li, L., Gannon, P., Linster, E., Huber, M., Kapos, P., Bienvenut, W., Polevoda, B., Meinnel, T., Hell, R., Giglione, C., Zhang, Y., Wirtz, M., Chen, S. and Li, X. (2015) Two N-terminal acetyltransferases antagonistically regulate the stability of a nod-like receptor in Arabidopsis. The Plant Cell **27:** 1547.

Yamaguchi-Shinozaki, K. and Shinozaki, K. (2006) Transcriptional regulatory networks in cellular responses and tolerance to dehydration and cold stresses. Annual Review of Plant Biology **57:** 781-803.

Yang, J., Kamide, K., Kokubo, Y., Takiuchi, S., Tanaka, C., Banno, M., Miwa, Y., Yoshii, M., Horio, T., Okayama, A., Tomoike, H., Kawano, Y. and Miyata, T. (2005) Genetic variations of regulator of G-protein signaling 2 in hypertensive patients and in the general population. Journal of Hypertension **23:** 1497-1505.

Zhang, J., Schurr, U. and Davies, W.J. (1987) Control of stomatal behaviour by abscisic acid which apparently originates in the roots. Journal of Experimental Botany **38:** 1174-1181.

Zhang, Y. and Li, X. (2019) Salicylic acid: biosynthesis, perception, and contributions to plant immunity. Current Opinion in Plant Biology **50:** 29-36.

Zhao, C., Nie, H., Shen, Q., Zhang, S., Lukowitz, W. and Tang, D. (2014) EDR1 physically interacts with MKK4/MKK5 and negatively regulates a MAP kinase cascade to modulate plant innate immunity. PLOS Genetics **10:** e1004389.

Zheng, X.-y., Spivey, Natalie W., Zeng, W., Liu, P.-P., Fu, Zheng Q., Klessig, Daniel F., He, Sheng Y. and Dong, X. (2012) Coronatine promotes *Pseudomonas syringae* virulence in plants by activating a signaling cascade that inhibits salicylic acid accumulation. Cell Host & Microbe **11:** 587-596.

Zhou, N., Tootle, T.L., Tsui, F., Klessig, D.F. and Glazebrook, J. (1998) PAD4 functions upstream from salicylic acid to control defense responses in Arabidopsis. The Plant Cell **10:** 1021-1030.

Zhu, J.-K. (2002) Salt and drought signaling transduction in plants. Annual Review of Plant Biology **53:** 247-273.

Chapter 2: Arabidopsis ENHANCED DISEASE RESISTANCE1 Protein Kinase Regulates the Association of ENHANCED DISEASE SUSCEPTIBILITY1 and PHYTOALEXIN DEFICIENT4 to Inhibit Cell Death

(Matthew P. Neubauer, Irene Serrano, Natalie Rodibaugh, Deepak D. Bhandari, Jaqueline Bautor, Jane E. Parker, and Roger W. Innes, *Molecular Plant-Microbe Interactions*)

Introduction

Loss-of-function mutations in the *ENHANCED DISEASE RESISTANCE1* (*EDR1*) gene of Arabidopsis confer enhanced resistance to the powdery mildew pathogen *Golovinomyces cichoracearum* (Frye and Innes, 1998). This enhanced resistance is correlated with enhanced cell death at the site of infection. The *edr1-1* mutation causes a premature stop codon in the *EDR1* gene, which encodes a protein kinase with homology to mitogen–activated protein kinase kinase kinases (MAPKKKs) belonging to the Raf family (Frye et al., 2001). The *edr1* mutant does not display constitutive expression of defense genes in the absence of a pathogen, indicating that the enhanced resistance is not caused by constitutive activation of systemic acquired resistance (Frye and Innes, 1998); however, *edr1*-mediated disease resistance is suppressed by mutations that block or reduce salicylic acid (SA) production or signaling (Frye and Innes, 1998; Frye et al., 2001; Christiansen et al., 2011; Hiruma et al., 2011; Hiruma and Takano, 2014; Tang et al., 2005), suggesting that *edr1*-mediated enhanced resistance against *G. cichoracearum* requires an intact SA signaling pathway.

In addition to enhancing resistance to powdery mildew, loss-of-function mutations in *EDR1* enhance drought-induced growth inhibition, ethylene induced senescence and sensitivity to abscisic acid (ABA) (Tang et al., 2005; Wawrzynska et al., 2008). The enhanced drought-induced growth inhibition and enhanced ABA sensitivity phenotypes, but not ethylene-induced senescence, are suppressed by mutations in the *ENHANCED DISEASE SUSCEPTIBILITY 1* (*EDS1*) and *PHYTOALEXIN DEFICIENT 4* (*PAD4*) genes, which encode sequence-related nucleocytoplasmic lipase-like proteins (Tang et al., 2005). The inability of these mutations to suppress the ethylene-induced senescence phenotype of *edr1* mutants suggests that EDR1may regulate multiple pathways.

The *pad4* mutant was originally isolated in an Arabidopsis screen for enhanced disease susceptibility to *Pseudomonas syringae* pv. *maculicola* (Glazebrook et al., 1996). PAD4 physically interacts with EDS1 as a heterodimer (Feys et al., 2001; Jirage et al., 1999; Rietz et al., 2011; Wagner et al., 2013), forming a nucleo-cytoplasmic complex that promotes accumulation of the plant defense signaling molecule SA (Cui et al., 2017; Feys et al., 2001; Feys et al., 2005). EDS1 and PAD4 also contribute to defense responses activated by intracellular nucleotide-binding, leucine rich repeat (NLR) receptors that have an N-terminal Toll-interleukin 1 receptor (TIR) domain (Aarts et al., 1998; Bhandari et al., 2019; Cui et al., 2018; Feys et al., 2001; Glazebrook et al., 1996). NLR-mediated immune responses are often associated with localized host-cell death as part of the hypersensitive response (HR) (Maekawa et al., 2011). Arabidopsis *pad4* mutants display a delayed HR against the oomycete pathogen *Hyaloperospora arabidopsidis* that is insufficient for preventing pathogen spread (Feys et al., 2001). This partially retained HR can be attributed to partial genetic redundancy between *PAD4* and the nuclear *SENESCENCE-*

ASSOCIATED GENE 101 (*SAG101*), another component of the EDS1 regulatory hub (Feys et al., 2005; Lipka et al., 2005). It was recently established that EDS1-SAG101 heterodimers promote HR cell death in TIR-NLR receptor immunity, whereas formation of EDS1-PAD4 heterodimers is necessary for transcriptionally mobilizing SA and other defense pathways (Bhandari et al., 2019; Feys et al., 2005; Gantner et al., 2019; Lapin et al., 2019; Rietz et al., 2011). Complementary studies have shown that EDS1 and PAD4 transduce photo-oxidative stress signals leading to cell death and the slowing of plant growth, and that they are involved in plant fitness regulation (Chandra-Shekara et al., 2007; Venugopal et al., 2009; Wituszynska et al., 2013; Xiao et al., 2001).

So far, all described mutations in *EDS1* and *PAD4* have caused a loss of function (Feys et al., 2001; Hu et al., 2005; Jirage et al., 1999; Rietz et al., 2011; Wagner et al., 2011). Here we describe a gain-of-function mutation in the *PAD4* gene that enhances a subset of *edr1* mutant phenotypes, including *edr1*-dependent cell death after powdery mildew infection, and *edr1* accelerated ethylene- and age-induced senescence. This mutation causes a serine to phenylalanine substitution at position 135 of PAD4. Furthermore, the PAD4^{S135F} substitution alone confers enhanced disease resistance and enhanced cell death after infection with the powdery mildew fungus *G. cichoracearum*. The molecular basis for these phenotypes remains unclear, however, the S135F substitution did not affect PAD4 protein accumulation, localization, or its ability to associate with EDS1. The discovery that PAD4^{S135F} enhances a subset of *edr1* phenotypes supports previous findings that the *edr1* phenotype is at least partially due to changes in SA signaling (Tang et al., 2005). Analysis of *edr1* and *pad4*/*eds1* transcriptome data revealed that a significant proportion of the PAD4/EDS1 gene network

is upregulated in *edr1* plants during the defense response. To follow up on these results, we investigated whether EDR1 plays a direct role in regulating PAD4. Significantly, we found that EDR1 interacts with both PAD4 and EDS1, and that EDR1 can inhibit the interaction between EDS1 and PAD4.

Results

Identification of a Mutation in *PAD4* That Enhances *edr1* Mutant Phenotypes

The *edr1* mutant displays enhanced sensitivity to *flg22*, a 22 amino-acid peptide derived from bacterial flagellin that is known to induce defense responses (Geissler et al., 2015). This sensitivity can be assayed in very young seedlings grown in liquid culture. We took advantage of this phenotype to screen for second site mutations that can suppress this enhanced flg22 sensitivity, restoring *edr1* mutants to a wild-type phenotype. Candidate suppressor mutants obtained in this screen were assessed for the presence of mutations in genes previously shown to be required for *edr1* mutant phenotypes (Tang et al., 2005; Wawrzynska et al., 2008), so that we could focus our efforts on new genes. To our surprise, all suppressor candidates analyzed (13 in total) carried an identical missense mutation in the *PAD4* gene, causing a change of amino acid Ser135 to Phe135 ($PAD4^{S135F}$). Because these 13 mutants were derived from multiple different ethylmethane sulphonate-mutagenized parents, it seemed likely that the parent population (prior to mutagenesis) carried this mutation, and that the mutation was not responsible for the suppressor phenotype. We therefore sequenced the *PAD4* gene in the *edr1-1* parental line used for suppressor mutagenesis. This analysis confirmed that the *edr1-1* parental line used for the suppressor mutagenesis carried the same mutation,

and that this mutation had arisen at some point during the backcrossing process of the original *edr1-1* mutant, which lacks this mutation (see Methods). We have designated this new *pad4* mutation as *pad4-13* as it represents the 13th mutant allele of *pad4* to be described. To separate the *pad4-13* mutation from the *edr1-1* mutation, the double mutant line was backcrossed to wild-type Col-0 and F2 plants identified that were homozygous mutant at one locus and homozygous wild-type at the other. Each separate mutant was then back-crossed to wild-type Col-0 three times to eliminate any other unlinked or loosely linked mutations.

The *pad4-13* Mutation Confers Enhanced Disease Resistance and Contributes to *edr1*-Dependent Enhanced Cell Death

Because we had previously shown that loss-of-function mutations in *PAD4* suppressed *edr1-1* mutant phenotypes (Tang et al., 2005), the discovery that a missense mutation in *PAD4* was present in the *edr1-1* mutant suggested that the *pad4-13* mutation might be contributing to *edr1* mutant phenotypes. To test this hypothesis, we infected wild-type Col-0, *edr1-1* (lacking *pad4-13*), *edr1-3* (contains a T-DNA insertion in *EDR1*), *pad4-13*, and *edr1-1 pad4-13* plants with *G. cichoracearum* and quantified fungal growth by counting conidiospores at 8 dpi. As expected, *edr1-1 pad4-13* plants had a reduced spore count compared to wild-type Col-0 (Figure 2-1A). This enhanced disease resistance was not influenced by the presence of the *pad4-13* mutation, as the *edr1-1* and *edr1-3* mutants had comparable spore counts (Figure 2-1A). Interestingly, the *pad4-13* mutant also had a reduced spore count, similar to that of the *edr1* mutants (Figure 2-1A). These results indicate that the *pad4-13* mutation alone confers an enhanced disease

resistance similar to *edr1* mutations, and that the mutations are not additive in their effects.

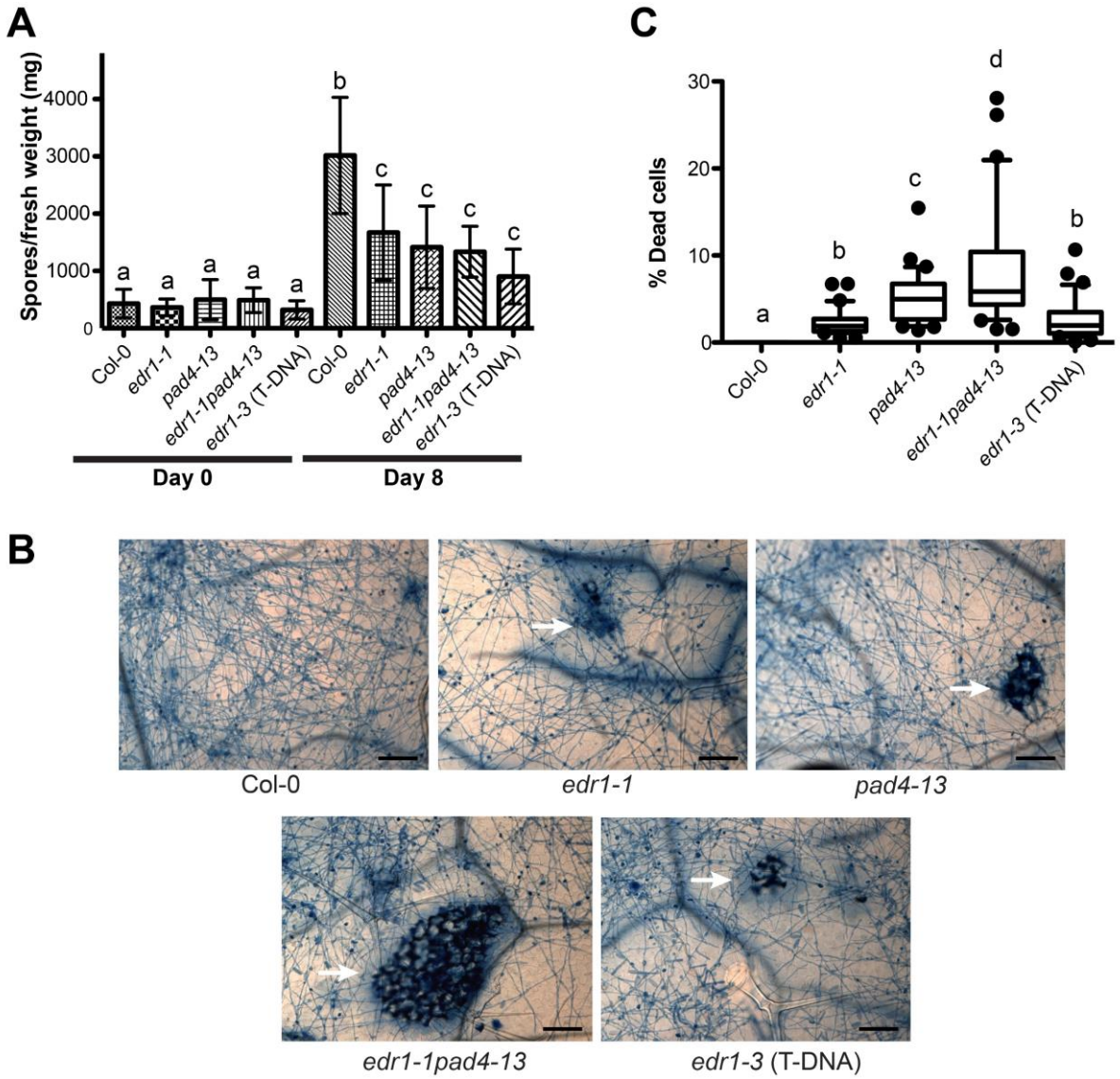

Figure 2-1. The *pad4-13* mutation confers enhanced disease resistance and contributes to *edr1*-associated cell death. **A**, Quantitative analysis of powdery mildew conidia (asexual spores) on Col-0, *edr1-1*, *pad4-13*, *edr1-1pad4-13* and *edr1-3* lines. Plants were inoculated with powdery mildew and conidia production was determined 8 dpi. Bars indicate the mean of three samples, each with three technical replicates. Error bars indicate SD. Results are representative of 3 independent experiments. **B**, Trypan blue staining of powdery mildew-infected Col-0, *edr1-1*, *pad4-13*, *edr1-1pad4-13* and *edr1-3* lines. The indicated lines were assessed for leaf mesophyll cell death 8 dpi and cell death was quantified using ImageJ. For quantification, six pictures from five independent experiments were randomly chosen (n=30). Results are provided as means with 10th and 90th percentiles (box) and range (whiskers). Statistical outliers are shown as a circle. Lower case letters indicate values that are significantly different ($P<0.01$; one-way ANOVA test using the Bonferroni method). **C**, Four-week old plants were infected with *G. cichoracearum* and phenotypes were scored 8 days post-infection. Trypan blue staining of infected leaves to reveal fungal hyphae and patches of dead mesophyll cells (arrows). Bars=50 µm. Pictures are representative of 3 independent experiments.

Loss-of-function mutations in *PAD4* have been shown to enhance disease susceptibility (Feys et al., 2001; Frye et al., 2001; Glazebrook et al., 1997; Zhou et al., 1998). Indeed, upon *G. cichoracearum* infection, *pad4-1* plants accumulate more fungal spores than wild-type (Figure 2-2). These data indicate that the *pad4-13* mutation causes a gain-of-function that enhances resistance to *G. cichoracearum*.

In addition to enhancing resistance to *G. cichoracearum*, the *edr1* mutation causes an increase in mesophyll cell death following infection by this fungus (Frye and Innes, 1998). To assess whether the *pad4-13* mutation contributes to this cell death phenotype, we used trypan blue staining to score cell death at 5 dpi. The *edr1-1 pad4-13* mutant displayed large patches of mesophyll cell death (Figure 2-1B). In comparison, the *edr1-1* and *edr1-3* mutants displayed fewer patches of dead cells, and these patches were smaller. Significantly, the *pad4-13* mutant also displayed patches of dead mesophyll cells, similar in appearance to the *edr1* mutants. No mesophyll cell death was detected in wild-type Col-0 plants. To further characterize the cell death response, the patches of dead mesophyll cells positive for trypan blue staining were quantified. The *edr1*-dependent cell death was enhanced by the presence of the *pad4-13* mutation, indicating that the two mutations are additive in their effect on powdery mildew-induced cell death (Figure 2-1C). Notably, *pad4-13* plants displayed a significantly higher level of cell death than *edr1* plants.

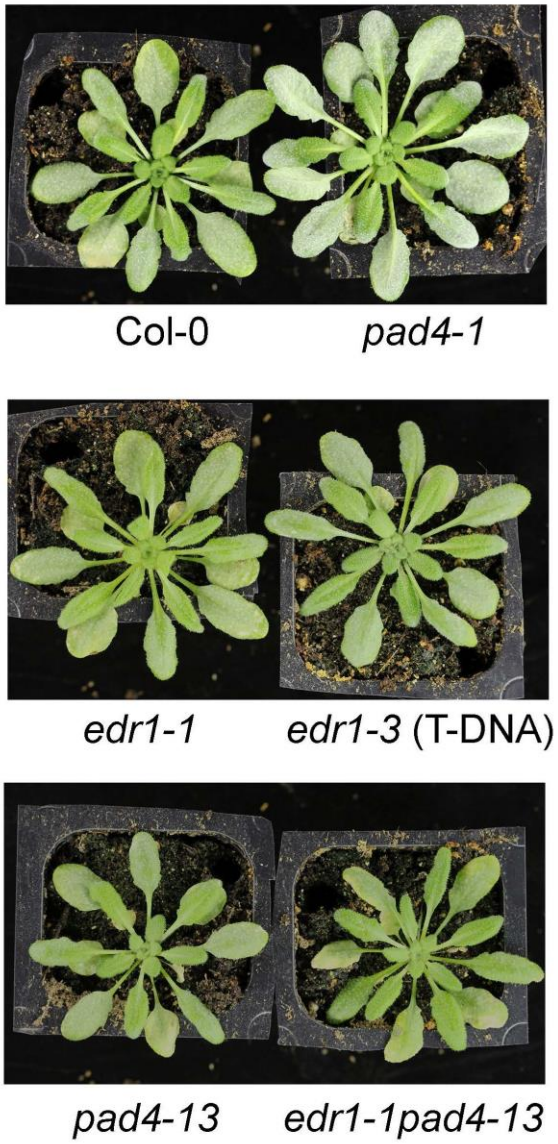

Figure 2-2. The *pad4-13* mutation does not result in a loss of function. Photographs of powdery mildew-infected plants 8 dpi. *pad4-1* plants display enhanced susceptibility and an increased level of powdery mildew growth, while *pad4-13* plants do not.

EDR1 Physically Interacts with EDS1 and PAD4

The conclusion that pad*4-13* can enhance some but not all *edr1* phenotypes prompted us to investigate whether EDR1 and PAD4 are part of a common regulatory complex. In support of this hypothesis, both proteins were previously shown to localize partially to the nucleus (Feys et al., 2005; Christiansen et al., 2011). To test whether EDR1

interacts with PAD4, we performed yeast two-hybrid analyses. Counter to expectations, we could not detect an interaction between wild-type EDR1 and PAD4 (Figure 2-3A). As described above, however, PAD4 is known to interact with EDS1, and this interaction is required for both basal disease resistance and TIR-NLR-mediated resistance (Feys et al., 2005; Feys et al., 2001; Rietz et al., 2011; Wagner et al., 2013), suggesting that the genetic interaction between *EDR1* and *PAD4* could be mediated by EDS1. We thus tested whether EDR1 interacts with EDS1, and observed a positive yeast two-hybrid interaction (Figure 2-3A). One possible reason we could not detect the interaction between PAD4 and EDR1 is that PAD4 could be a substrate of EDR1, and this interaction may be very transient. We therefore tested whether a substrate-trap mutant form of EDR1, EDR1ST (Gu and Innes, 2011), interacts with PAD4. EDR1ST results from an aspartic acid to alanine substitution in the catalytic site of EDR1 (amino acid 810), which inhibits phosphotransfer and thus stabilizes interactions with substrates. Indeed, EDR1ST was found to interact with both EDS1 and PAD4. However, the enhanced interaction of EDR1ST with PAD4 is possibly explained by enhanced stability of the mutant protein compared to wild-type EDR1 (Figure 2-3A).

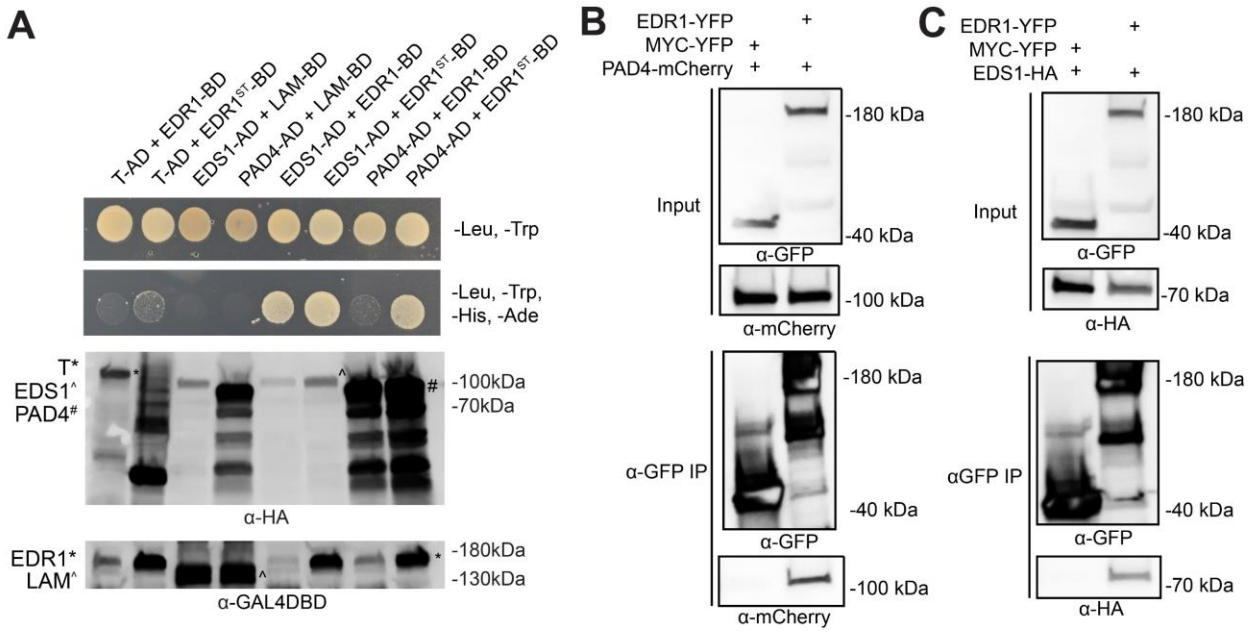

Figure 2-3. EDR1 physically interacts with EDS1 and PAD4. **A,** Yeast two-hybrid analysis of EDR1 interactions with EDS1 and PAD4. AD, GAL4 activation domain fusion; BD, GAL4 DNA binding domain fusion; T, SV40 large T antigen; LAM, lamin. Protein expression was verified through immunoblotting. AD-tagged proteins also contain an HA tag, which was used for detection. **B,** EDR1 co-immunoprecipitates with PAD4. **C,** EDR1 co-immunoprecipitates with EDS1. For both panels B and C, the indicated constructs were transiently expressed in *N. benthamiana* and then immunoprecipitated using GFP-Trap beads. These experiments were all repeated three times with similar results.

We then sought to determine whether the interactions observed in yeast also occur *in planta*. Co-immunoprecipitation (Co-IP) assays in *N. benthamiana* were performed. EDS1-3xHA and PAD4-mCherry were independently co-expressed with either EDR1-sYFP or 5xMYC-sYFP as a negative control. 5xMYC-sYFP was used as a negative control because it displays a nucleocytoplasmic distribution similar to PAD4 and EDR1, but would not be expected to interact with PAD4. Both PAD4 and EDS1 were found to Co-IP with EDR1, but not when co-expressed with 5xMYC-sYFP (Figure 2-3B, 2-3C). These assays indicate that both PAD4 and EDS1 can form complexes with EDR1 *in planta.* Although PAD4 did not interact with wild-type EDR1 in yeast two-hybrid, we did observe a PAD4-EDR1 interaction in Co-IP experiments. Based on these observations, we propose that EDR1 directly interacts with both EDS1 and PAD4.

EDR1 Inhibits the Interaction Between EDS1 and PAD4

The interaction between EDR1 and both PAD4 and EDS1 raised the question of whether EDR1 regulates PAD4-EDS1 heterodimer association. Formation of the EDS1-PAD4 heterodimer brings together α-helical coil surfaces in the partner C-terminal domains that are essential for basal and TIR-NLR immunity signaling (Bhandari et al., 2019; Lapin et al., 2019). To test whether EDR1 can affect this interaction, we performed a yeast three-hybrid analysis in which the kinase domain of EDR1 (EDR1-KD) was expressed as a third protein in the yeast cell under control of the methionine-regulated promoter Met25 (repressed in the presence of 1 mM methionine and induced in its absence). However, we still observed accumulation of EDR1-KD in the absence of methionine, perhaps due to leakiness of the promoter (Figure 2-4B). EDR1-KD

expression inhibited the interaction between EDS1 and PAD4 (Figure 2-4A). To test whether this effect of EDR1 was dependent on EDR1 kinase activity, we also performed the assay using EDR1-KDST, which is kinase-inactive. EDR1-KDST also blocked the EDS1-PAD4 interaction (Figure 2-4A). Expression of EDR1-KD and EDR1-KDST had no noticeable effect on the interaction between the bacterial effector AvrB and the soybean R protein RIN4b, indicating that the effect on the EDS1-PAD4 interaction was specific. Immunoblotting demonstrated that EDR1-KD and EDR1-KDST accumulated in yeast to similar levels, and that EDR1 expression did not interfere with the accumulation of EDS1 or PAD4 (Figure 2-4B). That EDR1 kinase activity was dispensable for blocking the EDS1-PAD4 interaction suggests that EDR1 may be interfering with EDS1-PAD4 association by competing for a common EDS1 binding site, rather than by phosphorylation of either protein.

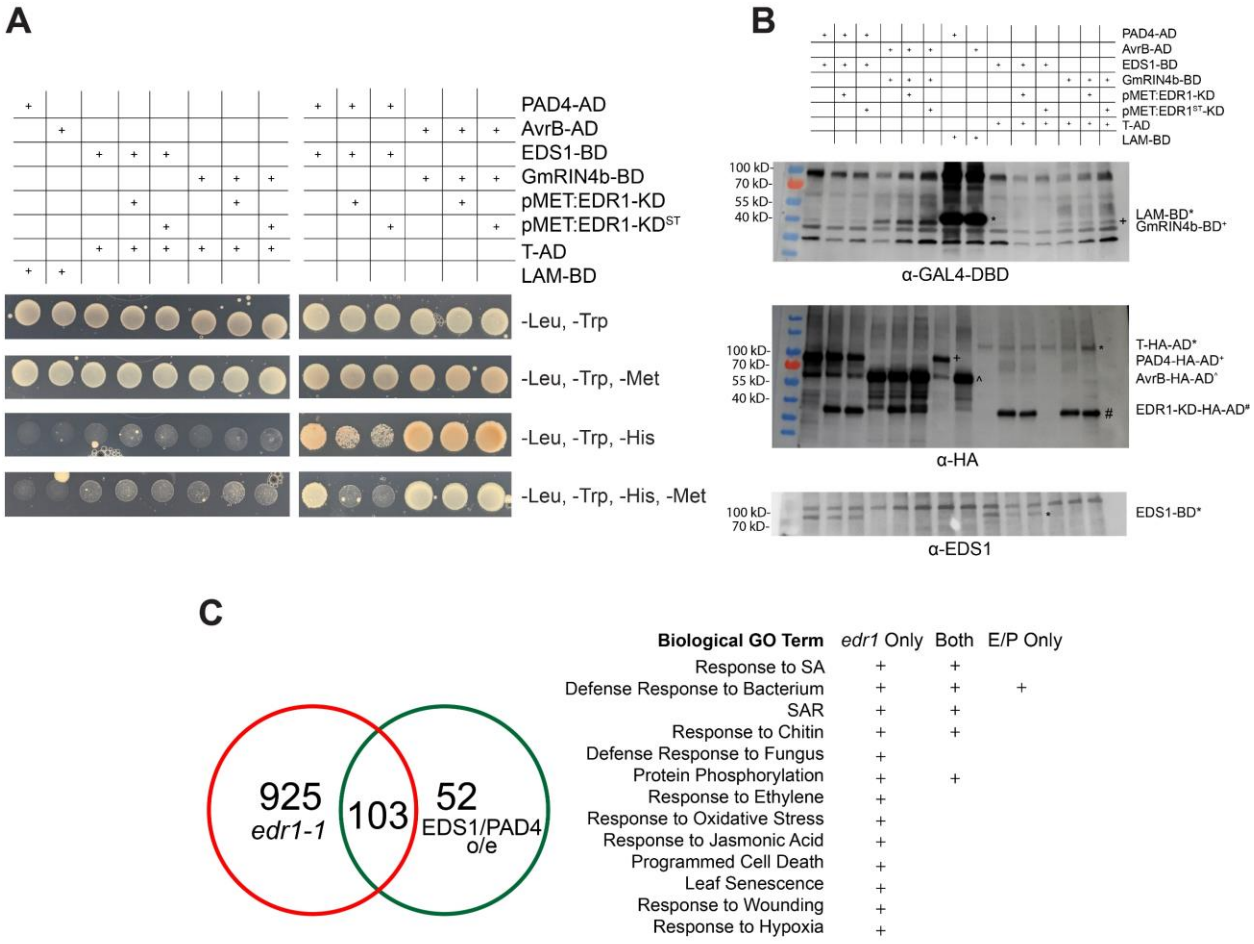

Figure 2-4. EDR1 interferes with EDS1:PAD4 association. **A,** The EDR1 kinase domain (KD) inhibits EDS1:PAD4 interaction in a yeast three-hybrid assay. The indicated constructs were transformed into yeast strains AH109 (activation domain constructs) and Y187 (DNA binding domain and methionine promoter constructs in pBridge vector) and then mated. Diploids were selected on minus Leu Trp plates, then replated on the indicated media. Growth on minus His plates indicates physical interaction between EDS1 and PAD4. Media lacking methionine induces the MET promoter. AvrB and RIN4b are positive controls for interaction. **B**, Immunoblot analysis confirms protein expression in yeast strains utilized in yeast three-hybrid assay. **C**, Loss of *EDR1* results in the upregulation of the EDS1-PAD4 network during a defense response. The *edr1* only dataset is enriched for a more diverse set of biological GO terms than the EDS1-PAD4 network.

edr1 Plants Display Enhanced EDS1/PAD4 Signaling During Defense Response

Recently, a network of 155 core genes was demonstrated to be upregulated during the overexpression of EDS1 with PAD4 (Cui at al., 2017). Previous work has demonstrated that loss of function mutations in either *EDS1* or *PAD4* inhibit a subset of *edr1* phenotypes (Tang et al., 2005). The discovery that EDR1 can interact with EDS1 and PAD4, as well as disrupt the formation of the EDS1/PAD4 complex, prompted us to investigate whether EDR1 negatively regulates the EDS1-PAD4 signaling network. We have previously demonstrated that the loss of *EDR1* results in the upregulation of many defense-related genes during powdery mildew infection (Christiansen et al., 2011). We found that the majority of the 155 genes that were upregulated during EDS1-PAD4 overexpression are significantly upregulated in *edr1* plants relative to wild type after powdery mildew infection (Figure 2-4C). 103 of the 155 EDS1-PAD4 upregulated transcripts were upregulated in *edr1* plants during infection. This demonstrates that EDR1 has a negative impact on the induction of many EDS1-PAD4 upregulated genes during the defense response.

Gene Ontology (GO) term enrichment analysis revealed that the genes belonging to both the EDS1-PAD4 upregulated and *edr1* upregulated networks are enriched for processes such as SA response, response to chitin, and protein phosphorylation (Figure 2-4C). Interestingly, those genes that were found to be upregulated in *edr1* plants, but not belonging to the EDS1-PAD4 network, were enriched for a more diverse set of processes, including response to JA, ethylene, oxidative stress, hypoxia, and wounding. This correlates with the previous discovery that *edr1* phenotypes are only partially supressed by mutations in *EDS1* or *PAD4* (Tang et al., 2005), as well as the observation that *pad4*-

13 enhances a subset of *edr1* phenotypes (Figure 2-1). These data demonstrate that EDR1 negatively regulates a broad set of defense responses, which includes but is not limited to, the EDS1-PAD4 network.

The S135F Substitution in PAD4 Does Not Affect Protein Accumulation, Localization, or Interaction with EDS1

To determine the effect of the S135F substitution on PAD4 function, we investigated possible changes that could result in PAD4 over-activity. We hypothesized that an increase in the stability of the PAD4 protein caused by the S135F substitution might result in enhanced SA signaling and cell death. However, we were unable to detect an increase in the accumulation of $PAD4^{S135F}$ relative to PAD4 in Arabidopsis plants undergoing a defense response elicited by the RPS4 TIR-NLR protein (unelicited plants have nearly undetectable levels of PAD4; Figure 2-5A).

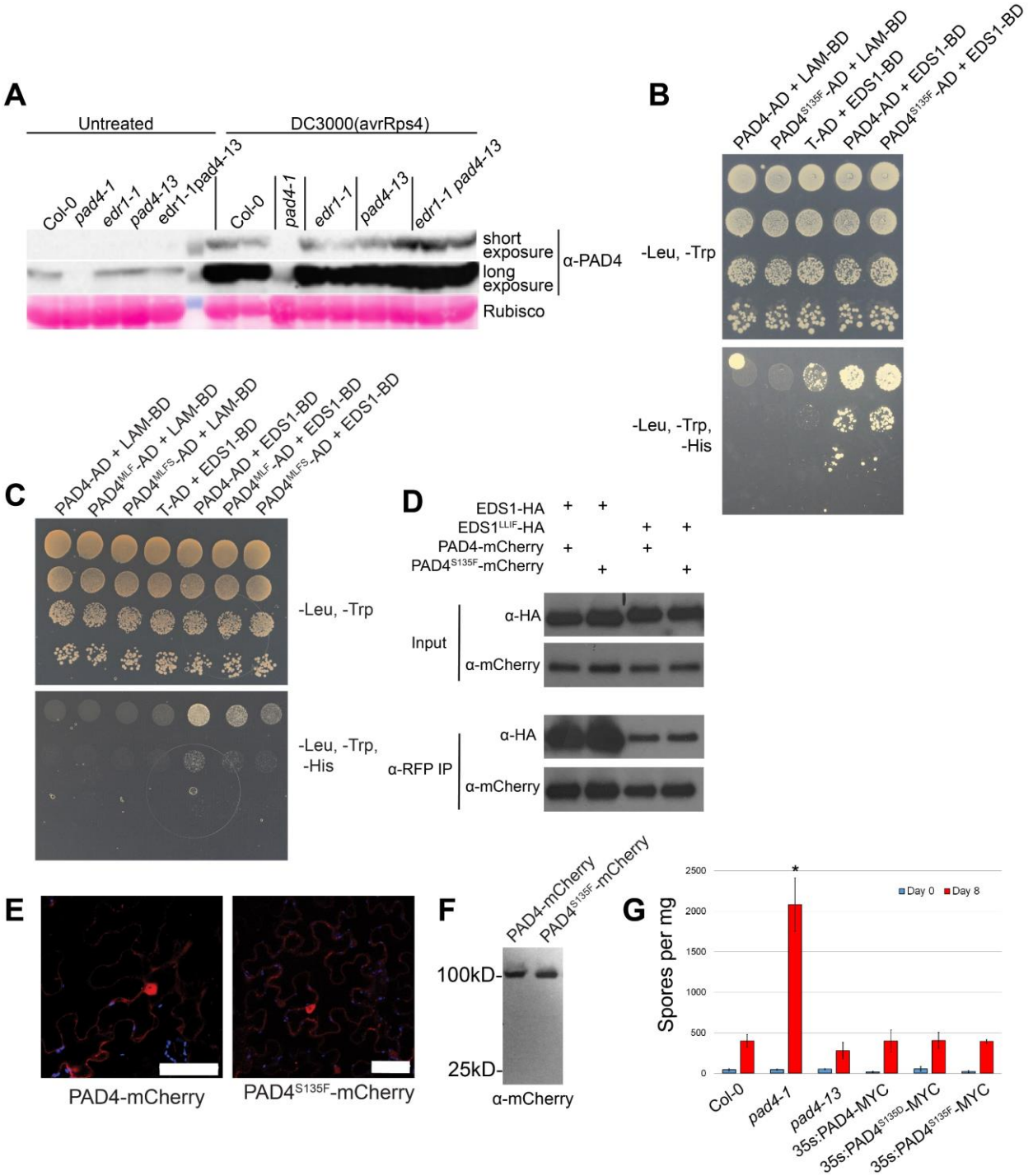

Figure 2-5. The S135F substitution in PAD4 does not affect its stability, interaction with EDS1, or subcellular localization pattern. **A,** PAD4 protein accumulates to similar levels in wild-type Col-0, *pad4-13*, *edr1* and double mutant Arabidopsis. Total protein was extracted from Arabidopsis rosette leaves that were either untreated or sprayed with *Pseudomonas syringae* DC3000(*avrRps4*), which induces PAD4 accumulation. **B,** PAD4^{S135F} interacts with EDS1 in a yeast two-hybrid assay. The indicated constructs were transformed into yeast strain AH109 (activation domain constructs, AD) and yeast strain Y187 (DNA binding domain constructs, BD) and the strains mated, with diploids plated on the indicated media. **C,** The S135F mutation does not enhance the ability of PAD4^{MLF} to interact with EDS1 in a yeast two-hybrid assay. The indicated constructs were transformed into yeast strain AH109 (activation domain constructs, AD) and yeast strain

Y187 (DNA binding domain constructs, BD) and the strains mated, with diploids plated on the indicated media. **D,** The S135F mutation does not increase the interaction between PAD4 and EDS1^{LLIF}. Constructs were expressed in *N. benthamiana* and protein immunoprecipitated using anti-RFP beads. **E,** PAD4^{S135F} displays a nucleocytoplasmic localization pattern indistinguishable from wild-type PAD4. The indicated constructs were transiently expressed in *N. benthamiana* and imaged using confocal microscopy. Scale bar = 50 µM. **F,** PAD4-mCherry and PAD4^{S135F}-mCherry accumulate at similar levels without free mCherry tag. Tissue from E was subjected to immunoblotting using an anti-mCherry antibody. **G,** PAD4^{S135D} and PAD4^{S135F} both can complement a *pad4-1* loss of function mutation. Four-week-old homozygous T3 Arabidopsis plants were infected with powdery mildew. Spore counts were taken immediately following infection and 8 dpi. Bars indicate the means ±SD of three biological replicates per genotype. Asterisk denotes a significant difference from wild-type Col-0 at 8 dpi using one-way ANOVA analysis ($P < 0.0001$). No other values differed significantly from wild-type Col-0 at 8 dpi, and there were no significant differences between any of the genotypes at 0 dpi.

Another possible explanation for the over-activity of PAD4^{S135F} is that it might have enhanced interaction with its partner, EDS1. The EDS1-PAD4 interaction is mediated principally by conserved residues in the partner N-terminal domains, respectively EDS1^{LLIF} and PAD4^{MLF} that form a hydrophobic groove (Wagner et al., 2013). In an Arabidopsis EDS1-PAD4 structural model based on the EDS1-SAG101 heterodimer crystal structure (Wagner et al., 2013), PAD4^{S135} is located in a loop close to, but facing away from the PAD4^{MLF} heterodimer contact site (Figure 2-6). We therefore assessed whether the S135F substitution in PAD4 affected its interaction with EDS1 in a yeast two-hybrid assay. We observed no obvious effect on the interaction (Figure 2-5B). In addition, we introduced the S135F mutation into the PAD4^{MLF} triple mutant, generating PAD4^{MLFS}. We found that the S135F mutation did not significantly enhance the weakened interaction between PAD4^{MLF} and EDS1 in yeast two-hybrid assays (Figure 2-5C). Similarly, we observed no change in the ability of PAD4^{S135F} to co-immunoprecipitate with EDS1 or with EDS1^{LLIF} compared to WT PAD4 (Figure 2-5D). These data indicate that the S135F mutation does not affect the ability of PAD4 to interact with EDS1.

Finally, we investigated whether the S135F mutation alters the localization of PAD4 in plant cells. Transient expression of PAD4-mCherry and PAD4^{S135F}-mCherry showed

that both proteins displayed a nucleocytoplasmic localization (Figure 2-5E). To verify that the observed localization was not the result of protein degradation, we performed immunoblotting, which also demonstrated a similar level of accumulation of the PAD4 and PAD4^{S135F} proteins (Figure 2-5F). We thus conclude that the S135F mutation does not alter PAD4 stability, localization, or its ability to interact with EDS1, but somehow still affects PAD4 function and signaling.

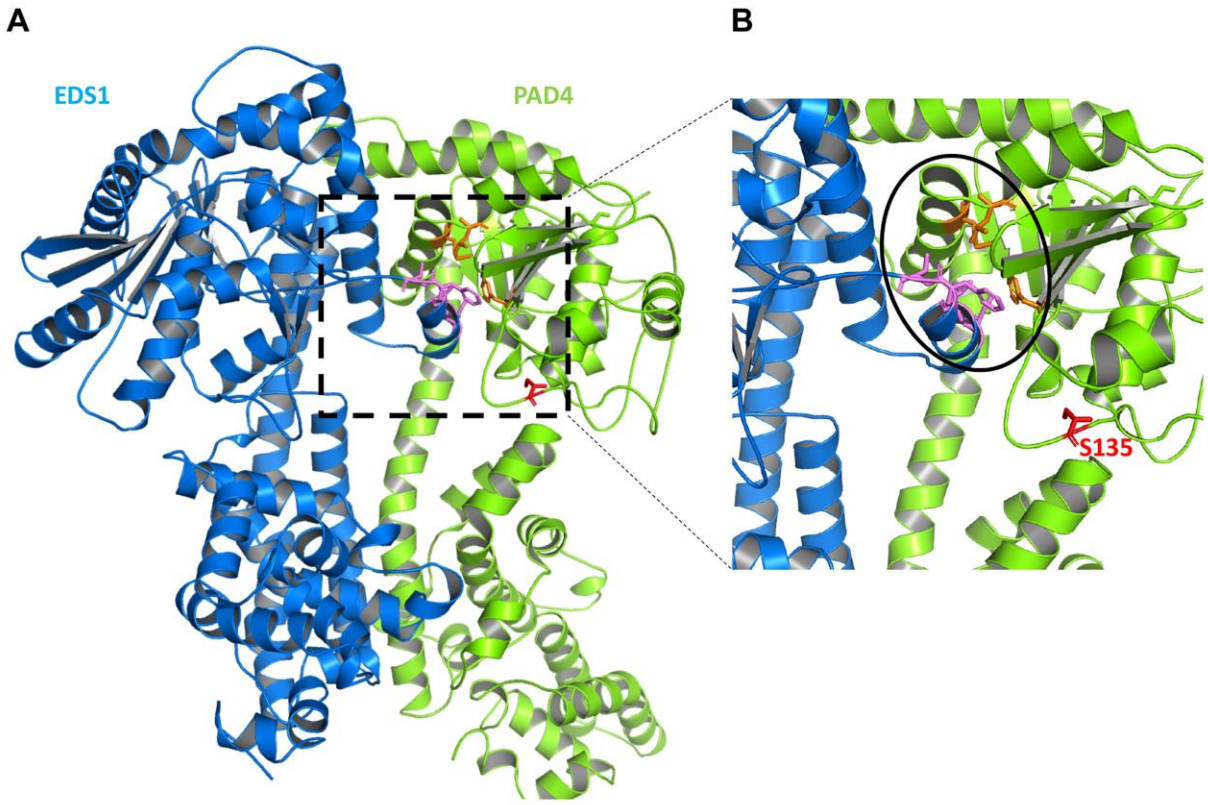

Figure 2-6. The S135F mutation in PAD4 is positioned away from the PAD4-EDS1 interaction surface. **A,** Cartoon representation of EDS1 (blue) and PAD4 (green) based on the EDS1-SAG101 structure (Wagner et al., 2013). **B,** Close-up of EDS1^{LLIF}-PAD4^{MLF} hydrophobic groove mediating N-terminal binding in the heterodimer. Key N-terminal domain residues that drive heterodimerization between EDS1 and PAD4 are shown as magenta and orange sticks, respectively. PAD4^{S135} (S135, red stick) is not in direct contact with the above residues and faces away from the binding groove. The S135F mutation is therefore unlikely to interfere with EDS1-PAD4 heterodimer formation. Substitution of the PAD4 polar serine (S) residue with a bulky phenylalanine (F) at this position might, however, cause structural reorganization that could affect EDS1-PAD4 signaling.

Phosphorylation of PAD4^{S135} is Unlikely to Negatively Regulate PAD4 Activity

Our data indicate that EDR1 functions as a negative regulator of EDS1/PAD4 signaling. As EDR1 has been demonstrated to have kinase activity (Tang and Innes, 2002), we hypothesized that EDR1-mediated regulation of EDS1/PAD4 is by direct phosphorylation. Therefore, we carried out IP-MS experiments in *N. benthamiana* using transient expression of Arabidopsis PAD4, EDS1, EDR1, and EDR1ST proteins. However, we were consistently unable to detect any phosphorylation of PAD4 or EDS1 in either the presence or absence of active EDR1. This result was repeated in three independent experiments. Importantly, the unphosphorylated S135-containing peptide was identified in all replicates, even though S135 is surface exposed in the structural model (Figure 2-6), making it potentially amenable for phosphorylation.

Although we could not detect EDR1-mediated phosphorylation of EDS1 or PAD4 in *N. benthamiana*, it remains a possibility that under specific conditions, EDR1 or some other kinase may regulate PAD4 via phosphorylation. Thus, we investigated whether the gain of function phenotype of S135F may be caused by the loss of an important phosphorylated serine residue. To test whether S135 is an important site of phosphorylation, we generated transgenic *pad4-1* PAD4^{S135D}-MYC phosphomimic Arabidopsis. If PAD4 is indeed negatively regulated by phosphorylation at S135, then the PAD4^{S135D}-MYC transgene should be unable to complement the *pad4-1* allele. However, we found that *pad4-1* plants were fully complemented by PAD4^{S135D}-MYC, PAD4-MYC, and PAD4^{S135F}-MYC expression in resistance to powdery mildew infection (Figure 2-5G). For this experiment, homozygous T3 plants were utilized. We observed a higher level of wild-type PAD4-MYC accumulation than that of PAD4^{S135D}-MYC and PAD4^{S135F}-MYC

(Figure 2-7). Despite accumulating to lower levels than WT PAD4, the PAD4^{S135D} and PAD4^{S135F} transgenes were equally able to complement the *pad4*-1 mutant phenotype (enhanced susceptibility). This result demonstrates that the gain of function phenotype of S135F is unlikely to be the result of blocking phosphorylation.

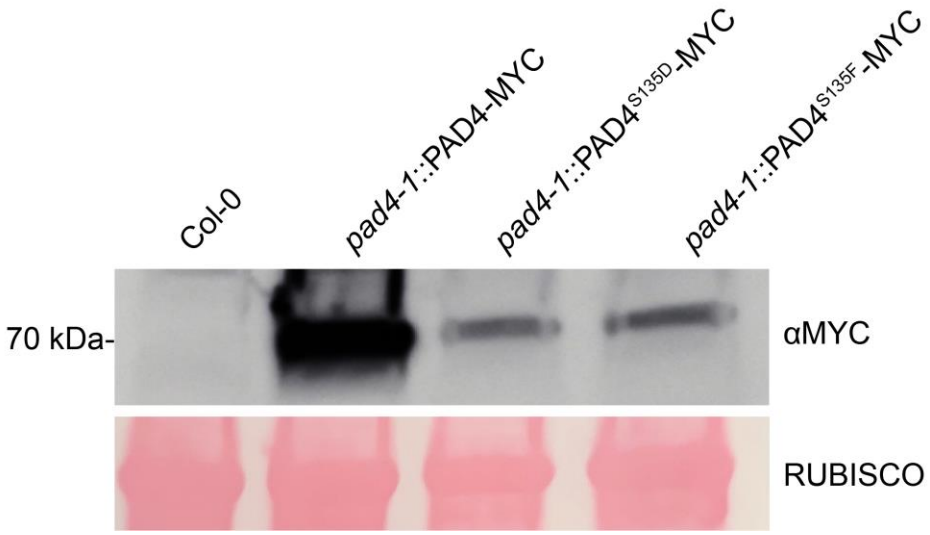

Figure 2-7. Accumulation of 5xMYC-tagged PAD4 protein from transgenic *pad4-1* plants was detected through immunoblotting. Total protein was extracted from 2-week-old homozygous T3 seedlings. Accumulation of PAD4-5xMYC was greater than that of PAD4^{S135D} and PAD4^{S135F}.

Discussion

Arabidopsis EDR1 acts as a negative regulator of cell death during both biotic and abiotic stress responses. Loss-of-function mutations in the *EDR1* gene confer enhanced disease resistance to powdery mildew infection and more rapid senescence than wild-type plants when exposed to ethylene (Frye and Innes, 1998; Frye et al., 2001; Tang et al., 2005). In this work, we report that a missense mutation in the *PAD4* gene (*pad4-13*) that causes an S135F substitution enhances *edr1*-dependent cell death after pathogen attack. Moreover, the *pad4-13* mutation alone confers enhanced disease resistance to the powdery mildew *G. cichoracearum* and accelerated cell death.

PAD4 is required for the accumulation of the signaling molecule SA (Jirage et al., 1999; Feys et al., 2005), and thus loss-of-function mutations in the *PAD4* gene severely compromise defense against biotrophic pathogens, including powdery mildew (Glazebrook et al., 1996; Gao et al., 2014). The *pad4-13* mutation, in contrast, enhances resistance to *G. cichoracearum*, indicating that this mutation causes a gain-of-function. Moreover, this enhanced disease resistance is accompanied by enhanced cell death (Figure 2-1B), similar to that observed in the *edr1* mutant (Frye and Innes, 1998). While the enhanced disease resistance is not additive in the *edr1-1 pad4-13* double mutant, the cell death is more extensive in the double mutant than in either of the single mutants, suggesting that *PAD4* and *EDR1* independently regulate the cell death pathway.

The enhanced disease resistance phenotype in both *edr1* and *pad4-13* without additive effects in the double mutant can be explained by both mutations causing a similar effect on SA signaling. Alternatively, $PAD4^{S135F}$ might be augmenting *edr1* cell death in parallel to SA, since PAD4 with EDS1 promotes both SA-dependent and SA-independent

pathways in basal and TIR-NLR-mediated resistance (Cui et al., 2018; Bhandari et al., 2019). We have shown that *pad4-13* does not alter PAD4 accumulation, localization, or interaction with EDS1 (Figure 2-5), yet it remains unclear what effect this mutation has on PAD4. While PAD4^{S135} is located close to the chief N-terminal PAD4^{MLF} interface with EDS1^{LLIF}, it is facing away from the interaction groove (Figure 2-6), consistent with the finding that the PAD4^{S135F} substitution does not obviously alter PAD4-EDS1 heterodimerization. It is possible that close proximity of PAD4^{S135F} to an α-helix of the PAD4 EP-domain (Figure 2-6) creates a loosening of N-terminal restraint on the PAD4 C-terminal signaling function. Recently, it has been demonstrated that EDS1/PAD4 functions to antagonize the activity of MYC2, a master regulator of JA signaling in TIR-NLR immunity (Cui et al., 2018). It is therefore a formal possibility that the S135F substitution enhances the interaction between PAD4 and MYC2, or some other unknown signaling partner.

Although we could not detect an enhanced interaction between PAD4^{S135F} and EDS1 using a yeast two-hybrid assay, we did observe that co-expression of EDR1 with EDS1 and PAD4 inhibited the EDS1-PAD4 interaction in a yeast three-hybrid assay. Furthermore, EDR1 interacts strongly with EDS1 and PAD4 in yeast, and in co-IPs from *N. benthamiana.* Collectively, these observations suggest that EDR1 functions, at least in part, to negatively regulate the interaction between EDS1 and PAD4. Because formation of an EDS1-PAD4 heterodimer is essential for the rapid transcriptional reprogramming of host defense pathways in pathogen resistance (Bhandari et al., 2019), EDR1 might exert important negative control on EDS1-PAD4 signaling activity in response to infection. In support of this model, mutations in either *EDS1* or *PAD4* block

edr1-mediated enhanced resistance and cell death (Frye et al., 2001). Furthermore, genes upregulated in the absence of EDR1 overlap significantly with genes upregulated by co-overexpression of EDS1 and PAD4 (Figure 2-4). Importantly, overexpression of either EDS1 or PAD4 alone does not upregulate these genes or enhance resistance (Cui et al., 2017), which indicates that it is the concentration of the EDS1- PAD4 complex, and not their individual protein levels, that determines the strength of defense signaling.

Materials and Methods

Plant Material and Growth Conditions

Arabidopsis thaliana accession Col-0, and Col-0 mutants *edr1-1* (Frye and Innes, 1998), *edr1-3* (salk_127158C), *pad4-13*, and *edr1-1 pad4-13* were used in this study. The *edr1-1* parental seed used for the suppressor mutagenesis was derived from a backcross 3 population. To confirm that the *pad4-13* mutation was present in this population, we sequenced *PAD4* amplified from multiple individuals of that population and found that the *pad4-13* mutation was segregating within the population. To assess whether the *pad4-13* mutation was present in our original *edr1-1* mutant, we sequenced *PAD4* in an *edr1-1* M6 population (8 individual plants) that had never been backcrossed. Surprisingly, none of these plants carried the *pad4-13* mutation, suggesting that the mutation had arisen spontaneously at some point during the backcrossing process. Consistent with this conclusion, an *edr1-1* population being used by a former lab member in China also lacks this mutation (D. Tang, personal communication).

To separate the *pad4-13* mutation from the *edr1-1* mutation, the double mutant line was backcrossed to wild-type Col-0 and F2 plants were screened for the presence of

these mutations by amplifying the mutant regions using PCR and sequencing. Individual F2 plants that were homozygous wild-type *EDR1* and homozygous mutant *pad4-13* were back-crossed to wild-type Col-0 three times to remove any other unlinked or loosely linked mutations. Similarly, individual F2 plants that were homozygous *edr1-1* and wild-type for *PAD4* were also backcrossed to wild-type Col-0 three times to isolate the *edr1-1* mutation.

Seeds were surface sterilized with 50% (v/v) bleach and planted on one-half-strength Murashige and Skoog plates supplemented with 0.8% agar and 1% sucrose. Plates were placed at 4ºC for 72 h for stratification and then transferred to a growth room set to 23ºC and 9 h light (150 µEm-2s-1)/15 h dark cycle. Seven-day-old seedlings were transplanted to MetroMix 360 (Sun Gro Horticulture) and grown for the indicated time for each experiment. For transient expression experiments, *Nicotiana benthamiana* was grown under the same growth room conditions as *A. thaliana*, but potted in Pro-Mix PGX Biofungicide plug and germination mix.

Quantifying Powdery Mildew Sporulation

G. cichoracearum strain UCSC1 was maintained on hyper-susceptible Arabidopsis *pad4-2* mutant plants. Inoculation was carried out as described in (Serrano et al., 2014). Briefly, four-week-old plants were inoculated using a settling tower approximately 0.8 m tall and covered with a 100 micron Nitex mesh screen. Plants with a heavy powdery mildew infection (leaves covered in white powder due to production of asexual spores) were passed over the mesh to transfer the conidiospores to the plants below. Twelve *pad4-2* mutant plants were used for inoculating each tray of 60 plants. Conidiospores were counted as described in (Serrano et al., 2014). Briefly, after inoculation, the

conidiospores were allowed to settle for 30 min and three leaves per genotype were harvested, weighed, and transferred to 1.5- ml microcentrifuge tubes. 500 µl of dH_2O were added and conidiospores were liberated by vortexing 30 s at maximum speed. Leaves were removed and conidiospores were concentrated by centrifugation at 4000 g for 5 min. For each sample, conidiospores were counted in eight 1 mm^2 fields of a Neubauer-improved haemocytometer (Marienfeld, Lauda-Königshofen, Germany). Spore counts were normalized to the initial weight of the leaves and results were averaged. The same procedure was repeated 8 days post inoculation (dpi).

Quantifying Cell Death

Staining with trypan blue was performed essentially as described by (Serrano et al., 2010). Arabidopsis plants were inoculated with *G. cichoracearum* as described above, leaves collected at 5 dpi, and boiled in alcoholic lactophenol (ethanol:lactophenol 1:1 v/v) containing 0.1 mg ml^{-1} trypan blue (Sigma) for 1 min. Leaves were then destained using a chloral hydrate solution (2.5 mg ml^{-1}) at room temperature overnight. Samples were observed under a Zeiss Axioplan microscope. To quantify cell death, 6 pictures of each of five experimental repetitions were randomly selected (n=30) and total leaf area and trypan-stained area were measured using ImageJ (Bethesda, MD, USA), and the percentage (area of cell death/ total leaf area) was calculated. Cell death measurements are provided as means with 10th and 90th percentiles (box) and range (whiskers).

Plasmid Construction and Generation of Transgenic Arabidopsis Plants

EDS1^{LLIF} and PAD4^{MLF} clones used in this study were derived from pENTR cDNA clones (Bhandari et al., 2019). Site-directed mutagenesis was utilized to introduce the PAD4^{S135F} mutation into PAD4^{MLF}, generating PAD4^{MLFS}. All primers used in this study for cloning and site-directed mutagenesis are listed in Table 2-1.

For yeast-two hybrid assays, the full-length open reading frames of EDR1, EDR1 (D810A), and EDS1 were cloned into the DNA-binding domain vector pGBKT7 (Clontech Matchmaker System). The full-length open reading frame of PAD4, PAD4^{MLF}, PAD4^{MLFS}, and EDS1 were cloned into the activation domain vector pGADT7. The SV40 Large T Antigen (T) and Lamin (LAM) cloned into pGADT7 and pGBKT7 respectively, were used as negative controls.

For yeast three-hybrid assays, EDS1 and RIN4b cDNA sequences were inserted into multiple cloning site I of the pBridge vector (Clontech) using the SmaI and SalI restriction sites (separate constructs). The EDR1 kinase domain (amino acids 587-933) and EDR1 kinase domain substrate trap mutant form (EDR1^{D810A}) were cloned into multiple cloning site II of the pBridge vector using NotI and BglII restriction sites. PAD4 cDNA was inserted into the pGADT7 (Clontech) plasmid using NdeI and SmaI restriction sites. To clone AvrB into pGADT7, NdeI and BamHI restriction sites were used.

For EDR1 yeast two-hybrid experiments, EDR1 full-length wild-type cDNA and EDR1ST (D810A) was cloned into pGBKT7 using SmaI and SalI restriction sites. EDS1 and PAD4 were cloned into pGADT7 using NdeI and SmaI restriction sites.

For transient expression in *N. benthamiana,* PAD4-mCherry, PAD4^{S135F}-mCherry, EDS1-3xHA, EDS1^{LLIF}-3xHA, and 5xMYC-sYFP were cloned into the cauliflower mosaic

virus 35S promoter vector pEarleyGate100 (Earley et al., 2006) using a modified multisite Gateway recombination cloning system (Invitrogen) as described in (Qi et al., 2012). PAD4-cYFP and EDS1-nYFP were cloned into the dexamethasone-inducible vectors pTA7001-DEST (Aoyama and Chua, 1997) and pBAV154 (Vinatzer et al., 2006), respectively, using multisite Gateway cloning. EDR1-sYFP and EDR1ST-sYFP were also cloned into pBAV154 using multisite Gateway cloning.

Transgenic *pad4-1* plants expressing PAD4-5xMYC, PAD4^{S135D}-5xMYC, and PAD4^{S135F}-5xMYC were generated using the floral dip method (Clough and Bent, 1998). PAD4^{S135D} clones were generated using site-directed mutagenesis of PAD4 cDNA. PAD4, PAD4^{S135D}, and PAD4^{S135F} full-length cDNA tagged with 5xMYC were cloned into the pEarleyGate100 vector (Earley et al., 2006) using multisite Gateway cloning. Plasmids were transformed into Agrobacterium strain GV3101 (pMP90) by electroporation with selection on Luria-Bertani plates containing 50 µg/mL kanamycyin sulfate (Sigma-Aldrich) and 20 µg/mL gentamycin (Gibco). Selection of transgenic plants was performed by spraying 1-week old seedlings with 300 µM BASTA (Finale). Protein expression was verified via immunoblot using mouse anti-MYC-HRP antibody (ThermoFisher).

Yeast Two-Hybrid and Yeast Three-Hybrid Assays

For yeast two-hybrid assays between EDR1 and PAD4 or EDS1, pGBKT7 and pGADT7 clones were transformed into haploid yeast strain AH109 (Clontech) by electroporation, and selected on SD-Trp-Leu medium. For yeast two-hybrid assays between EDS1 and PAD4, the full-length EDS1 open reading frame was cloned into an

empty pBridge vector. Full-length PAD4, PAD4^{S135F}, PAD4^{MLF}, and PAD4^{MLFS} open reading frames were cloned into pGADT7. Yeast strain AH109 was transformed with pGADT7 vectors by electroporation and transformants were selected on SD-Leu. Yeast strain Y187 was transformed with pBridge plasmids by electroporation and transformants were elected on SD-Trp.

For yeast three-hybrid assays, EDR1-KD and EDR1-KDST were cloned into pBridge vectors, under the control of the MET25 promoter. EDS1 and RIN4b were cloned into pBridge. PAD4, PAD4^{S135F}, and AvrB were cloned into pGADT7. Yeast strains AH109 and Y187 were transformed with pGADT7 and pBridge, respectively.

Matings between the Y187 and AH109 strains carrying the appropriate constructs were performed in yeast peptone dextrose medium at 30°C for 16 hours. Mating cultures were then diluted and plated on SD-Trp-Leu. Before carrying out yeast two-hybrid or three-hybrid assays, yeast were grown for 16 hours at 30ºC. Cultures were re-suspended in water to an OD_{600} of 1.0, serially diluted, and plated on appropriate SD media. Plates were allowed to grow for up to 5 days at 30ºC.

β-Galactosidase Assays

β-galactosidase assays using ortho-Nitrophenyl-β-galactoside (ONPG) were performed as described in the Clontech Yeast Protocols Handbook 2009. Diploid yeast was grown overnight in SD–Leu-Trp at 30ºC. A subculture was made by adding 4 mL of fresh SD–Leu-Trp to 1 mL of the overnight culture. The subculture was grown at 30ºC until OD_{600} reached 0.3. Cells were pelleted and re-suspended in Z buffer. A 100 µL fraction was then subjected to three cycles of freezing in liquid nitrogen and thawing in a

37ºC water bath. 700 µL of Z buffer containing β-mercaptoethanol was then added. 170 µL Z buffer with ONPG was then added to each reaction. Samples were incubated at 30°C for up to 24 hours. OD_{600} and OD_{420} readings were taken and β-Gal units calculated.

Immunoprecipitations and Immunoblots

For total protein extraction, four leaves of infiltrated *N. benthamiana* were collected, frozen with liquid nitrogen, and ground in lysis buffer (50 mM Tris-HCl, pH 7.5, 150 mM NaCl, 1% Nonidet P-40, 1% Plant Proteinase Inhibitor Cocktail [Sigma], and 50 mM 2,2′-Dithiodipyridine [Sigma]) or, for co-IPs, IP Buffer (50 mM Tris, pH 7.5, 150 mM NaCl, 50 mM NaF, 50 mM Na-β-glycerophosphate, pH 7.4, 2 mM EGTA, 1mM EDTA, 0.1% Nonidet P-40, 0.1% Triton X-100, 10% glycerol, 1% Plant Proteinase Inhibitor Cocktail [Sigma], and 50 mM 2,2′-Dithiodipyridine [Sigma]). Samples were centrifuged at 10,000 g at 4°C for 5 minutes, and supernatants were transferred to new tubes.

Immunoprecipitations were performed as described previously (Shao et al., 2003) using GFP-Trap_A and RFP-Trap beads (Chromotek). Total proteins were mixed with 1 volume of 2x Laemmli sample buffer [Bio-Rad], supplemented with 5% β-mercaptoethanol, 1% Protease Inhibitor Cocktail [Sigma], and 50 mM 2,2′-Dithiodipyridine [Sigma]). Samples were then boiled for 5 min before loading. Total proteins and/or immunocomplexes were separated by electrophoresis on a 4-20% Mini-PROTEAN TGX Stain-Free protein gel (Bio-Rad). Proteins were transferred to a nitrocellulose membrane and probed with anti-HA-HRP (Sigma,), anti-mCherry-HRP (Santa Cruz), mouse anti-GFP (Invitrogen), and goat anti-mouse-HRP antibodies (Invitrogen).

For protein extraction from yeast, yeast grown on solid -Leu, -Trp plates were resuspended in lysis buffer (100 mM NaCl, 50 mM Tris-Cl, pH 7.5, 50 mM NaF, 50 mM Na-β-glycerophosphate, pH 7.4, 2 mM EGTA, 2 mM EDTA, 0.1% Triton X-100, 1 mM Na_3VO_4). Glass beads were then added to the suspension and the solution was vortexed three times for 1 minute. Samples were then boiled for 10 minutes. Immunoblots were performed using anti-HA-HRP (Sigma), mouse anti-GAL4DBD (RK5C1) (Santa Cruz Biotechnology), rabbit anti-EDS1 (Agisera), goat anti-mouse-HRP (abcam), and goat anti-rabbit-HRP (abcam) antibodies. Visualization of immunoblots from yeast strains used in three-hybrid assay were performed using the KwikQuant Imager (Kindle Biosciences).

Transcriptome Analysis

The *edr1* dataset was based upon previously generated microarray data of *edr1* plants 18 hours post inoculation with powdery mildew (Christiansen et al., 2011; GEO Accession GSE26679). Upregulated genes were identified as having higher expression in *edr1* plants compared to wildtype plants (p value < 0.05) using the NCBI GEO2R tool (Edgar et al., 2002). GENE IDs were converted to TAIR using the DAVID Gene ID Conversion Tool (Huang et al., 2008). The EDS1-PAD4 dataset was based upon 155 genes previously identified as being significantly upregulated due to EDS1 and PAD4 coexpression (Cui et al., 2017). Comparison of the *edr1* and PAD4-EDS1 datasets was performed using the Venny 2.1 tool (Oliveros, 2007). Gene Ontology enrichment analysis was performed using PANTHER gene list analysis (Mi et al., 2019).

Co-Expression of EDR1, PAD4, and EDS1 for Mass Spectrometry

To detect phosphorylation of PAD4 or EDS1 via EDR1, PAD4-mCherry and EDS1-3xHA, were transiently co-expressed with either EDR1 or EDR1-ST(D810A)-sYFP in *N. benthamiana*. 24 hours after agrobacterium infiltration, plants were sprayed with dexamethasone to induce EDR1 and EDR1-ST expression. Immunoprecipitation and gel electrophoresis was carried out as noted above using RFP-trap (Chromotek) beads. Following gel electrophoresis, PAD4-mCherry and EDS1-HA bands were visualized using UV light, and excised. EDS1-HA and PAD4-mCherry bands were then sent for MS analysis.

Gel bands were diced into 1 mm cubes and incubated for 45 min at 57 °C with 2.1 mM dithiothreitol to reduce cysteine residue side chains. These side chains were then alkylated with 4.2 mM iodoacetamide for 1 h in the dark at 21 °C. Proteins were digested with either trypsin, chymotrypsin, or pepsin. For the trypsin digestion, a solution containing 1 µg trypsin, in 25 mM ammonium bicarbonate was added and the samples were digested for 12 hours at 37 °C. For the chymotrypsin digestion, a solution containing 1 µg chymotrypsin, in 25 mM ammonium bicarbonate was added and the samples were digested for 12 hours at 25 °C. For the pepsin digestion, a solution containing 0.5 µg of pepsin in 5% formic acid was added and the samples were digested for 12 hours at 21°C. The resulting peptides were desalted using a ZipTip (Millipore, Billerica MA). The samples were dried down and injected into an EasyNano HPLC coupled to an Orbitrap Fusion Lumos mass spectrometer (Thermo Fisher Scientific, Waltham MA) operating in data dependent MS/MS selection mode. The peptides were separated using a 75 micron, 25 cm column packed with C18 resin

(Thermo Fisher Scientific, Waltham MA) at a flow rate of 300 nl/min. A one hour gradient was run from Buffer A (0.1% formic acid) to 60% Buffer B (100% acetonitrile, 0.1% formic acid).

Table 2-1. Primers used in this study.

Name	Purpose	Sequence (5' to 3')
T7 F	Sequencing Y2H plasmids	TAATACGACTCACTATAGGGC
PGADT7 INS R	Sequencing Y2H plasmids	AGATGGTGCACGATGCACAG
PGBKT7 INS R	Sequencing Y2H plasmids	TAGCTTGGCTGCAAGCGCGC
pBridge Ins F	Sequencing Y3H plasmids	GACAGCATAGAATAAGTGCG
pBridge Ins R	Sequencing Y3H plasmids	CCTGACCTACAGGAAAGAG
AvrB NdeI F	For PGADT7	GCGCCATATGATGGGCTGCGTCTCGTCA
AvrB BamHI R	For PGADT7	GCGCGGATCCTTAAAAGCAATCAGAATC
EDS1 NdeI F	For PGADT7	CGCGCATATGATGGCGTTTGAAGCTCTTACC
EDS1 XhoI R	For PGADT7	CGCGCTCGAGTCAGGTATCTGTTATTTCATC
PAD4 NdeI F	For PGADT7	CGCGCATATGATGGACGATTGTCGATTC
PAD4 SmaI R	For PGADT7	CGCGCCCGGGCTAAGTCTCCATTGCGTC
EDS1 SmaIF	For PGBKT7 and pBridge	CGCGCCCGGGCATGGCGTTTGAAGCTCTT
EDS1 SalIR	For PGBKT7 and pBridge	CGCGGTCGACTCAGGTATCTGTTATTTC
EDR1 SmaI F	For PGBKT7	GAGCCCGGGGATGAAGCATATTTTCAAGAAGC
EDR1 SalI R	For PGBKT7	ACCGGTCGACCTATTGTGGTGTAGGAAGTACA
RIN4B SmaI F	For pBridge	GCGCCCCGGGGATGGCACAACGTTCTCATG
RIN4B SalI R	For pBridge	GCGCGTCGACTCATTTTTTCCCACCCCA
NotI-EDR1-KD F	For pBridge	GATCAC GCG GCC GCA TGTGAAATTCCTTGGAATGATC
BglII-EDR1-KD R	For pBridge	GATCAC AGA TCT CTATTGTGGTGTAGGAAGTAC
PAD4S135F F	Mutagenesis	TTTGGCTTCTATCTCAATTTTCTCCGCCGTCATTCC
PAD4S135F R	Mutagenesis	GGAATGACGGCGGAGAAAATTGAGATAGAAGCCAAA
PAD4S135A F	Mutagenesis	GGCTTCTATCTCAAGCTTCTCCGCCGTCATTCCGCG
PAD4S135A R	Mutagenesis	GACGGCGGAGAAGCTTGAGATAGAAGCCAAAGTGCG
PAD4S135D F	Mutagenesis	TTTGGCTTCTATCTCAAGATTCTCCGCCGTCATTCCGCG
PAD4S135D R	Mutagenesis	CGCGGAATGACGGCGGAGAATCTTGAGATAGAAGCCAAA
EDS1attb1	Gateway Cloning	GGGGACAAGTTTGTACAAAAAAGCAGGCTCGATGGCGTTTGAAGCTCTT
EDS1attb4	Gateway Cloning	GGGGACAACTTTGTATAGAAAAGTTGGGTGGGTATCTGTTATTTCATC
PAD4attb1	Gateway Cloning	GGGGACAAGTTTGTACAAAAAAGCAGGCTCGATGGACGATTGTCGATT C
PAD4attb4	Gateway Cloning	GGGGACAACTTTGTATAGAAAAGTTGGGTGAGTCTCCATTGCGTCACT
PAD4 BSMFI F	Genotyping	GCGATGCATCAGAAGAG
PAD4 BSMFI R	Genotyping	TAGCCCAAAAGCAAGTATC
PAD4MF	Genotyping	TTGTACTCTCAGAAGGAAGGT
PAD4MR	Genotyping	CCTCCTTTGTCGGAACAGAAC

Literature Cited

Aarts, N., Metz, M., Holub, E., Staskawicz, B. J., Daniels, M. J., and Parker, J. E. 1998. Different requirements for EDS1 and NDR1 by disease resistance genes define at least two R gene-mediated signaling pathways in Arabidopsis. Proc. Natl. Acad. Sci. U.S.A. **95**:10306-10311.

Aoyama, T., and Chua, N.H. 1997. A glucocorticoid-mediated transcriptional induction system in transgenic plants. Plant J. **11**:605–612.

Bhandari, D.D., Lapin, D., Kracher, B., von Born, P., Bautor, J., Niefind, K., and Parker, J.E. 2019. An EDS1 heterodimer signalling surface enforces timely reprogramming of immunity genes in Arabidopsis. Nat. Commun. **10**:772.

Chandra-Shekara, A.C., Venugopal, S.C., Barman, S.R., Kachroo, A., and Kachroo, P. 2007. Plastidial fatty acid levels regulate resistance gene-dependent defense signaling in Arabidopsis. Proc. Natl. Acad. Sci. U.S.A. **104**:7277–7282.

Christiansen, K.M., Gu, Y., Rodibaugh, N., and Innes, R.W. 2011. Negative regulation of defence signaling pathways by the EDR1 protein kinase. Mol. Plant Pathol. **12**:746–758.

Clough, S.J., and Bent, A.F. 1998. Floral dip: a simplified method for Agrobacterium-mediated transformation of *Arabidopsis thaliana*. Plant J. **16**: 735–743.

Cui, H., Gobbato, E., Kracher, B., Qiu, J., Bautor, J., and Parker, J.E. 2017. A core function of EDS1 with PAD4 is to protect the salicylic acid defense sector in Arabidopsis immunity. New Phytol. **213**:1802-1817.

Cui, H., Qiu, J., Zhou, Y., Bhandari, D.D., Zhao, C., Bautor, J., and Parker, J. E. 2018. Antagonism of transcription factor MYC2 by EDS1/PAD4 complexes bolsters salicylic acid defense in Arabidopsis effector-triggered immunity. Mol. Plant **11**:1053-1066.

Earley, K.W., Haag, J. R., Pontes, O., Opper, K., Juehne, T., Song, K., and Pikaard, C.S. 2006. Gateway-compatible vectors for plant functional genomics and proteomics. Plant J. **45**:616–629.

Edgar, R., Domrachev, M., Lash, A.E. 2002. Gene Expression Omnibus: NCBI gene expression and hybridization array data repository Nucl. Acids Res. **30**:207-210.

Feys, B.J., Moisan, L.J., Newman, M.A., and Parker, J.E. 2001. Direct interaction between the Arabidopsis disease resistance signaling proteins, EDS1 and PAD4. EMBO J. **20**:5400–5411.

Feys, B.J., Wiermer, M., Bhat, R.A., Moisan, L.J., Medina-Escobar, N., Neu, C., Cabral, A., and Parker, J.E. 2005. Arabidopsis SENESCENCE-ASSOCIATED GENE101 stabilizes and signals within an ENHANCED DISEASE SUSCEPTIBILITY1 complex in plant innate immunity. Plant Cell **17**:2601–2613.

Frye, C.A., and Innes, R.W. 1998. An Arabidopsis mutant with enhanced resistance to powdery mildew. THE PLANT CELL ONLINE. **10**:947–956.

Frye, C.A., Tang, D., and Innes, R.W. 2001. Negative regulation of defense responses in plants by a conserved MAPKK kinase. Proc. Natl. Acad. Sci. U.S.A. **98**:373–378.

Gao, F., Dai, R., Pike, S.M., Qiu, W., and Gassmann, W. 2014. Functions of EDS1-like and PAD4 genes in grapevine defenses against powdery mildew. Plant Mol. Biol. **86**:381–393.

Gantner, J., Ordon, J., Kretschmer, C., Guerois, R., and Stuttmann, J. 2019. An EDS1-SAG101 complex is essential for TNL-mediated immunity in *Nicotiana benthamiana*. Plant Cell **31**:2456-2474.

Geissler, K., Eschen-Lippold, L., Naumann, K., Schneeberger, K., Weigel, D., Scheel, D., Rosahl, S., and Westphal, L. 2015. Mutations in the EDR1 gene alter the response of *Arabidopsis thaliana* to *Phytophthora infestans* and the bacterial PAMPs flg22 and elf18. Mol. Plant-Microbe Interact. **28**:122–133.

Glazebrook, J., Rogers, E.E., and Ausubel, F.M. 1996. Isolation of Arabidopsis mutants with enhanced disease susceptibility by direct screening. Genetics **143**:973-982.

Glazebrook, J., Zook, M., Mert, F., Kagan, I., Rogers, E.E., Crute, I.R., Holub, E.B., Hammerschmidt, R., and Ausubel, F.M. 1997. Phytoalexin-deficient mutants of Arabidopsis reveal that PAD4 encodes a regulatory factor and that four PAD genes contribute to downy mildew resistance. Genetics. **146**:381–392.

Gu, Y., and Innes, R.W. 2011. The KEEP ON GOING protein of Arabidopsis recruits the ENHANCED DISEASE RESISTANCE1 protein to trans-Golgi network/early endosome vesicles. Plant Physiol. **155**:1827–1838.

Hiruma, K., and Takano, Y. 2014. Roles of EDR1 in non-host resistance of Arabidopsis. Plant Signal. Behav. **6**:1831–1833.

Hiruma, K., Nishiuchi, T., Kato, T., Bednarek, P., Okuno, T., Schulze-Lefert, P., and Takano, Y. 2011. Arabidopsis ENHANCED DISEASE RESISTANCE 1 is required for pathogen-induced expression of plant defensins in nonhost resistance, and acts through interference of MYC2-mediated repressor function. Plant J. **67**:980–992.

Hu, G., deHart, A.K., Li, Y., Ustach, C., Handley, V., Navarre, R., Hwang, C.F., Aegerter, B.J., Williamson, V.M., and Baker, B. 2005. EDS1 in tomato is required for resistance mediated by TIR-class R genes and the receptor-like R gene Ve. Plant J. **42**:376-391.

Huang, D., Sherman, B.T., Stephens, R., Baseler, M.W., Lane, H.C., & Lempicki, R.A. 2008. DAVID gene ID conversion tool. Bioinformation, **2**:428–430.

Jirage, D., Tootle, T.L., Reuber, T.L., Frost, L.N., Feys, B.J., Parker, J.E., Ausubel, F.M., and Glazebrook, J. 1999. *Arabidopsis thaliana* PAD4 encodes a lipase-like gene that is important for salicylic acid signaling. Proc. Natl. Acad. Sci. U.S.A. **96**:13583–13588.

Lapin, D., Kovacova, V., Sun, X., Dongus, J. A., Bhandari, D., von Born, P., Bautor, J., Guarneri, N., Rzemieniewski, J., Stuttmann, J., Beyer, A., and Parker, J. E. 2019. A coevolved EDS1-SAG101-NRG1 module mediates cell death signaling by TIR-domain immune receptors. Plant Cell **31**:2430-2455.

Lipka, V., Dittgen, J., Bednarek, P., Bhat, R., Wiermer, M., Stein, M., Landtag, J., Brandt, W., Rosahl, S., Scheel, D., Llorente, F., Molina, A., Parker, J., Somerville, S., and Schulze-Lefert, P. 2005. Pre- and postinvasion defenses both contribute to nonhost resistance in Arabidopsis. Science **310**:1180–1183.

Maekawa, T., Kufer, T.A., and Schulze-Lefert, P. 2011. NLR functions in plant and animal immune systems: so far and yet so close. Nat. Immunol. **12**:817–826.

Mi, H., Muruganujan, A., Ebert, D., Huang, X., Thomas, P.D. 2019. PANTHER version 14: more genomes, a new PANTHER GO-slim and improvements in enrichment analysis tools. Nucl. Acids Res. **47**:D419-D426.

Oliveros, J.C. (2007–2017) Venny. An interactive tool for comparing lists with Venn's diagrams, Madrid, Spain. URL http://bioinfogp.cnb.csic.es/tools/venny/index.html.

Qi, D., DeYoung, B.J., and Innes, R.W. 2012. Structure-function analysis of the coiled-coil and leucine-rich repeat domains of the RPS5 disease resistance protein. Plant Physiol. **158**:1819–1832.

Rietz, S., Stamm, A., Malonek, S., Wagner, S., Becker, D., Medina-Escobar, N., Vlot, A.C., Feys, B.J., Niefind, K., and Parker, J.E. 2011. Different roles of ENHANCED DISEASE SUSCEPTIBILITY1 (EDS1) bound to and dissociated from PHYTOALEXIN DEFICIENT4 (PAD4) in Arabidopsis immunity. New Phytol. **191**:107–119.

Serrano, I., Gu, Y., Qi, D., Dubiella, U., and Innes, R.W. 2014. The Arabidopsis EDR1 protein kinase negatively regulates the ATL1 E3 ubiquitin ligase to suppress cell death. Plant Cell. **26**:4532–4546.

Serrano, I., Irene, S., Pelliccione, S., Salvatore, P., Olmedilla, A., and Adela, O. 2010. Programmed-cell-death hallmarks in incompatible pollen and papillar stigma cells of *Olea europaea* L. under free pollination. Plant Cell Rep. **29**:561–572.

S**hao, F., Golstein, C., Ade, J., Stoutemyer, M., Dixon, J.E., and Innes, R.W.** 2003. Cleavage of Arabidopsis PBS1 by a bacterial type III effector. Science **301**:1230–1233.

Tang, D., and Innes, R.W. 2002. Overexpression of a kinase-deficient form of the EDR1 gene enhances powdery mildew resistance and ethylene-induced senescence in Arabidopsis. Plant J. **32**:975-983.

Tang, D., Christiansen, K.M., and Innes, R.W. 2005. Regulation of plant disease resistance, stress responses, cell death, and ethylene signaling in Arabidopsis by the EDR1 protein kinase. Plant Physiol **138**:1018-1026.

Venugopal, S. C., Jeong, R.-D., Mandal, M. K., Zhu, S., Chandra-Shekara, A. C., Xia, Y., Hersh, M., Stromberg, A. J., Navarre, D., Kachroo, A., and Kachroo, P. 2009. ENHANCED DISEASE SUSCEPTIBILITY 1 and salicylic acid act redundantly to regulate resistance gene-mediated signaling. PLoS Genet. **5**:e1000545.

Vinatzer, B. A., Teitzel, G. M., Lee, M.-W., Jelenska, J., Hotton, S., Fairfax, K., Jenrette, J., and Greenberg, J. T. 2006. The type III effector repertoire of Pseudomonas syringae pv. syringae B728a and its role in survival and disease on host and non-host plants. Mol. Microbiol. **62**:26–44.

Wagner, S., Stuttmann, J., Rietz, S., Guerois, R., Brunstein, E., Bautor, J., Niefind, K., and Parker, J. E. 2013. Structural basis for signaling by exclusive EDS1 heteromeric complexes with SAG101 or PAD4 in plant innate immunity. Cell Host Microbe **14**:619-630.

Wawrzynska, A., Christiansen, K.M., Lan, Y., Rodibaugh, N.L., and Innes, R.W. 2008. Powdery mildew resistance conferred by loss of the ENHANCED DISEASE RESISTANCE1 protein kinase is suppressed by a missense mutation in KEEP ON GOING, a regulator of abscisic acid signaling. Plant Physiol. **148**:1510–1522.

Wituszynska, W., Slesak, I., Vanderauwera, S., Szechynska-Hebda, M., Kornas, A., Van Der Kelen, K., Mühlenbock, P., Karpinska, B., Mackowski, S., Van Breusegem, F., and Karpinski, S. 2013. LESION SIMULATING DISEASE1, ENHANCED DISEASE SUSCEPTIBILITY1, and PHYTOALEXIN DEFICIENT4 conditionally regulate cellular signaling homeostasis, photosynthesis, water use efficiency, and seed yield in Arabidopsis. Plant Physiol. **161**:1795–1805.

Xiao, S., Ellwood, S., Calis, O., Patrick, E., Li, T., Coleman, M., and Turner, J. G. 2001. Broad-spectrum mildew resistance in Arabidopsis thaliana mediated by RPW8. Science **291**:118–120.

Zhou, N., Tootle, T.L., Tsui, F., Klessig, D.F., and Glazebrook, J. 1998. PAD4 functions upstream from salicylic acid to control defense responses in Arabidopsis. Plant Cell. **10**:1021-1030.

Chapter 3: The Arabidopsis N-terminal Acetyltransferase NAA50 Regulates Plant Growth and Defense

(Matthew P. Neubauer and Roger W. Innes, *In review*)

Introduction

As sessile organisms, plants frequently encounter and respond to stress conditions such as drought, salinity, heat, and microbial infection. Various adaptations enable plants to defend themselves against these stresses, however, they often come at a significant cost (Cipollini et al., 2014). Plant defense responses require significant sacrifices by infected cells and tissues, which can negatively impact plant growth. The Hypersensitive Response (HR), a form of programmed cell death, is a primary mode of defense for infected plant cells (Greenberg and Yao, 2004). Thus, plants must carefully tailor their defense responses to conserve energy for growth and reproduction (Huot et al., 2014). This tradeoff is exhibited by enhanced resistance mutants such as *snc1-1* and *cpr1* which have constitutively active defense responses and are dwarfed (Li et al. 2001; Bowling et al., 1994).

Stress responses place strain upon the cellular machinery, which can result in endoplasmic reticulum (ER) stress (Bao and Howell, 2017). ER stress can occur during biotic or abiotic stress, as well as during normal developmental processes that place increased demands on the protein translation and protein secretion machinery (Vitale and Boston, 2008). Response to ER stress is mediated by the unfolded protein response (UPR), which occurs in two phases. The first phase aims to alleviate ER stress through

increased expression of chaperones, removal and degradation of misfolded proteins from the ER, and reduction of protein translation (Williams et al., 2014; Liu and Howell, 2010). If these attempts are unsuccessful, the UPR transitions into a pro-apoptotic phase (Woehlbier and Hetz, 2011; Walter and Ron, 2011; Srivastava et al., 2018). Recent studies have demonstrated that UPR genes are required for plant growth and development (Kim et al., 2018; Bao et al., 2019). On the other hand, mutations that constitutively activate the UPR cause dwarfism (Iwata et al., 2018). Just as stress responses to external stimuli must be regulated to ensure proper growth and development, so must responses to internal stress and the UPR.

We have previously identified and characterized the *EDR1* gene and demonstrated its role in negatively regulating plant stress response signaling (Frye and Innes, 1998; Christiansen et al., 2011; Serrano et al., 2014). In particular, *EDR1* negatively regulates the salicylic acid (SA) and ethylene pathways (Frye et al., 2001; Tang et al., 2005). Mutant *edr1* plants display enhanced sensitivity to a variety of stimuli, including drought, pathogen infection, abscisic acid (ABA), and ethylene (Frye and Innes, 1998; Frye et al., 2001; Tang et al., 2005; Wawrzynska et al., 2008). The variety of *edr1*-related phenotypes implies that *EDR1* function impacts a diversity of plant stress responses. Interestingly, *edr1* plants appear phenotypically wildtype in the absence of external stresses. This transitory requirement of *EDR1* indicates that it may be functionally active only after a stress response has been induced.

There remain many unanswered questions regarding EDR1 function. EDR1 is believed to negatively regulate KEG, an E3 ubiquitin ligase required for post-embryonic development and endomembrane trafficking (Wawrzynska et al., 2008; Gu and Innes,

2011; Gu and Innes, 2012). However, it is unclear whether EDR1 itself is a regulator of development or endomembrane trafficking. Interestingly, EDR1 primarily localizes to the ER, yet no ER-associated function of EDR1 has been demonstrated (Christiansen et al., 2011).

To gain a greater understanding of EDR1 function, we performed a yeast two-hybrid screen to identify potential substrates of EDR1. These screens yielded a particularly interesting hit, At5g11340, a predicted N-terminal acetyltransferase (NAT) that bears similarity to the human Naa50 protein (Figure 3-1A).

NATs serve as the catalytic components of larger complexes, designated as NatA-F in humans (Polevoda et al., 2009; Aksnes et al., 2016). Human Naa50 serves as the catalytic component of the NatE complex, which also includes the Naa10 and Naa15 subunits (Arnesen et al., 2006). Naa10, Naa15, and Naa50 are also found in the NatA complex, for which Naa10 provides catalytic function. NAT complexes mediate N-terminal acetylation (NTA), a widespread co-translational protein modification believed to affect the majority of eukaryotic proteins (Brown and Roberts, 1976; Polevoda and Sherman, 2003; Arnesen et al., 2009). These complexes target unique N-terminal sequences. Human Naa50 preferentially targets N-termini that have retained their initiator methionine and have a hydrophobic residue in the second position (Evjenth et al., 2009; Van Damme et al., 2011).

Based on work in yeast and humans, there is a solid biochemical understanding of how NATs function; however, the purpose of NTA is not well understood. Emerging evidence suggests that NTA serves various functions. In humans, the Golgi-localized Naa60 specifically targets transmembrane proteins and is required for the maintenance

of Golgi integrity (Aksnes et al., 2015). Recent work in plants has implicated NTA in the regulation of stress responses and development. Both *NAA10* and *NAA15* are essential for plant embryonic development, and knockdown of either results in morphological defects and drought resistance (Feng et al., 2016; Linster et al., 2015). Differential NTA of the SNC1 receptor was found to have significant impacts on its activity, demonstrating a role for NTA in the regulation of defense signaling (Xu et al., 2015). Plant NATs bear strong similarity to their non-plant orthologues; however, the discovery of the plant-specific, plastid-localized NatG indicates that NTA in plants may serve unique purposes (Dinh et al., 2015). This early work demonstrates that NTA plays an important role in plant physiology and stress responses. However, many aspects of plant NATs have yet to be investigated.

Here, we demonstrate a role for the uncharacterized Arabidopsis *NAA50* gene in regulating plant growth and stress responses. Using knockout and transgenic knockdown lines, we show that *NAA50* is indispensable for normal plant growth and development. Loss of *NAA50* triggers defense response pathways in Arabidopsis, implicating *NAA50* in the negative regulation of defense signaling. Loss of *NAA50* also induces constitutive ER stress, while loss of *EDR1* leads to enhanced sensitivity to ER stress. Thus, *EDR1* and *NAA50* appear to be involved in the negative regulation of ER stress. This work demonstrates the importance of NTA in plant stress responses and development, as well as a potential link between NTA and ER stress.

Results

NAA50 is Highly Conserved and Interacts with EDR1

To verify the initial yeast two-hybrid screen which identified NAA50 as a potential interactor of EDR1, we performed additional assays to detect protein-protein interaction. To test for physical interactions between EDR1 and potential substrates, we utilized a "substrate-trap" mutant of EDR1, EDR1ST (Gu and Innes, 2011). EDR1ST contains a D810A substitution in the phosphotransfer domain, which is necessary for substrate phosphorylation, thus stabilizing the potential interaction between EDR1 and its substrates (Gibbs and Zoller, 1991). Our initial yeast two-hybrid screen was carried out using EDR1ST as bait. In yeast two-hybrid, NAA50 was found to physically interact with EDR1ST, but not wildtype EDR1 (Figure 3-1B). This result indicates that NAA50 may be a substrate of EDR1. However, immunoblotting demonstrated that wildtype EDR1 accumulation is significantly lower than that of EDR1ST in yeast, potentially explaining the absence of an interaction (Figure 3-1C). Co-immunoprecipitation using proteins expressed transiently in *N. benthamiana* demonstrated that NAA50 physically associates with both EDR1 and EDR1ST *in vivo*, contrasting with our yeast two-hybrid results (Figure 3-1D). We did not observe NAA50 co-immunoprecipitating with the sYFP-tagged MYC negative control, demonstrating that this interaction is specific (Figure 3-1D). EDR1 has been previously demonstrated to localize to the ER (Christiansen et al., 2011). We similarly observed an ER localization of NAA50 tagged with mCherry when transiently expressed in *N. benthamiana* (Figure 3-1E). NAA50 co-localized with the GFP-tagged ER marker SDF2 (Nekrasov et al., 2009). These experiments indicate that EDR1 and NAA50 physically interact, that both proteins localize to the ER.

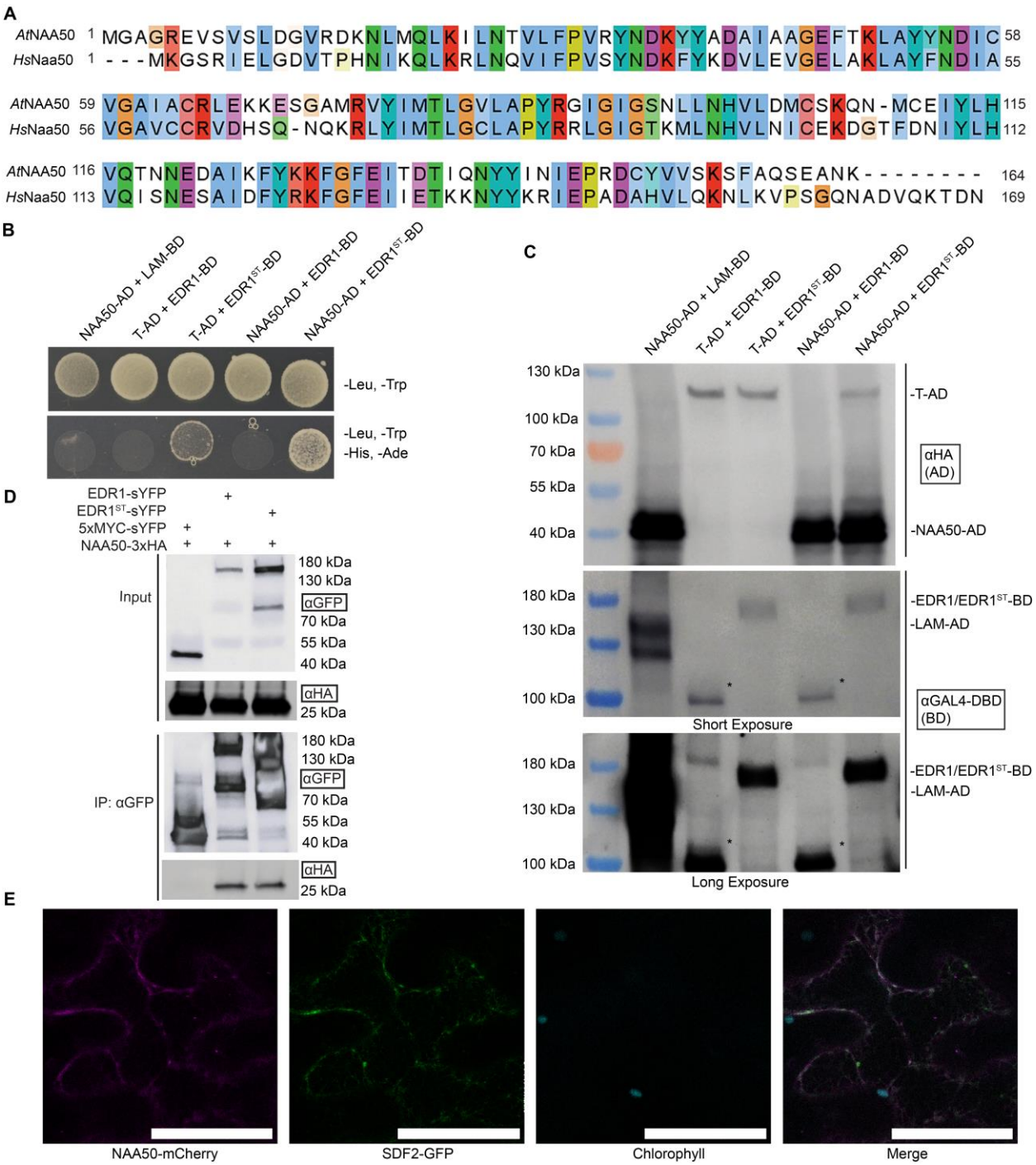

Figure 3-1. Arabidopsis NAA50 physically interacts with EDR1. **A,** Naa50 is conserved in Arabidopsis. Amino acid alignment depicting Arabidopsis NAA50 and human Naa50. This alignment was generated using Clustal Omega (https://www.ebi.ac.uk/Tools/msa/clustalo/) and visualized in Jalview (Waterhouse et al., 2009). **B,** EDR1 interacts with NAA50 in yeast two-hybrid. AD, GAL4 activation domain fusion; BD, GAL4 DNA binding domain fusion. **C,** Immunoblot analysis of yeast strains from panel B. EDR1-BD accumulated poorly in yeast, and a significant accumulation of degraded EDR1-BD (*) was visible. **D,** NAA50 co-immunoprecipitates with EDR1. The indicated constructs were transiently expressed in *N. benthamiana* and then immunoprecipitated using GFP-Trap beads. **E,** NAA50 co-localizes with the ER marker SDF2. mCherry-tagged NAA50 and GFP-tagged SDF2 were transiently co-expressed in *N. benthamiana*. Bars = 50 microns. These experiments were repeated three times with similar results.

Arabidopsis *NAA50* is Essential for Development

The discovery that NAA50 physically interacts with EDR1 prompted us to investigate its potential functions in Arabidopsis. There is a 51.25% identity match between Arabidopsis and human NAA50 proteins (Figure 3-1A). This high degree of sequence similarity indicates that NAA50 function is likely conserved between plants and animals.

To investigate the role of NAA50 in plants, we characterized two T-DNA insertion mutants (SAIL_210_A02 and SAIL_1186_A03), which we designated *naa50-1* and *naa50-2*. Both mutant lines were found to be severely dwarfed compared to wild-type plants (Figure 3-2, A–B). Knockout *naa50* seedlings displayed abnormal and dwarfed growth (Figure 3-2A). As they developed, *naa50* plants remained dwarfed and were sterile, although stems and flowers did form (Figure 3-2C). We were able to fully complement the *naa50-1* mutant phenotypes by transformation of a transgene carrying NAA50 tagged with sYFP under the control of the native NAA50 promoter, demonstrating that loss of NAA50 is responsible for the dwarf phenotype and sterility (Figure 3-2B). These observations establish that *NAA50* is essential for normal plant growth and development.

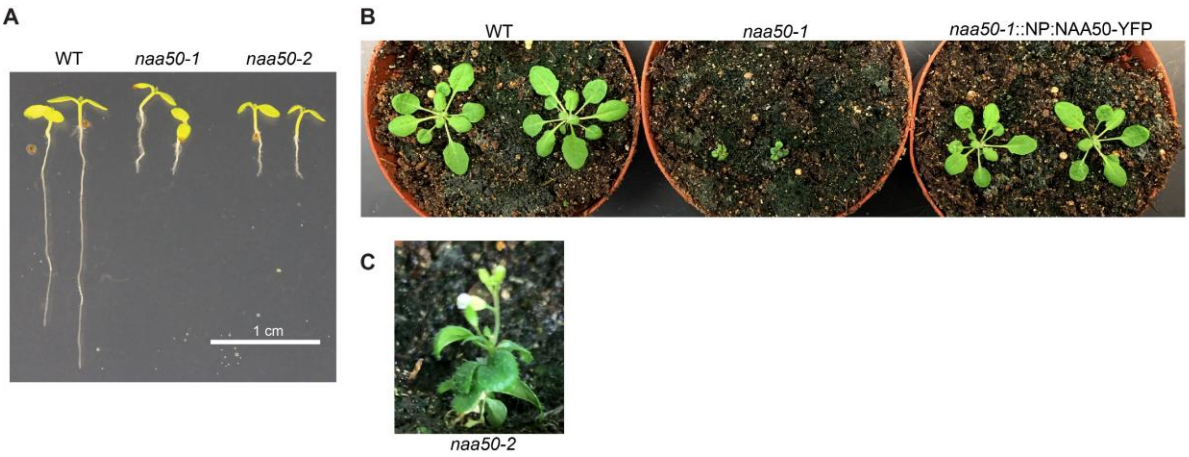

Figure 3-2. *NAA50* is required for plant development. **A,** Loss of *NAA50* results in dwarfed seedlings. Representative seven-day-old, MS-grown seedlings are depicted. **B,** *NAA50*-sYFP complements *naa50*-mediated dwarfism. Four-week-old adult plants are shown. NP, Native *NAA50* Promoter. **C,** *naa50* plants can develop stems and flowers. A five-week-old *naa50-2* plant is shown.

Loss of *NAA50* Alters Plant Growth

In addition to being dwarfed, *naa50* seedlings displayed a variety of developmental phenotypes. Root hair growth in *naa50* plants was irregular, and root hairs were elongated (Figure 3-3A). This led us to hypothesize that loss of NAA50 may result in altered vacuole development. Loss of KEG, another EDR1-interacting protein, has been shown to result in altered vacuolar development (Gu and Innes, 2012). In *naa50-1* seedlings expressing the tonoplast marker γTIP (Nelson et al., 2007), altered vacuole shape was observed (Figure 3-3B). Many *naa50-1* vacuoles appeared fractured and contained many “blebs”, similar to those observed in *keg* mutant seedlings (Gu and Innes, 2012). Additionally, *naa50-1* root cells were larger and irregularly shaped. This could indicate that NAA50 is involved in vacuole maturation.

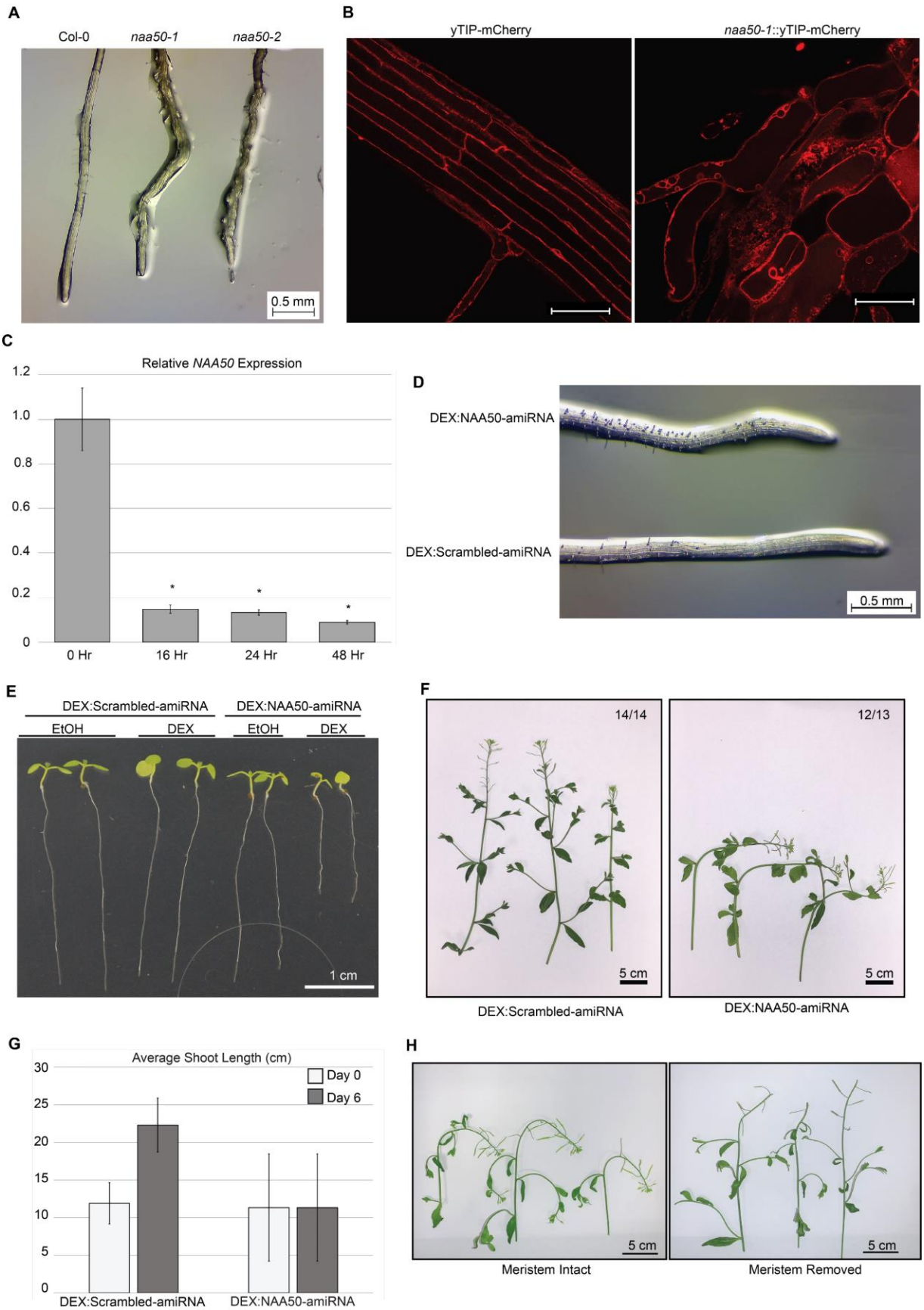
A
Col-0
naa50-1
naa50-2
0.5 mm
B
yTIP-mCherry
naa50-1::yTIP-mCherry
C
Relative NAA50 Expression
1.2
1.0
0.8
0.6
0.4
0.2
0
0 Hr
16 Hr
24 Hr
48 Hr
D
DEX:NAA50-amiRNA
DEX:Scrambled-amiRNA
0.5 mm
E
DEX:Scrambled-amiRNA
DEX:NAA50-amiRNA
EtOH
DEX
EtOH
DEX
1 cm
F
14/14
12/13
5 cm
5 cm
DEX:Scrambled-amiRNA
DEX:NAA50-amiRNA
G
Average Shoot Length (cm)
30
25
20
15
10
5
0
Day 0
Day 6
DEX:Scrambled-amiRNA
DEX:NAA50-amiRNA
H
5 cm
5 cm
Meristem Intact
Meristem Removed

Figure 3-3. Loss of *NAA50* results in developmental changes. **A,** *naa50* seedlings have altered root morphology. The seedling roots depicted are from one-week-old seedlings. **B,** Vacuole and cell morphology are altered in *naa50* seedling roots. Shown are fluorescence micrographs taken of seven-day-old wildtype and *naa50-1* seedlings expressing mCherry-tagged γTIP. Scale bars = 50 microns. **C,** Dexamethasone treatment induces knockdown of *NAA50* in DEX:NAA50-ami plants. q-RT PCR was performed on cDNA generated from multiple adult DEX:NAA50-ami plants following dexamethasone treatment. Displayed are the averages of three replicates. Asterisk denotes *P* value < 0.05. Expression values were normalized to *ACTIN2*. This experiment was repeated three independent times with similar results. **D,** *NAA50* knockdown induces changes to root cell morphology. Five-day-old seedlings were transferred from MS plates to MS plates supplemented with dexamethasone. Images were taken three days after dexamethasone exposure. **E,** *NAA50* knockdown slows root elongation. Seven-day-old seedlings were transferred to MS plates supplemented with ethanol or dexamethasone. Images were taken three days after transfer to ethanol- or dexamethasone-supplemented media. **F,** *NAA50* knockdown induces stem bending. Images were taken 24 hours after dexamethasone treatment. Numbers indicate proportion of all stems which displayed the given morphology. **G,** *NAA50* knockdown stalls stem growth. Stem measurements were taken on DEX:Scrambled-ami (n = 8) and DEX:NAA50-ami (n = 10) immediately before and six days after dexamethasone treatment. No stem growth was detected in DEX:NAA50-ami plants. **H,** Removal of the apical meristem inhibits *NAA50* knockdown-mediated stem bending. Adult DEX:NAA50-ami plants were sprayed with dexamethasone and images were taken twenty-four hours later. The shoot apical meristem was removed immediately prior to dexamethasone treatment.

The severe dwarfing and sterility of *naa50-1* homozygous mutant plants compromised our ability to study the role of *NAA50* in later stages of plant development. To overcome this limitation, we generated inducible knockdown plants based on the expression of an artificial microRNA (amiRNA) driven by a dexamethasone-inducible promoter (DEX:NAA50-ami). We identified a transgenic line carrying this construct that displayed a significant knockdown of *NAA50* as early as 16 hours after dexamethasone treatment (Figure 3-3C). As a control, we utilized a scrambled amiRNA line (DEX:Scrambled-ami), which contains a dexamethasone-inducible amiRNA with no predicted targets.

Knockdown of *NAA50* in the DEX:Naa50-ami plants resulted in severe morphological changes. Growth of DEX:NAA50-ami seedlings on MS media supplemented with dexamethasone increased the length of root hairs, recapitulating the *naa50* root hair phenotype (Figure 3-3D). Additionally, dexamethasone treatment caused DEX:NAA50-ami seedlings to grow significantly slower than the control lines, resulting in

shorter roots (Figure 3-3E). *NAA50* knockdown also elicited changes in stem growth. 24 hours after dexamethasone treatment, the stems of DEX:NAA50-ami plants bent approximately 90º (Figure 3-3F). As in the roots, dexamethasone treatment completely halted any growth of the primary stem in DEX:NAA50-ami plants (Figure 3-3G). Interestingly, this shoot bending phenotype was suppressed by removal of the shoot apical meristem prior to dexamethasone treatment (Figure 3-3H), suggesting that the bending phenotype is dependent on auxin redistribution. Our observations of knockout and knockdown plants confirm that *NAA50* is essential for normal plant growth and development.

Loss of *NAA50* Triggers Cell Death

As well as inducing growth changes, knockdown of *NAA50* caused early senescence in leaves. Leaves of adult DEX:NAA50-ami plants turned yellow and became necrotic following dexamethasone treatment (Figure 3-4A). Senescence also occurred in DEX:NAA50-ami seedlings after transfer to MS plates supplemented with dexamethasone (Figure 3-4B). In both adults and seedlings, the senescence phenotype developed about 4 days after the initial dexamethasone treatment, long after the changes in growth rate and stem bending occurred.

The discovery that knockdown of *NAA50* induces cell death prompted us to investigate whether loss of *NAA50* results in cell death in *naa50-1* seedlings. Indeed, roots of *naa50-1* and *naa50-2* seedlings were readily stained by trypan blue dye, indicating that loss of *NAA50* leads to the accumulation of dead cells in roots (Figure 3-4C). Trypan blue staining of *naa50* roots was spotty and irregular, indicating that only a

subset of *naa50* root cells died (Figure 3-4D). Taken together, these results demonstrate that in addition to being essential for plant development, *NAA50* is also required for the repression of cell death and senescence.

Given the interaction between EDR1 and NAA50, we hypothesized that introduction of the *edr1-1* allele into *NAA50* knockdown plants may affect the senescence phenotype. However, we did not observe any major change in the senescence phenotype when *edr1-1* was introduced (Figure 3-4E). That the *edr1-1* mutation did not enhance or suppress the senescence phenotype indicates that *NAA50* and *EDR1* may regulate senescence through a shared mechanism.

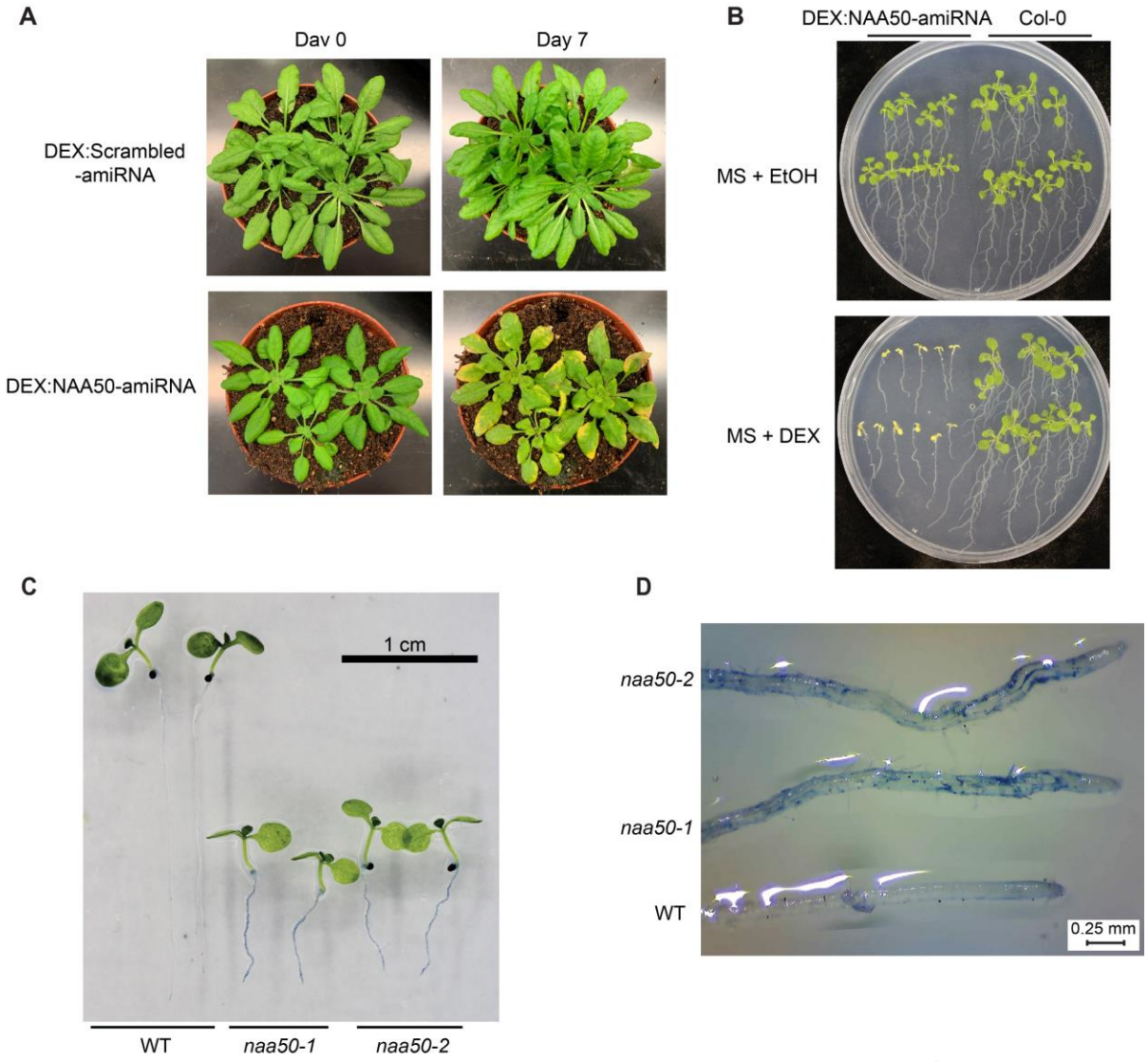
A
Dav 0
Day 7
DEX:Scrambled
-amiRNA
DEX:NAA50-amiRNA
B
DEX:NAA50-amiRNA
Col-0
MS + EtOH
MS + DEX
C
1 cm
WT
naa50-1
naa50-2
D
naa50-2
naa50-1
WT
0.25 mm
E
DEX:Scrambled-amiRNA
DEX:NAA50-amiRNA
DEX:NAA50-amiRNA x edr1-1
Day 0
Day 6

Figure 3-4. Loss of *NAA50* induces cell death and senescence. **A,** *NAA50* knockdown induces senescence in adult leaves. Four-week-old plants were sprayed with dexamethasone. Images were taken immediately before, and seven days after treatment. **B,** *NAA50* knockdown induces senescence in seedlings. Seedlings were grown on MS plates for seven days, and then transferred to MS plates supplemented with ethanol or dexamethasone. Images were taken seven days after transfer to ethanol- or dexamethasone-supplemented media. **C,** *naa50* seedling roots contain dead cells. Seven-day-old seedlings were stained with trypan blue dye. **D,** Cell death staining in *naa50* roots is spotty and irregular. Images depict trypan blue-stained roots from seven-day-old seedlings. **E,** Loss of *EDR1* does not alter senescence in *NAA50* knockdown plants. Images were taken of four-week-old plants immediately before, and seven days after dexamethasone treatment.

Constitutive Knockdown of *NAA50* Induces Developmental Changes and Drought Tolerance

In addition to characterizing DEX:NAA50-amiRNA plants, I also generated transgenic Arabidopsis that constitutively express the *NAA50*-targetting amiRNA (35s:NAA50-amiRNA). Adult 35s:NAA50-amiRNA plants exhibited a significant reduction in *NAA50* transcript level (Figure 3-5A). Previous work exploring the effect of constitutive *NAA10* and *NAA15* knockdown implicated the NatA complex in the regulation of development and osmotic stress. Loss of *NAA10* and *NAA15* resulted in dwarfed plants that displayed enhanced drought tolerance (Linster et al., 2015). This led me to question whether constitutive knockdown of *NAA50* may lead to similar changes. Indeed, constitutive knockdown of *NAA50* resulted in significant developmental changes, including smaller rosette size, shorter petioles, and broader leaves (Figure 3-5B). As with the previously reported *NAA10* and *NAA15* knockdown plants, I found that 35s:NAA50-amiRNA plants display enhanced drought tolerance (Figure 3-5C). These results provide additional evidence that NAA50 is involved in the regulation of plant development and stress responses.

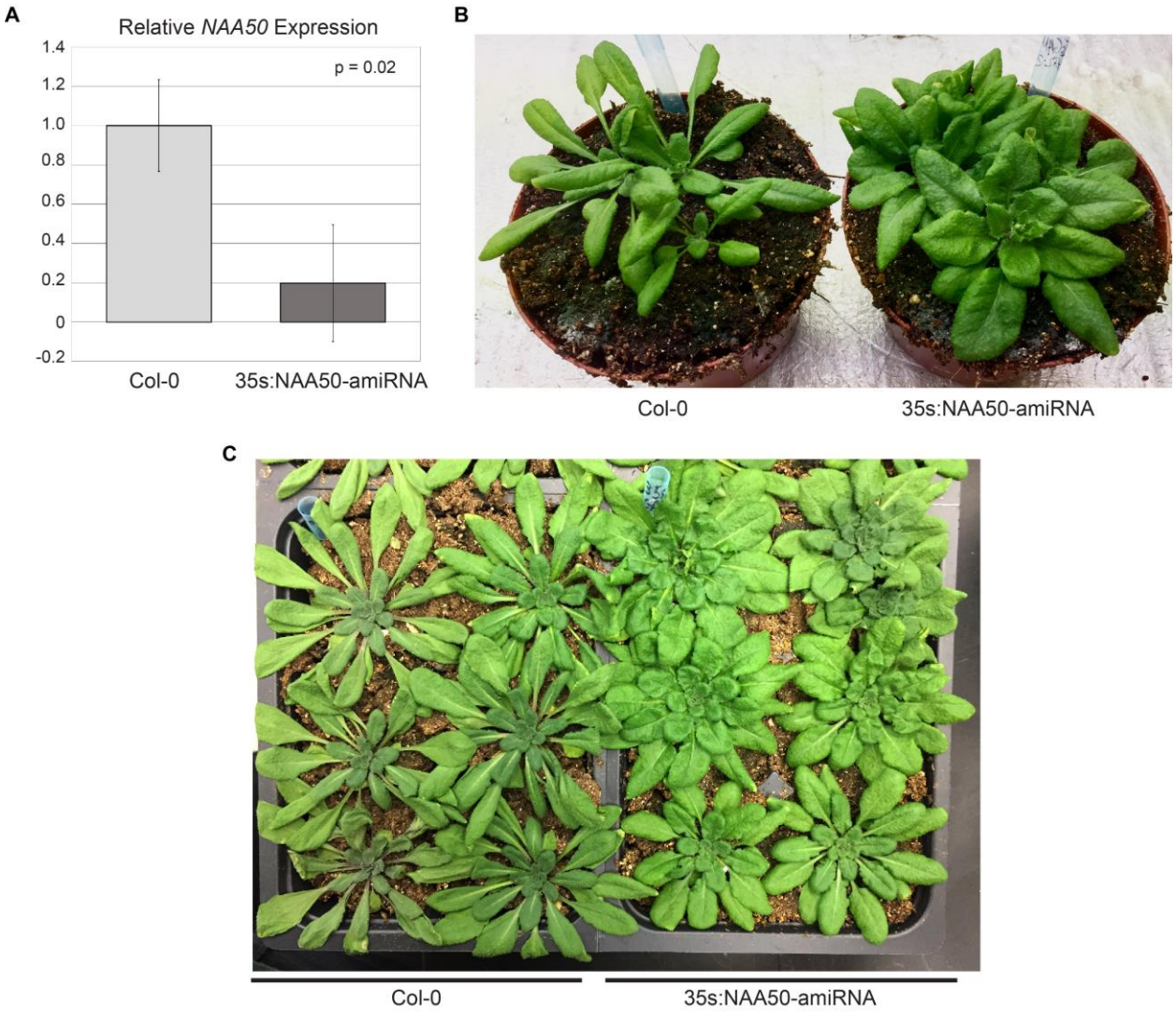

Figure 3-5. Constitutive knockdown of *NAA50* induces developmental changes and drought tolerance. **A,** 35s:NAA50-amiRNA plants exhibit a significant reduction in *NAA50* transcript level. qPCR was performed on cDNA generated from the leaves of 4-week-old plants. *NAA50* expression level was determined by calculating the average of three technical replicates per biological replicate. Bars indicate the average of three biological replicates. *NAA50* transcript level was normalized to *ACTIN2*. Error bars represent the standard deviation of 3 biological replicates. **B,** Constitutive *NAA50* knockdown alters plant development. 4-week-old plants are shown. **C,** 35s:NAA50-amiRNA plants display enhanced drought tolerance. 5-week-old plants are depicted. Water was withheld for 5 days prior to image being taken. Similar results were observed in three independent experiments.

Loss of *NAA50* Represses Growth and Induces Stress Signaling

The discovery that knockdown of *NAA50* triggers changes in plant growth and senescence prompted us to investigate the transcriptional changes taking place in these plants. We therefore conducted an RNA sequencing-based analysis of the DEX:NAA50-ami transcriptome. Four-week-old plants were treated with dexamethasone, and RNA was collected 0, 12, and 24 hours later. Dexamethasone-treated DEX:Scrambled-ami plants were utilized as a control, with RNA samples collected at the same time points. Transcripts from dexamethasone-treated DEX:NAA50-ami plants were deemed significantly altered only if they differed significantly (adjusted *P* value <0.05) from the dexamethasone-treated Scrambled-ami plants at the same time point. To determine whether these transcripts were significantly up- or down-regulated, we compared expression levels in the 12 and 24 hour DEX:NAA50-ami transcriptomes to the time zero DEX:NAA50-ami transcriptome. Transcripts were considered significantly up- or downregulated if they differed from the time zero DEX:NAA50-ami expression level (adjusted *P* value <0.05 and $\log_2$ fold-change >1.5). This design enabled a comparison of the DEX:NAA50-ami transcriptome at various time points, while also excluding potential off-target effects of dexamethasone treatment, amiRNA overexpression, or circadian-influenced expression changes.

Our RNA sequencing analysis indicated that *NAA50* knockdown resulted in altered expression of approximately 2,000 genes by 12 hours post-dexamethasone application (GEO Accession GSE145580). To determine the biological processes most impacted by loss of *NAA50*, we analyzed the biological gene ontology (GO) term enrichment in the 12 and 24 hour DEX:NAA50-ami datasets. This analysis demonstrated that *NAA50*

knockdown leads to upregulation of genes involved in stress hormone signaling (Figure 3-6A). Responses to the stress hormones abscisic acid, jasmonic acid, and salicylic acid were induced 12 hours after dexamethasone treatment. On the other hand, *NAA50* knockdown resulted in the downregulation of a variety of plant growth and photosynthetic processes (Figure 3-6A). In particular, transcripts of genes involved in photosynthesis, light responses, and growth hormone responses were negatively impacted. These changes in expression correlate with the altered development and induced senescence phenotypes observed during *NAA50* knockdown. For instance, we found that auxin signaling was significantly reduced following *NAA50* knockdown, potentially explaining the meristem-dependent stem-bending that occurs following *NAA50* knockdown (Figure 3-3F, H). The increase in the expression of defense genes and salicylic acid signaling correlates with the cell death and senescence that results from *NAA50* knockdown (Figure 3-4).

To further analyze our transcriptome data, we searched for studies that had identified similar transcriptional changes using the Genevestigator Signature tool (Hruz et al., 2008). We selected the 330 most significantly altered transcripts (greatest $\log_2$ fold-change relative to DEX:NAA50-ami at 0 hours) from the 12 hour DEX:NAA50-ami dataset, and searched for studies that displayed similar expression profiles. We found that the most similar expression profiles were those of studies investigating plant-pathogen interactions, or light stress (Figure 3-6B). This overlap demonstrates that *NAA50* knockdown elicits stress signaling in plants.

A

Downregulated

GO TERM	Adj. P Value 12 Hr	Adj. P Value 24 Hr
Photosynthesis	1.21E-10	2.11E-21
DNA Replication	1.27E-07	NS
Response to Blue Light	9.57E-07	1.32E-08
Response to Red Light	1.92E-06	3.00E-08
Response to Hormone Stimulus	3.45E-06	2.85E-06
Peptide Transport	1.48E-05	2.34E-03
Response to Auxin Stimulus	2.96E-03	5.76E-05
Response to Water Deprivation	3.63E-03	NS
Response to Water	5.51E-03	NS
Response to Gibberellin Stimulus	5.98E-03	7.78E-03
Plant-Type Cell Wall Modification	8.12E-03	NS
Cell Growth	8.77E-03	NS
Phototropism	1.64E-02	2.34E-03
Pigment Biosynthetic Process	7.58E-02	1.73E-02
Tropism	8.14E-02	3.12E-03
Response to Stress	8.82E-02	NS
Negative Gravitropism	NS	3.39E-02
Response to Cytokinin Stimulus	NS	3.44E-02

Upregulated

GO TERM	Adj. P Value 12 Hr	Adj. P Value 24 Hr
Response to Hormone Stimulus	3.70E-06	1.72E-05
Response to Abscisic Acid Stimulus	1.04E-05	7.74E-09
Response to Salicylic Acid Stimulus	7.29E-05	NS
Response to Jasmonic Acid Stimulus	2.05E-04	NS
Response to Osmotic Stress	2.36E-04	5.19E-09
Response to Metal Ion	5.79E-04	NS
Response to Light Stimulus	6.56E-04	NS
Response to Salt Stress	8.68E-04	1.62E-06
Response to Stress	5.04E-03	3.03E-12
Cell Wall Organization or Biogenesis	2.00E-02	1.21E-03
Response to Cold	NS	2.55E-05
Defense Response to Fungus	NS	6.32E-05
Response to Temperature Stimulus	NS	2.37E-04
Defense Response	NS	5.23E-04
Response to Wounding	NS	9.01E-04

B

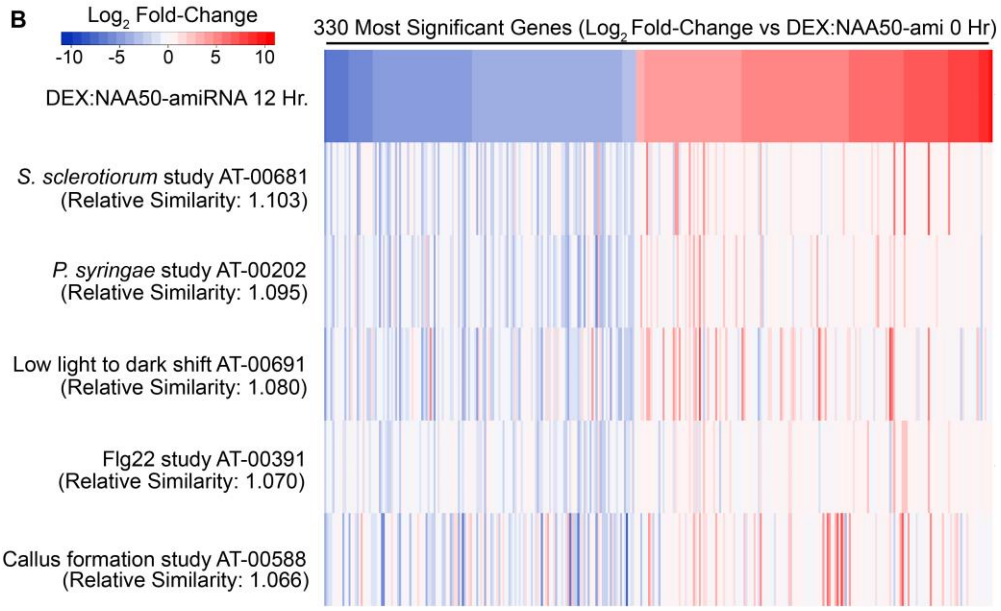

Figure 3-6. *NAA50* knockdown induces changes to growth and defense signaling. **A,** *NAA50* knockdown results in a downregulation of growth signaling, and an upregulation of defense signaling. Significantly altered transcripts were identified by comparing expression levels in dexamethasone-treated DEX:NAA50-amiRNA plants at the given time point to Scrambled-amiRNA plants at the same time point. Furthermore, expression levels in DEX:NAA50-amiRNA plants at 12 and 24 hours were compared to NAA50-amiRNA plants at 0 hours after dexamethasone treatment. Gene Ontology (GO) term enrichment analysis was performed using the BiNGO application to determine whether the DEX:NAA50-ami transcriptome was enriched for specific biological processes. NS, not statistically significant. **B,** The DEX:NAA50-ami transcriptome bears similarity to biotic and abiotic stress studies. The 330 most significantly altered transcripts (based on Log_2 fold-change) from the DEX:NAA50-ami 12 hour dataset were compared to previous studies using the Genevestigator Signature tool. The five most related transcriptomes based on the calculated Relative Similarity scores are shown. A heatmap was generated using Heatmapper (http://www2.heatmapper.ca/expression/) to display the relative log_2 fold-change for each of the 330 transcripts for each study.

NAA50 and *EDR1* Repress ER Stress

We have previously found that plants lacking *EDR1* display an enhanced ER stress phenotype (unpublished). To verify this, we tested *edr1-1* plants for ER stress sensitivity by injecting leaves with tunicamycin (TM), an inhibitor of protein glycosylation that induces ER stress. Injected regions of *edr1-1* leaves senesced more rapidly than wild-type leaves (Figure 3-7A). This observation suggests that *EDR1* is required for proper execution of the unfolded protein response, or that loss of *EDR1* results in enhanced cell death signaling during ER stress signaling.

NTA has been shown to alter protein stability, localization, and transport (Arnesen, 2011). This raised the question of whether loss of NAA50 may lead to induction of ER stress. Indeed, many of the observed *naa50*-mediated developmental phenotypes, such as stunted growth and cell death, can be caused by ER stress. Treatment with TM or dithiothreitol (DTT), which reduces disulfide bonds and induces ER stress, resulted in shorter roots, increased root hair length, and altered cell morphology in wild-type seedlings (Figure 3-7, B–C). Additionally, TM and DTT treatments resulted in root cell death like that observed in *naa50* seedlings (Figure 3-7D). These results demonstrate that ER stress treatment and loss of *NAA50* produce similar physiological changes.

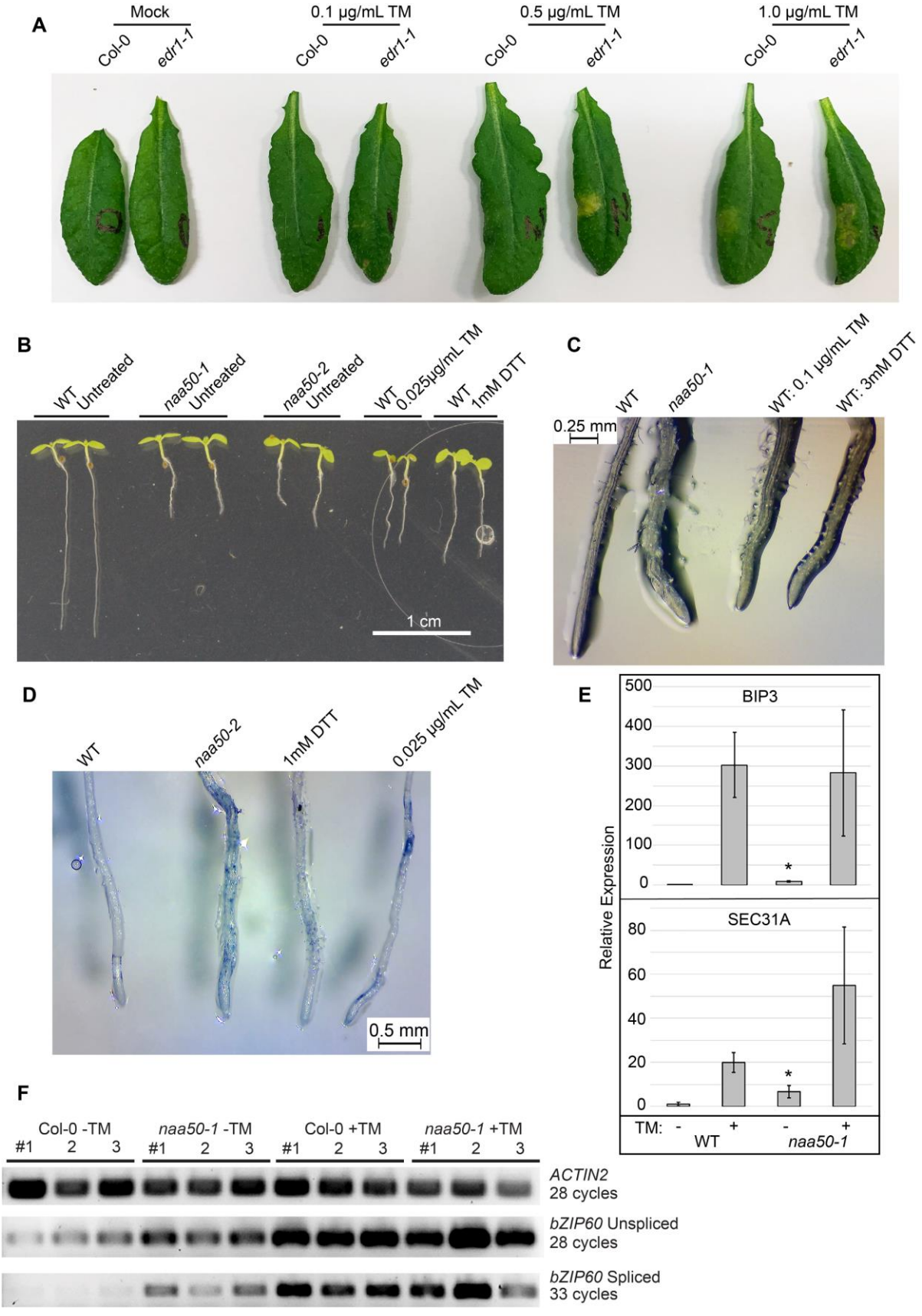
A
Mock
0.1 µg/mL TM
0.5 µg/mL TM
1.0 µg/mL TM
Col-0
edr1-1
B
WT Untreated
naa50-1 Untreated
naa50-2 Untreated
WT 0.025µg/mL TM
WT 1mM DTT
1 cm
C
WT
naa50-1
WT: 0.1 µg/mL TM
WT: 3mM DTT
0.25 mm
D
WT
naa50-2
1mM DTT
0.025 µg/mL TM
0.5 mm
E
BIP3
SEC31A
Relative Expression
TM: - + - +
WT
naa50-1
F
Col-0 -TM
naa50-1 -TM
Col-0 +TM
naa50-1 +TM
#1 2 3
ACTIN2
28 cycles
bZIP60 Unspliced
28 cycles
bZIP60 Spliced
33 cycles

Figure 3-7. Loss of *EDR1* and *NAA50* result in changes to ER stress signaling. **A,** *edr1-1* mutants display heightened ER stress sensitivity. Leaves from six-week-old plants were infiltrated with various concentrations of tunicamycin using a needleless syringe. Leaves were removed, and images taken three days after injection. **B,** ER stress induces *naa50*-like root dwarfism. Seedlings were germinated on MS plates or MS supplemented with TM or DTT. Representative ten-day-old seedlings are shown. **C,** ER stress induces *naa50*-like root cell morphology. Roots of ten-day-old seedlings are depicted. Seedlings were grown on regular MS plates or MS plates supplemented with TM or DTT. **D,** ER stress induces cell death in roots. Ten-day-old seedlings were stained with trypan blue after growth on MS or MS supplemented with TM or DTT. **E,** *naa50-1* seedlings display heightened ER stress signaling in the absence of TM treatment. qRT-PCR was performed on cDNA generated from wildtype and *naa50-1* seedlings. Seedlings were germinated on MS plates and 5 days later transferred to regular MS or MS supplemented with 1 µg/mL TM. RNA was collected twenty hours after transfer to new plates. Gene expression values were normalized to *ACTIN2*. Values depict the averages of three biological replicates, each consisting of twenty individual seedlings. Error bars represent standard deviation between three independent biological replicates. Asterisk denotes *P* value <0.05. **F,** *bZIP60* splicing is induced in *naa50-1* seedlings. RT-PCR was performed on the same cDNA used in panel E. Each lane represents a unique biological replicate derived from twenty seedlings.

To test whether *naa50* seedlings display constitutive ER stress responses, we measured transcription of ER stress marker genes by qPCR. *naa50-1* seedlings were found to have significantly higher levels of *BIP3* and *SEC31A* expression in the absence of any treatment (Figure 3-7E). However, *BIP3* and *SEC31A* expression did not significantly differ between WT and *naa50* seedlings that had been treated with TM. During ER stress, the transcription factor *bZIP60* undergoes splicing, leading to its activation (Deng et al., 2011). Thus, detection of the spliced form of *bZIP60* indicates an active ER stress response. Untreated *naa50-1* seedlings were found to contain significantly higher levels of spliced *bZIP60* relative to WT (Figure 3-7F). However, similar levels of *bZIP60* splicing occurred in TM-treated *naa50-1* and WT seedlings. These results demonstrate that loss of *NAA50* leads to constitutive ER stress, but not an increase in maximum ER stress response signaling. Thus, *EDR1* and *NAA50* both appear to play important roles in regulating ER stress in plants.

NAA50 Enzymatic Activity is Required for Development

Given the high sequence conservation between Arabidopsis and human NAA50 proteins (Figure 3-1A), we hypothesized that the enzymatic activity of NAA50 would be conserved. In addition to functioning as an N-terminal acetyltransferase, human Naa50 has been shown to be capable of auto-acetylation (Evjenth et al., 2009). We therefore tested NAA50 for auto-acetylation activity using recombinant NAA50 protein. *In vitro* auto-acetylation assays using recombinant NAA50 protein demonstrated that Arabidopsis NAA50 is indeed capable of auto-acetylation (Figure 3-8A).

Human Naa50 has previously been shown to associate with the NatA complex, which includes the Naa10 subunit (Arnesen et al., 2006). Transient expression of sYFP-tagged *At*NAA50 with mCherry-tagged *At*NAA10 indeed demonstrated that these proteins co-localize in plants (Figure 3-8B).

Based on the sequence conservation between Arabidopsis NAA50 and human Naa50, as well as the co-localization of *At*NAA50 with *At*NAA10, we hypothesized that *At*NAA50 likely functions as an N-terminal acetyltransferase. To determine whether NAA50 is active in N-terminal acetylation, we tested whether various loss of function NAA50 mutants could complement *naa50-2* mutant phenotypes. *naa50-2* plants were transformed with NAA50^{Y34A}-HA and NAA50^{I145A}-HA. It has been demonstrated that the comparable Y31A and I142A mutations in human Naa50 reduce enzyme efficiency to below 10% and 42.2% of wild-type levels, respectively (Liszczak et al., 2011). Thus, if NAA50-mediated NTA is indeed required for plant development, these mutations may prevent full rescue of the *naa50-2* allele.

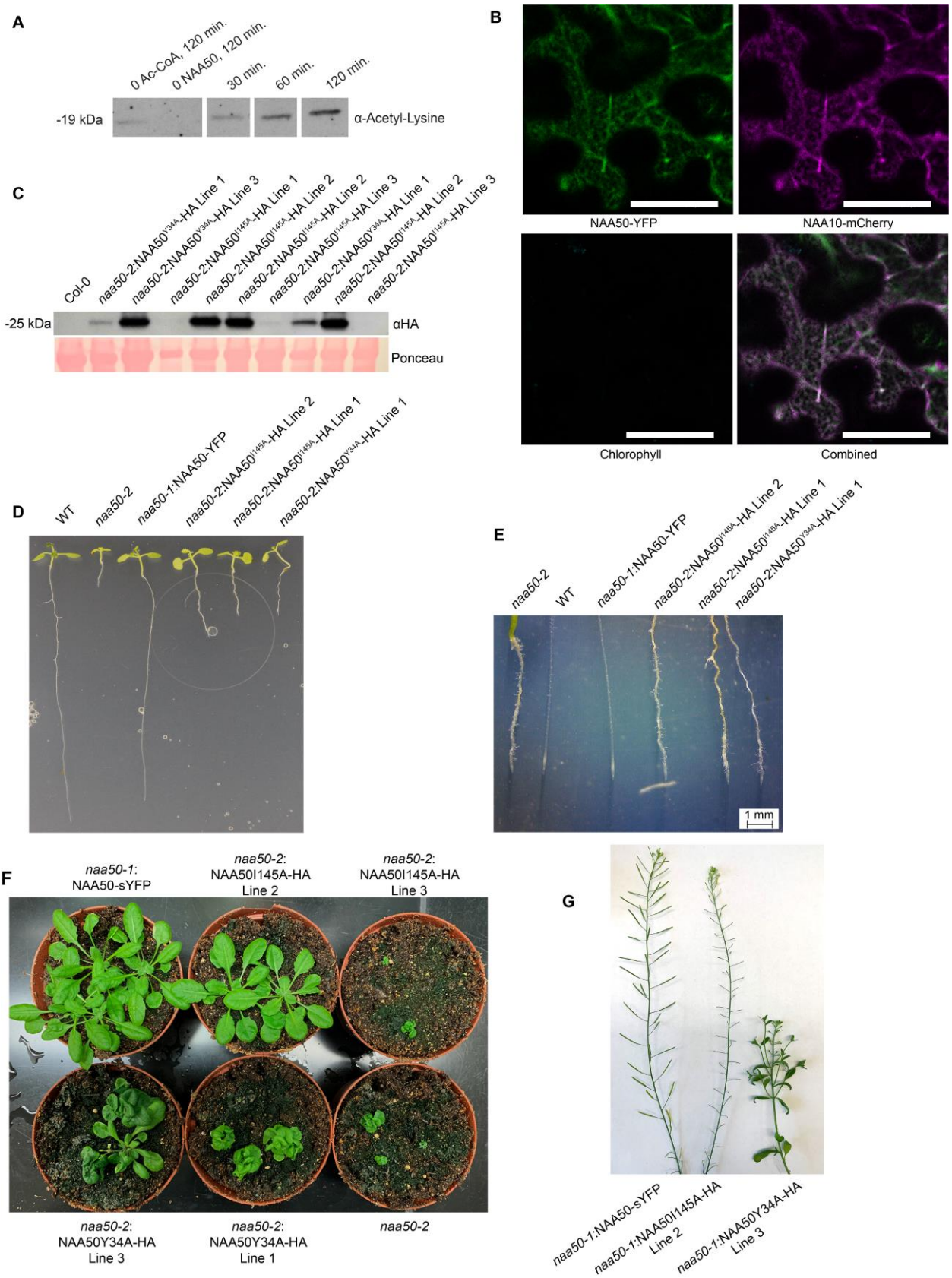
A
0 Ac-CoA, 120 min.
0 NAA50, 120 min.
30 min.
60 min.
120 min.
-19 kDa
α-Acetyl-Lysine
B
NAA50-YFP
NAA10-mCherry
Chlorophyll
Combined
C
Col-0
naa50-2:NAA50Y34A-HA Line 1
naa50-2:NAA50Y34A-HA Line 3
naa50-2:NAA50I145A-HA Line 1
naa50-2:NAA50I145A-HA Line 2
naa50-2:NAA50I145A-HA Line 3
naa50-2:NAA50Y34A-HA Line 1
naa50-2:NAA50Y34A-HA Line 2
naa50-2:NAA50I145A-HA Line 2
naa50-2:NAA50I145A-HA Line 3
-25 kDa
αHA
Ponceau
D
WT
naa50-2
naa50-1:NAA50-YFP
naa50-2:NAA50I145A-HA Line 2
naa50-2:NAA50I145A-HA Line 1
naa50-2:NAA50Y34A-HA Line 1
E
naa50-2
WT
naa50-1:NAA50-YFP
naa50-2:NAA50I145A-HA Line 2
naa50-2:NAA50I145A-HA Line 1
naa50-2:NAA50Y34A-HA Line 1
1 mm
F
naa50-1: NAA50-sYFP
naa50-2: NAA50I145A-HA Line 2
naa50-2: NAA50I145A-HA Line 3
naa50-2: NAA50Y34A-HA Line 3
naa50-2: NAA50Y34A-HA Line 1
naa50-2
G
naa50-1:NAA50-sYFP
naa50-1:NAA50I145A-HA Line 2
naa50-1:NAA50Y34A-HA Line 3

Figure 3-8. NAA50 enzymatic activity is required for plant development. **A,** Recombinant NAA50 displays auto-acetylation activity *in vitro*. Recombinant HIS-tagged NAA50 was expressed and purified from *E. coli. In vitro* reactions were performed at 30°C for the indicated time points. Samples were then boiled and subjected to gel electrophoresis and immunoblotting using an anti-acetyl-lysine antibody. This experiment was repeated three times with similar results. This figure was generated from one immunoblot derived from a single experiment with irrelevant lanes removed. **B,** NAA50 co-localizes with NAA10. sYFP-tagged NAA50 was transiently co-expressed with mCherry-tagged NAA10 in *N. benthamiana.* Bars = 50 microns. **C,** Immunoblotting demonstrates that HA-tagged NAA50 mutant transgenes are expressed in transgenic plants. Leaf tissue from hygromycin-resistant T3 plants was subjected to gel electrophoresis and immunoblotting using an anti-HA antibody. **D,** Mutant *NAA50* transgenes do not complement *naa50* root dwarfism. Representative ten-day-old seedlings are depicted. **E,** Mutant *NAA50* transgenes do not complement *naa50* root cell morphology defects. Images were taken of representative ten-day-old seedlings. **F,** NAA50I145A can complement *naa50*-mediated rosette dwarfism. The image depicts representative six-week-old plants. **G,** NAA50I145A does not complement *naa50*-mediated sterility. Stems were removed from 7-week-old plants.

We were able to identify numerous transgenic lines expressing both the Y34A and I145A proteins (Figure 3-8C). Following transformation with the NAA50^{I145A}-HA transgene, we observed that the *naa50* root phenotype was not fully complemented in the transgenic lines, as roots retained their dwarf phenotype and altered cell morphology (Figure 3-8, D-E). Despite retaining the *naa50* root phenotypes, some NAA50^{I145A} lines did not display the *naa50* dwarfism phenotype and had wildtype-sized rosettes (Figure 3-8F). I145A line 2 plants displayed the greatest expression of the I145A transgene and had a more wildtype-like rosette size than lines 1 and 3 (Figure 3-8C, F). However, although line 2 NAA50^{I145A} transgenic plants had wildtype-sized rosettes, normal siliques did not develop and viable seed was not produced (Figure 3-8G).

The Y34A mutation, which has been shown to have a more significant impact on human Naa50 enzymatic activity than I145A (Liszczak et al., 2011), also prevented full rescue of *naa50-2* plants. NAA50^{Y34A} transgenic plants did not have normal roots or rosettes and were infertile (Figure 3-8, D-F). As with the I145A transgenic lines, we observed a correlation between NAA50^{Y34A} protein accumulation and rosette size (Fig. 3-8C, F). However, unlike NAA50^{I145A}, NAA50^{Y34A} was unable to fully complement the

rosette dwarfism phenotype (Figure 3-8F). Even in Y34A line 3 plants, which displayed a similar level of NAA50 accumulation to I145A line 2 plants, rosette size was not fully restored.

The inability of NAA50^{I145A} and NAA50^{Y34A} transgenes to fully rescue *naa50-2* plants demonstrates the importance of NAA50-mediated NTA in plant growth and development. That the NAA50^{I145A} mutant was able to complement the rosette dwarfism, but not the root phenotypes or sterility demonstrates that NAA50-mediated NTA may be especially required for the growth and development of roots as well as fertility. Furthermore, the inability of the NAA50^{Y34A} transgene to rescue the rosette dwarfism phenotype indicates that this mutation is indeed more deleterious than the I145A mutation.

Detecting NAA50-Mediated NTA

Since NAA50 is highly conserved (Figure 3-1A), and conserved NAA50 residues are required for proper plant development (Figure 3-8, D-G), I sought to demonstrate NAA50 NTA activity. *In vitro* reactions to detect NAA50-mediated NTA were performed using recombinant NAA50 protein incubated with synthetic N-terminal peptides. A total of 6 peptides were tested in these reactions (Figure 3-9A). Four of these peptides were 10mers based on actual Arabidopsis proteins bearing N-termini that make them either highly likely, or highly unlikely to be NAA50 targets. Two of the tested peptides were 24mers that have been previously used in similar *in vitro* reactions with recombinant human Naa50 (Foyn et al., 2017). However, I was unable to detect NAA50-mediated NTA

using any of these peptides. This may be due to Arabidopsis NAA50 requiring another factor, such as NAA15 to be enzymatically active.

I also attempted to detect NAA50-mediated NTA *in vivo*. To do this, protein extract was enriched for N-terminal peptides through liquid chromatography. Followoing this enrichment step, mass spectrometry was performed to identify N-terminally acetylated peptides. We compared the N-terminal acetylomes of wildtype and *naa50-1* seedlings using this technique. Since Naa50 targets peptides with an N-terminal methionine, we did not analyze peptides that had lost their N-terminal methionine residue. Ultimately, we were unable to detect significant differences in the N-terminal acetylomes of wildtype and *naa50-1* plants. 174 N-terminally acetylated peptides that had retained their N-terminal methionine were identified in the *naa50-1* sample while 184 were identified in the wildtype sample. Since NAT complexes display sequence specificity for their targets, we hypothesized that specific populations of the N-terminal acetylome may be affected by the loss of NAA50. However, the frequency with which specific amino acids appeared at the second position of N-terminally acetylated proteins was not significantly different in wildtype and *naa50-1* (Figure 3-9B). A similar approach was used to compare the effect of knocking down or overexpressing *NAA50* on the N-terminal acetylome. Protein from mock and dexamethasone-treated DEX:NAA50-amiRNA and DEX:NAA50-YFP plants was analyzed, yet no significant differences were observed (Figure 3-9C). 174 and 182 N-terminally acetylated peptides that retained an N-terminal methionine were identified in mock-treated DEX:NAA50-amiRNA and DEX:NAA50-sYFP samples, respectively. 140 and 192 N-terminally acetylated peptides that retained an N-terminal methionine were

identified in dexamethasone-treated DEX:NAA50-amiRNA and DEX:NAA50-sYFP samples, respectively.

Our inability to detect NAA50-mediated NTA *in vivo* may be due to redundancy between NAA50 and other N-terminal acetyltransferases. It is also worth noting that we extracted protein from either whole seedlings, or from adult rosettes. Given that *naa50* mutants display severe root phenotypes, it is possible that NAA50-mediated NTA is most prevalent in root tissue.

An *E. coli*-based approach has been previously utilized for the characterization of the NTA activity of the plant-specific NatG (Dinh et al., 2015). I took a similar approach to characterizing NAA50 activity, by identifying N-terminally acetylated peptides in *E. coli* expressing NAA50. We made use of an *E. coli* strain carrying an inducible HIS-tagged NAA50. We compared the effect of NAA50 induction in *E. coli* yet observed no significant difference in the total number of N-terminally acetylated peptides identified. 66 N-terminally acetylated peptides that retained their N-terminal methionine were identified in the NAA50-expressing *E. coli*, while 72 were identified in the un-induced *E. coli* (Figure 3-9D). The majority of the identified N-terminally acetylated peptides were found in both samples (Figure 3-9D). This again indicates that NAA50 may not be active in NTA in the absence of a partner, such as NAA15.

A

Peptide Sequence	Predicted NAA50 Target?	Reference	Arabidopsis Protein
MLGPSLLGRS	Yes		AT5G41610.2
MLGNQSADFS	Yes		AT2G43040.1
ATEDVQDPRI	No		AT1G27450.2
MNNDDIILAE	No		AT1G12610.1
MLGPEGGRWGRPVGRRRRPVRVYP	Yes	Foyn et al., 2017	
MDELDLDRWGRPVGRRRRPVRVYP	No	Foyn et al., 2017	

B

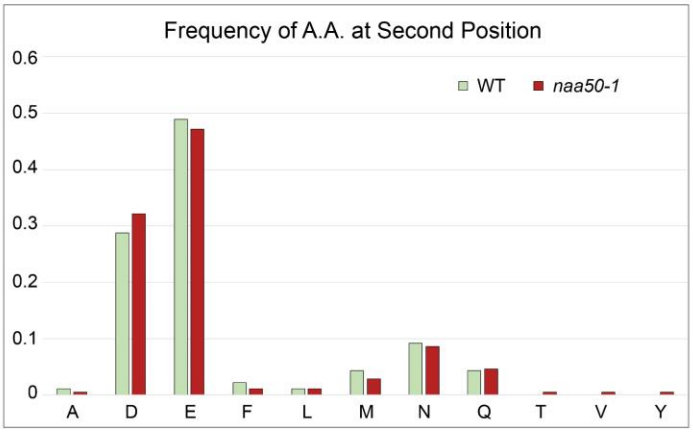

C

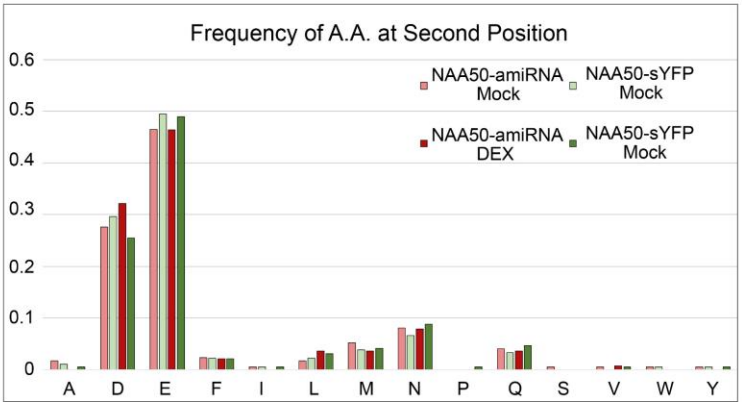

D

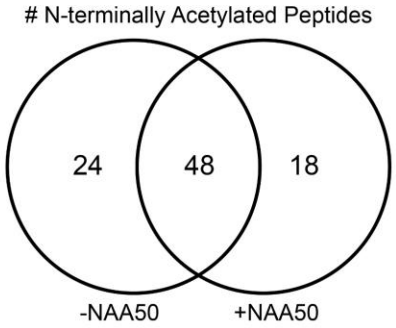

Figure 3-9. Detecting NAA50-mediated NTA. **A,** Table of the peptides utilized for *in vitro* NTA assays using recombinant NAA50. **B,** Mass spectrometry was performed on protein isolated from one-week-old wildtype and *naa50-1* seedlings. Depicted are the frequencies that a given amino acid appeared at the second position of an N-terminally acetylated peptide. **C,** Mass spectrometry was performed on protein isolated from four-week-old DEX:NAA50-amiRNA and DEX:NAA50-sYFP plants 48 hours after mock or dexamethasone treatment. Depicted are the frequencies that a given amino acid appeared at the second position of an N-terminally acetylated peptide. **D,** Protein was isolated from *E. coli* expressing or not expressing HIS-tagged NAA50. The Venn diagram depicts the total number of N-terminally acetylated peptides identified in each protein sample.

Discussion

NAA50 is Required for Growth and the Suppression of Stress Responses

The investigation of NTA in regulating cell signaling in eukaryotes is still in its infancy, and identification and characterization of all plant NATs is incomplete. Our understanding of how NATs function comes primarily from work in human cell culture and yeast. However, recent work in plants has demonstrated a role for NTA in regulating diverse processes (Linster et al., 2015; Xu et al., 2015; Huber et al., 2019). Post-translational modification of proteins has long been appreciated as a mechanism by which cell signaling and crosstalk is regulated (Hunter, 2007). NTA may provide a mechanism by which plants regulate responses to external and internal stress signals at the translational level.

With this work, we have begun to characterize the role of Arabidopsis *NAA50* in regulating plant growth and development. Complete loss of *NAA50* results in severely dwarfed and sterile plants, as well as altered root morphology. By using hormone-inducible amiRNA transgenic plants, we demonstrated that *NAA50* knockdown results in reduced expression of developmental process and inhibits growth. Taken together, these results indicate that *NAA50* is required for plant growth and development.

Our work adds to growing evidence that NATs are required for plant development. *NAA10* and *NAA15* have previously been demonstrated to be essential for development. Loss of function mutations in *NAA10* or *NAA15* are embryonic lethal (Linster et al., 2015; Feng et al., 2016), while partial loss of *NAA15* results in dwarfism and enhanced defense signaling (Xu et al., 2015). Knockdown of *NAA10* and *NAA15* alters root morphology, enhances the growth of the primary root and inhibits the growth of lateral roots (Linster et

al., 2015). NatB also appears to be required for development, as partial loss of NatB components NAA20 and NAA25 result in dwarfism (Ferrandez-Ayela et al., 2013; Xu et al., 2015; Huber et al., 2019). Loss of NAA30, the catalytic component of NatC, results in minor dwarfism as well as defects in photosystem II efficiency (Pesaresi et al., 2003). The range of developmental phenotypes resulting from mutations in NATs demonstrate that NATs differ in their involvement in plant development.

Our results demonstrate that, in addition to altering plant development, loss of *NAA50* results in the activation of plant stress signaling. Knockdown of *NAA50* elicits senescence in adults as well as seedlings, while the roots of *naa50* seedlings contain an abundance of dead cells. Gene expression analysis confirmed that knockdown of *NAA50* results in an upregulation of defense signaling.

NATs appear to play unique roles in the regulation of plant stress responses. Loss of NatA has been shown to increase drought tolerance (Linster et al., 2015). The NatA and NatB complexes have been previously implicated in the regulation of the NLR protein SNC1 (Xu et al., 2015). Partial loss of *NAA15* results in increased stability and accumulation of SNC1, as well as enhanced defense signaling and resistance. Interestingly, loss of NatB leads to decreased accumulation of SNC1, and suppression of *snc1*-induced dwarfism (Xu et al., 2015). Partial loss of NAA20 and NAA25 results in enhanced sensitivity to osmotic stress and altered expression of stress-related transcripts (Huber et al., 2019). Our observations add to the growing list of evidence that NATs play an important role in plant stress signaling.

In addition to its role in negatively regulating defense signaling, our results implicate *NAA50* in the repression of ER stress. The developmental defects observed in

naa50 plants can be recapitulated by TM and DTT treatment, indicating that they may result from constitutive activation of ER stress responses. In support of this hypothesis, we observed increased expression of ER stress genes and *bZIP60* splicing in untreated *naa50* seedlings (Figure 3-7). Following TM treatment, *naa50-1* seedlings displayed WT levels of ER stress signaling. Therefore, loss of *Naa50* induces ER stress signaling, but does not lead to greater induction during TM treatment. Additionally, the expression of *BIP3* and *SEC31A* in *naa50-1* seedlings was significantly lower in the absence of TM than during TM treatment. This indicates that the level of constitutive ER stress which occurs in *naa50-1* plants is significantly lower than that elicited by chemical treatment. Based on these results, we believe that NAA50 is required for the prevention of protein misfolding and aggregation, which contribute to ER stress. Plant NATs have not previously been demonstrated to play a role in the regulation of ER stress. Although NatE seems to be required for the repression of ER stress, it is possible that other NAT complexes may be required as well.

Our results demonstrate that NAA50-mediated NTA is likely required for plant development. Although we were unable to detect NAA50-mediated NTA *in vivo*, our complementation experiments demonstrate that the $NAA50^{I145A}$ and $NAA50^{Y34A}$ mutations, which inhibit NTA activity, prevent the NAA50 transgene from fully complementing *naa50* plants. This demonstrates an essential role for NAA50-mediated NTA in root development and fertility.

NTA May Regulate ER Stress

The enzymatic function of human Naa50 has been demonstrated previously (Liszczak et al., 2011; Van Damme et al., 2011; Reddi et al., 2016; Evjenth et al., 2009). A high degree of conservation has been demonstrated for other NATs. For instance, human NatA can complement yeast NatA mutants (Arnesen et al., 2009). Based on the high level of sequence similarity between Arabidopsis and human Naa50, it is probable that enzymatic function is conserved. We were able to detect auto-acetylation of recombinant Arabidopsis NAA50 *in vitro*, demonstrating that it is indeed a functional acetyltransferase (Figure 3-8A). In addition, we found that mutations that alter NAA50 NTA activity prevent complementation of *naa50* mutant phenotypes (Figure 3-8, D-G). As in other organisms, Arabidopsis NAA50 localizes primarily to the ER (Figure 3-1E, Figure 3-8B). These similarities to other Naa50 proteins demonstrate that NAA50 likely functions as an NTA in plants.

There is evidence from human and yeast systems for the involvement of NATs in responding to ER stress and protein aggregates. NTA is known to contribute to protein stability, trafficking, and translocation to the ER (Arnesen, 2011; Forte et al., 2011). The NatA complex has been implicated in the regulation of protein aggregation (Arnesen et al., 2010). HYPK, a NatA component, has chaperone activity, and has been shown to inhibit the formation of protein aggregates (Raychaudhuri et al., 2007). Loss of NatA components in yeast results in compromised heat shock sensitivity and signaling, indicating a potential role for NTA in regulating heat shock (Gautschi et al., 2003; Das and Bhattacharyya, 2016). There is an established link between the UPR and heat stress responses in plants. Heat shock can induce protein aggregation and ER fragmentation

(Richter et al., 2010). During heat stress, the UPR is activated and ensures proper reproductive development (Deng et al., 2011; Deng et al., 2016). We have demonstrated that loss of *NAA50* in plants results in constitutive ER stress, adding additional evidence that NTA is involved in the repression of protein aggregation and ER stress.

There is a well-established link between ER stress, the UPR, and defense signaling in plants. Plants carrying loss of function mutations in the stearoyl-ACP desaturase *SSI2* exhibit dwarfism, enhanced accumulation of ER stress marker BiP3, and higher PR-1 expression (Iwata et al., 2018; Kachroo et al., 2001). This mirrors the increased biotic and ER stress signaling observed in *naa50* plants. Mutants lacking UPR regulators IRE1 and bZIP60 display enhanced susceptibility to bacterial pathogens, demonstrating a link between the UPR and SA-based defense signaling (Moreno et al., 2012). If ER stress cannot be properly maintained, the UPR shifts into a cell death phase (Woehlbier and Hetz, 2011; Walter and Ron, 2011). A recent investigation of the transcriptional changes that occur during a prolonged UPR demonstrated that transcripts associated with biotic stress responses are elicited during the UPR (Srivastava et al., 2018). Biotic stress signaling is also impacted by the ER Quality Control (ERQC) pathway. The membrane-bound receptors upon which plant defense signaling relies undergo maturation through the ERQC pathway. Impairment of ERQC machinery can result in enhanced susceptibility, as the receptors required for pathogen recognition are unable to function (Tintor and Saijo, 2014). Thus, compromised ER integrity can hinder plant pathogen responses. Unsurprisingly, plant pathogens have been found to attack the host ER for their own benefit. The mutualistic fungus *Piriformospora indica* induces cell death using an ER stress-dependent mechanism, enabling its colonization of the Arabidopsis

root (Qiang et al., 2012). The high degree of overlap between ER stress and biotic stress responses opens the possibility that the observed increase in stress signaling in *NAA50* knockout and knockdown plants results from changes to ER stress, rather than direct regulation of stress responses by *NAA50.*

A link between NTA and osmotic stress in plants has been recently proposed (Linster et al., 2015; Asknes et al., 2016). It was demonstrated that NatA knockdown plants display enhanced drought tolerance. Furthermore, levels of NatA-mediated NTA were shown to fluctuate in response to ABA treatment (Linster et al., 2015). Here, we have demonstrated that plant NATs may be required for proper protein folding and the repression of ER stress. There is a demonstrated link between ER stress and osmotic stress in plants. Overexpression of the chaperone BiP in tobacco and soybean results in enhanced drought tolerance (Valente et al., 2008). BiP expression in soybean was found to inhibit both ER- and osmotic stress-induced cell death (Reis et al., 2011). In wheat, treatment with Tauroursodeoxycholic Acid alleviates osmotic stress-induced cell death and ER stress signaling (Zhang et al., 2017). Strong osmotic stress alters root architecture and induces cell death through an ER stress-dependent mechanism (Duan et al., 2010).

If NTA is indeed required to prevent induction of ER stress, then the enhanced drought resistance of NAT-deficient plants may be an indirect result of changes to ER stress signaling. We have demonstrated that loss of *NAA50* alters root morphology, resulting in shorter roots, longer root hairs, and the accumulation of dead cells. Furthermore, these changes appear to be the result of constitutive ER stress. Constitutive ER stress resulting from reduction in NAT expression may lead to priming of stress

responses, which ultimately results in a resistance phenotype. Thus, the enhanced drought tolerance of NatA knockdown plants observed by Linster et al., 2015 may result from enhanced ER stress and UPR signaling, rather than a direct effect on osmotic stress responses.

Although loss of *NAA50* has a significant impact on Arabidopsis development, it does not result in lethality, as in *Naa10 and Naa15* knockouts (Linster et al., 2015; Feng et al., 2016). This indicates potential redundancy for NAA50-mediated NTA, or that NAA50 is only essential for certain developmental processes. Human NatE, NatC, and NatF target a common set of N-terminal peptides (Aksnes et al., 2016). Given this overlap of function, other NATs may be capable of acetylating NatE targets in its absence. It is unclear whether Arabidopsis NAA50 can function similarly to NatF. NAA50 does not appear to have the same Golgi localization as human Naa60 (Aksnes et al., 2015), as we observed it primarily localizing to the ER (Figure 3-1E). NatC may be able to fulfill some functions for NatE, however, loss of function mutations in Arabidopsis NatC are less severe than that of NatE, producing only minor dwarf phenotypes (Pesaresi et al., 2003).

Most work on NTA has been performed in unicellular organisms, making it impossible to study whether NATs display tissue-specific functions. There are likely to be differences in the expression patterns of NATs in different tissues. According to the BAR ePlant browser (http://bar.utoronto.ca/eplant), root expression of NAA50 and NAA10 is predicted to be the highest in the meristematic region. It is likely that some NAT complexes are specifically active at certain developmental periods, or in specific tissues. If other plant NAT complexes are indeed able to fulfill some functions of NAA50, it is also possible that they are only able to do so in certain tissues or at certain points in

development, based upon their own expression profiles. The study of plant NATs has the potential to expose tissue- and development-specific NAT activity.

Loss of *NAA50* especially affected certain cell types and tissues. In *NAA50* knockdown plants, loss of *NAA50* led to reduced growth of both roots and stems. Furthermore, stem bending and altered root morphology were observed. The use of an inducible knockdown line enabled us to compare the effects of *NAA50* knockdown in new and old cells. Interestingly, phenotypes resulting from *NAA50* knockdown were mainly exhibited in newly developed cells. The sterility of *naa50* plants demonstrates that *NAA50* is required for reproductive as well as vegetative development. These observations demonstrate that NAA50 activity may be especially required by developing cells, or cells undergoing rapid growth and division.

If *NAA50* is indeed required for the regulation of ER stress, it follows that roots, shoots, and anthers would be especially impacted by its loss. There is evidence that plant vegetative and reproductive development require an intact UPR to manage ER stress. Roots have been shown to be particularly sensitive to ER stress (Cho and Kanehara, 2017). Significant changes in root and shoot development result from mutations in UPR genes, indicating that a functional UPR is essential for vegetative development (Deng et al., 2013; Kim et al., 2018; Bao et al., 2019). Mutations in UPR genes also have a significant impact on plant reproductive development (Deng et al., 2013; Deng et al., 2016). In fact, the UPR is constitutively active in anthers (Iwata et al., 2008). The requirement for UPR signaling in unstressed plants implies that ER stress occurs during normal development and must be managed by the UPR, or that UPR genes are involved in the direct regulation of developmental genes (Kim et al., 2018). A requirement for the

UPR in development has long been demonstrated in animals. The rapid production of immunoglobulins by B cells is preceded by an upregulation of the UPR, which manages potential ER stress (van Anken et al., 2003). Roots, shoots, and anthers may rely upon UPR signaling due to the high level of protein translation that occurs in these tissues during development. That these tissues were indeed particularly affected by the loss of NAA50 demonstrates that NAA50 may be required for the management of ER stress which occurs during development.

Model for EDR1 and NAA50 Regulation of ER Stress

Our initial interest in NAA50 was based on its physical interaction with EDR1. Indeed, the enhanced defense signaling observed in *NAA50* knockout and knockdown plants correlates with many *edr1* phenotypes. *EDR1* and *NAA50* also appear to play a role in the regulation of ER stress. *edr1* plants were found to have enhanced sensitivity to TM treatment, while loss of *NAA50* induced constitutive ER stress.

Our work indicates that EDR1 and NAA50 may be involved in the repression of ER stress (Figure 3-10). Since NAA50 likely functions primarily in the NTA of target peptides, loss of NAA50 may result in the translation of proteins which lack a required N-terminal acetylation mark. Loss of NAA50-mediated NTA likely results in the misfolding, improper trafficking, or aggregation of proteins, ultimately producing ER stress. We have found that loss of EDR1 results in increased ER stress sensitivity. It is possible that EDR1 activates NAA50, perhaps during a stress event. Thus, when plants lacking EDR1 encounter stress, NAA50 would lack proper activation. The lack of NAA50-mediated NTA would therefore lead to mild ER stress, ultimately resulting in enhanced senescence and cell

death. This model provides a potential explanation for the wide range of stimuli to which *edr1* plants display enhanced senescence and sensitivity.

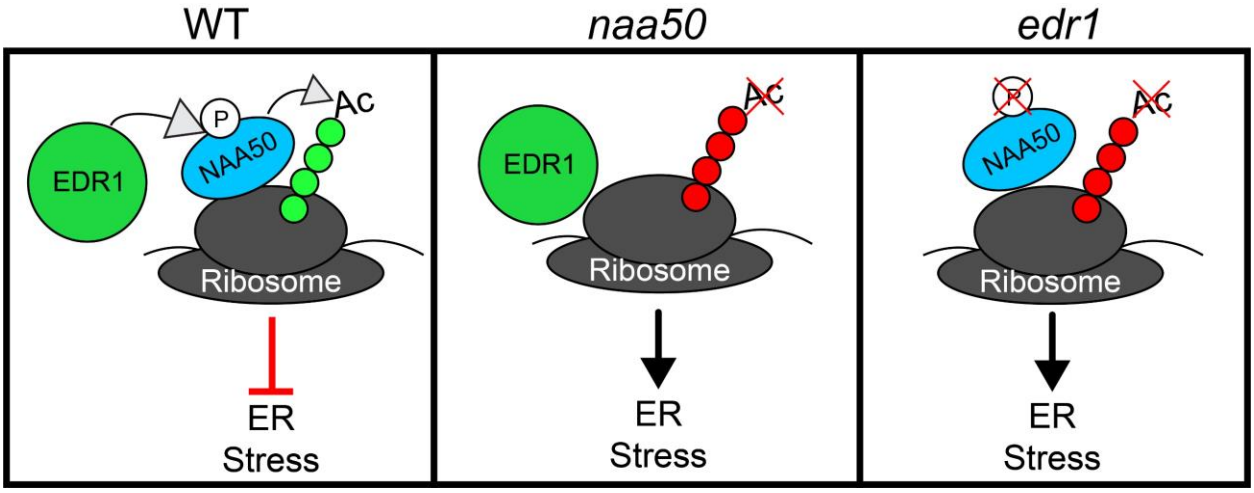

Figure 3-10. Model for EDR1- and NAA50-mediated regulation of ER stress. Left: In wildtype plants, EDR1 activates NAA50-mediated NTA, possibly through phosphorylation. NAA50-mediated NTA ensures proper protein folding, thereby inhibiting ER stress. Middle: In plants lacking functional NAA50, the absence of NAA50-mediated NTA results in protein aggregation and ER stress. Right: Biotic and abiotic stress events strain the translational machinery requiring altered or enhanced NAA50-mediated NTA. In plants lacking EDR1, NAA50 is not properly activated during these events, resulting in enhanced ER stress and senescence.

Material and Methods

Plant Material and Growth Conditions

Arabidopsis thaliana accession Col-0, and Col-0 mutants *edr1-1* (Frye and Innes 1998), *naa50-1* (SAIL_210_A02), and *naa50-2* (SAIL_1186_A03) were used in this study. For growth on Murashige and Skoog (MS) plates, seeds were surface sterilized with a solution of hydrogen peroxide and ethanol (1:19) and planted on one-half-strength MS plates supplemented with 0.8% agar. For soil-grown plants, seed was directly sowed onto Pro-Mix PGX Biofungicide plug and germination mix supplemented with Osmocote 14-14-14 fertilizer (ICL Fertilizers). Plates and flats were placed at 4ºC for 48 hours for stratification before being transferred to a growth room set to 23ºC and 12 hour light (150 µEm-2s-1)/12 hour dark cycle. For transient expression experiments, *Nicotiana benthamiana* was grown under the same growth room conditions as *A. thaliana*.

Plasmid Construction and Generation of Transgenic Arabidopsis Plants

NAA50 clones were derived by PCR amplification using cDNA from Col-0. Site-directed mutagenesis was utilized to introduce the I145A and Y34A mutations into *NAA50* (Qi and Scholthof, 2008). All primers used in this study for cloning and site-directed mutagenesis are listed in Table 3-1.

For yeast-two hybrid assays, the full-length open reading frames of EDR1, EDR1 (D810A), and Lamin (LAM) were cloned into the DNA-binding domain vector pGBKT7 (Clontech Matchmaker System). The full-length open reading frame of NAA50, and the SV40 Large T Antigen (T) were cloned into pGADT7. EDR1 full-length wild-type cDNA

and EDR1ST (D810A) were cloned into pGBKT7 using SmaI and SalI restriction sites. NAA50 was cloned into pGADT7 using ClaI and XhoI restriction sites.

For transient expression in *N. benthamiana*, NAA50 was cloned into the cauliflower mosaic virus 35S promoter vector pEarleyGate100 (Earley et al., 2006) using a modified multisite Gateway recombination cloning system (Invitrogen) as described in (Qi et al., 2012). EDR1-sYFP and EDR1ST-sYFP were cloned into the dexamethasone-inducible pBAV154 (Vinatzer et al., 2006) using multisite Gateway cloning. A sYFP-tagged 5xMYC construct was generated in pEarlyGate100 using multisite gateway cloning.

For the generation of amiRNA transgenic plants, a *NAA50*-specific amiRNA construct was created by PCR amplification following the procedures of Schwab et al. (2006), which included insertion of the *NAA50* sequence flanked by regions of the MIR319 microRNA. The resulting amiRNA construct was cloned into pBAV154 and PMDC32 (Qi and Katagiri, 2009) using Gateway cloning.

To generate transgenic plants containing NAA50-sYFP under the control of a native promoter, the 297 nucleotides upstream of the NAA50 start site were cloned into PMDC32 using KpnI and HindIII restriction sites. NAA50^{I145A} and NAA50^{Y34A} were generated using site-directed mutagenesis (Qi and Scholthof, 2008), and cloned into PMDC32 containing the NAA50 native promoter with a C-terminal 3xHA tag using multisite Gateway cloning.

Transgenic plants were generated using the floral dip method (Clough and Bent, 1998). Plasmids were transformed into Agrobacterium strain GV3101 (pMP90) by electroporation with selection on Luria-Bertani plates containing 50 µg/mL kanamycyin sulfate (Sigma-Aldrich) and 20 µg/mL gentamicin (Gibco). Selection of transgenic plants

carrying a BASTA resistance cassette was performed by spraying 1-week old seedlings with 300 µM BASTA (Finale), or by selection on MS plates supplemented with 300 µM BASTA. Selection of plants carrying a hygromycin resistance cassette was performed by germinating seed on MS plates supplemented with 20 µg/mL hygromycin (Fischer Scientific).

For expression in *E. coli*, NAA50 was cloned into pDEST17 using Gateway cloning. The resulting plasmid was transformed into *E. coli* strain BL21.AI (Invitrogen).

Yeast Two-Hybrid Assays

For yeast two-hybrid assays between EDR1 and NAA50, pGBKT7 and pGADT7 clones were transformed into haploid yeast strain AH109 (Clontech) by electroporation and selected on SD-Trp-Leu medium. Successful transformants were selected after 48 hours of growth at 30ºC and then struck onto fresh SD-Trp-Leu medium and allowed to grow for another 48 hours. Before carrying out yeast two-hybrid assays, yeast was grown in liquid SD-Trp-Leu medium for 16 hours at 30ºC. Cultures were re-suspended in water to an OD_{600} of 1.0, serially diluted, and plated on appropriate SD media. Plates were grown for up to 4 days at 30ºC.

Immunoprecipitations and Immunoblots

For total protein extraction, tissue was ground in lysis buffer (50 mM Tris-HCl, pH 7.5, 150 mM NaCl, 0.1% Nonidet P-40, 1% Plant Proteinase Inhibitor Cocktail [Sigma], and 50 mM 2,2′-Dithiodipyridine [Sigma]) or, for co-IPs, IP Buffer (50 mM Tris, pH 7.5, 150 mM NaCl, 1mM EDTA, 0.1% Nonidet P-40, 10% glycerol, 1% Plant Proteinase

Inhibitor Cocktail [Sigma], and 50 mM 2,2′-Dithiodipyridine [Sigma]). For expression of dexamethasone-inducible proteins, plants were sprayed with a 50 μM dexamethasone solution containing 0.02% (v/v) Silwet L-77 (OSi Specialties) 16 hours before tissue was harvested. Samples were centrifuged at 10,000 g at 4°C for 5 minutes, and supernatants were transferred to new tubes.

Immunoprecipitations were performed as described previously (Shao et al., 2003) using GFP-Trap_A (Chromotek). Total proteins were mixed with 1 volume of 2x Laemmli sample buffer, supplemented with 5% β-mercaptoethanol, 1% Protease Inhibitor Cocktail (Sigma), and 50 mM 2,2′-Dithiodipyridine (Sigma). Samples were then boiled for 5-10 minutes before loading. Total proteins and/or immunocomplexes were separated by electrophoresis on a 4-20% Mini-PROTEAN TGX Stain-Free protein gel (Bio-Rad). Proteins were transferred to a nitrocellulose membrane and probed with anti-HA-HRP (3F10) (Sigma), mouse anti-GFP (ab6556) (Abcam), and goat anti-mouse-HRP antibodies (A-10668) (Invitrogen).

For protein extraction from yeast, yeast grown on solid SD -Leu, -Trp plates were resuspended in lysis buffer (100 mM NaCl, 50 mM Tris-Cl, pH 7.5, 50 mM NaF, 50 mM Na-β-glycerophosphate, pH 7.4, 2 mM EGTA, 2 mM EDTA, 0.1% Triton X-100, 1 mM Na_3VO_4). Glass beads were then added to the suspension and the solution was vortexed for 1 minute three times. After the addition of 1 volume of 2x Laemmli sample buffer supplemented with 5% β-mercaptoethanol, samples were boiled for 10 minutes. Immunoblots were performed using anti-HA-HRP (3F10) (Sigma), mouse anti-GAL4DBD (RK5C1) (Santa Cruz Biotechnology), goat anti-mouse-HRP (A-10668) (Invitrogen),

antibodies. Visualization of immunoblots from yeast strains used in two-hybrid assay were performed using the KwikQuant Imager (Kindle Biosciences).

Fluorescence and Light Microscopy

Confocal laser scanning microscopy was performed on a Leica TCS SP8 confocal microscope (Leica Microsystems) equipped with a 63X, 1.2-numerical aperture water objective lens and a White Light Laser. sYFP fusions were excited at 514-nm and detected using a 522 to 545 nm band-pass emission filter. mCherry fusions were excited at 561 nm and detected using a custom 595 to 620 nm band-pass emission filter.

To capture detailed images of Arabidopsis roots, images were captured using a Stemi 305 compact Greenough stereo microscope (Zeiss). Digital images were captured using Labscope software (Zeiss).

Quantitative-PCR

For RT-PCR and quantitative RT-PCR experiments, RNA was extracted using the Spectrum plant total RNA kit (Sigma-Aldrich) according to manufacturer's instructions. cDNA was produced from 1 µg total RNA using the Verso cDNA synthesis kit (Thermo Fisher Scientific). Relative RNA amounts were determined by quantitative RT-PCR using the Power Up SYBR Green Master Mix (Thermo Fisher Scientific). A comparative Ct method was used to determine relative quantities (Schmittgen and Livak, 2008). *ACTIN2* was used for normalization.

NAA50 Knockdown Transcriptome Profiling

For RNA sequencing, plants were first sprayed with a solution containing 50 μM dexamethasone and 0.02% (v/v) Silwet L-77 (OSi Specialties) 24 hours, 12 hours, and immediately before tissue collection. Three biological replicates were performed per genotype per treatment, each consisting of approximately 0.4 g leaf tissue taken from the 4th leaf of 4 unique plants. RNA was extracted from 4-week-old Arabidopsis leaves using the Spectrum plant total RNA kit (Sigma-Aldritch) according to manufacturer's instructions.

Total RNA was prepared into equimolar pools for each sample submitted to Indiana University's Center for Genomics and Bioinformatics for cDNA library construction using a TruSeq Stranded mRNA LT Sample Prep Kit (Illumina) following the standard manufacturing protocol. Sequencing was performed using an Illumina NextSeq500 platform with 75 cycle sequencing kit generating 84bp single-end reads. After the sequencing run, demultiplexing was performed with bcl2fastq v2.20.0.422.

Trimmomatic (1; version 0.33; non-default parameters = ILLUMINACLIP<adapter_file>:2:20:6 LEADING:3 TRAILING:3 SLIDINGWINDOW:4:20 MINLEN:35) was used to trim reads of adapter and low-quality bases. Reads were mapped to the *Arabidopsis thaliana* genome using STAR with the final parameters (4; version 2.5.2a; --outSAMattributes All --outSAMunmapped Within --outReadsUnmapped Fastx --outFilterMultimapNmax 1 --seedSearchStartLmax 25 --chimSegmentMin 20 --quantMode GeneCounts --twopassMode Basic --outWigType wiggle --outWigStrand Unstranded --outWigNorm None --sjdbGTFtagExonParentTranscript Parent --sjdbGTFtagExonParentGene ID --outSAMtype BAM SortedByCoordinate). Read counts

were determined using a custom perl script. Differential expression comparisons of all features with 5 or more reads (in total across all samples) were carried out with DESeq2 (2; R package version 3.4.0) along with the IHW (3) package to adjust for multiple testing procedures.

Identification of significantly altered transcripts was performed by comparing ‘DEX:NAA50-ami’ and ‘DEX:Scrambled-ami’ datasets. Transcripts which differed significantly (adjusted *P*-value <0.05) between the ‘DEX:NAA50-ami’ and ‘DEX:Scrambled-ami’ datasets were then analyzed to determine whether expression had increased or decreased relative to the ‘DEX:NAA50-ami 0 hr’ dataset. Those transcripts which were significantly (adjusted *P*-value <0.05 and $\log_2$ fold-change >1.5) up- or downregulated relative to the ‘DEX:NAA50-ami 0 Hr’ dataset were then used for GO term enrichment analysis. Gene Ontology (GO) term enrichment analysis was performed in Cytoscape using the BiNGO app (Maere et al., 2005).

Transcriptome similarity analysis was performed using the Genevestigator Signature tool (https://genevestigator.com/gv/doc/signature.jsp). For this analysis, a list of the 330 most significantly altered (greatest $\log_2$ fold-change) transcripts at 12 hours was used as input. A heatmap comparing this input to similar transcriptomes was generated using the Heatmapper Expression tool (http://www2.heatmapper.ca/expression) (Babicki et al., 2016).

Trypan Blue Staining

Trypan blue staining of Arabidopsis roots was performed by soaking seedlings in a solution of 10 mg/mL trypan blue (Sigma) in water for twenty minutes. Seedlings were then washed three times with deionized water.

ER Stress Treatments

ER stress treatments of Arabidopsis seedlings were performed by growing seeds directly on MS plates supplemented with TM (Sigma) or DTT (Bio-Rad). For treatment of adult plants, TM was injected directly into one half of an Arabidopsis leaf using a needleless syringe.

***In Vitro* Acetylation Assays**

E. coli strain BL21.AI was transformed with a pDEST17 vector carrying NAA50. 5xHIS-tagged NAA50 was purified from *E. coli* using a Nickel-His column (Sigma). A 5 mL culture was incubated at 37ºC for 16 hours, and then subcultured to a final volume of 100 mL. The culture was grown until the OD_{600} reached 0.5. Expression of NAA50 was induced by adding 1 mM IPTG and 0.2% Arabinose to the culture. The culture was then incubated at 30ºC for 3 hours. Cells were then harvested and resuspended in 8 mL of Native Purification Buffer (50 mM NaH2PO4, 500 mM NaCl) supplemented with 8 mg lysozyme and a protease inhibitor tablet (Roche). The suspension was then incubated on ice for thirty minutes, and then sonicated. After sonication, the cell debris was pelleted by centrifugation (5,000 x g, 15 minutes) at 4ºC. The Ni-NTA resin was washed twice with Native Purification Buffer and then incubated with the lysate for 1 hour at 4ºC. The resin

was then washed 4 times with Wash Buffer (Native Purification Buffer supplemented with 6 mM Imidazole). Fractions were eluted with Elution Buffer (Native Purification Buffer supplemented with 250 mM Imidazole).

For *in vitro* auto-acetylation assays, 4 µg recombinant NAA50 was incubated with 100 µM Acetyl-Coenzyme A (Roche) in a 2X acetylation buffer (50mM Tris HCl pH 7.5, 2mM EDTA, 200mM NaCl, 10% Glycerol) at 30°C. Detection of auto-acetylation activity was performed through immunoblotting using acetylated lysine monoclonal antibody (1C6) (Invitrogen).

In vitro N-terminal acetylation assays were performed according to Foyn et al., 2017, using recombinant HIS-tagged NAA50 that was purified using the method described above. Synthetic peptides used in N-terminal acetylation assays were procured from GenScript.

Detecting NAA50-Mediated NTA by Mass Spectrometry

Liquid chromatography was performed on protein extracts from Arabidopsis seedlings and rosettes. Arabidopsis protein extraction was performed by grinding tissue in lysis buffer (50mM Tris-HCl pH 7.5, 150mM NaCl, 0.5% NP-40). Plant cell debris was pelleted by centrifugation (10 minutes, 10,000g). For protein extraction from *E. coli*, cultures were resuspended in lysis buffer (50 mM Tris-HCl pH 7.5, 50mM NaCl, 5% glycerol). Cultures were then sonicated and cell debris pelleted (5 minutes, 5,000g). Protein was precipitated using TCA/ethanol

Protein samples were resuspended and denatured in 8M urea with 100mM ammonium bicarbonate, pH 7.8. Disulfide bonds were reduced by incubation for 45

minutes at 57°C with a final concentration of 10mM Tris (2-carboxyethyl) phosphine hydrochloride (C4706, Sigma Aldrich). A final concentration of 20 mM iodoacetamide (I6125, Sigma Aldrich) was then added to alkylate these side chains and the reaction was allowed to proceed for one hour in the dark at 21°C. The samples were diluted to 1M urea using 100mM ammonium bicarbonate, pH 7.8. Trypsin (V5113, Promega) was added, and the samples were digested for 14 hours at 37°C.

The digested lysates were desalted using C18 SepPaks (WAT051910, Waters) and dried down. Dried pellets were resuspended in 50 µL 5mM KH2PO4 in 30% acetonitrile (34998, Sigma Aldrich), pH 2.7 (buffer A) and then fractionated using strong cation exchange chromatography on an AKTA Pure 10 (GE Healthcare) equipped with a Luna 5µm 100 angstrom 150 x 2.1 mm strong cation exchange (SCX) column (00F-4398-B0, Phenomenex). Buffer B was 350mM KCl (PX1405, EM Science) in buffer A. A 200 µL/min gradient was run from 0% B to 50% B over 10 mL, then up to 100% B over 1 mL. Fractions were collected and N-terminally acetylated peptides eluted between two and four mL into the gradient.

Individual fractions from the SCX chromatography were desalted using ZipTips (ZTC18S096, EMD Millipore), dried down and resuspended in 0.1% formic acid (94138, Honeywell). Fractions were analyzed by LC-MS on an Orbitrap Fusion Lumos mass spectrometer equipped with an Easy NanoLC1200 HPLC (ThermoFisher). Buffer A was 0.1% formic acid in water. Buffer B was 0.1% formic acid in 80% acetonitrile. Peptides were separated on a two-hour gradient from 0% B to 35% B. Peptides were collisionally fragmented using HCD mode. Precursor ions were measured in the Orbitrap with a

resolution of 120,000. Fragment ions were measured in the Orbitrap with a resolution of 60,000.

LC-MS/MS data generated from *E. coli* was searched against an *Eschericia coli* database (strain K12) downloaded from Uniprot. LC-MS/MS data generated from Arabidopsis was searched against an *Arabidopsis thaliana* database downloaded from Uniprot. Proteome Discoverer version 2.1.1.21 (ThermoScientific) was used to interpret the MS/MS files. Data was searched using the Sequest HT algorithm and the results were filtered via Percolator with a decoy database false discovery rate (FDR) set to < 1%. The database search parameters were set as follows: two missed trypsin cleavage sites were allowed per peptide. A mass tolerance of 5 ppm and 0.04 Da were used for precursor and fragment ions, respectively. Oxidation of methionine, pyroglutamine on peptide amino termini and protein N-terminal acetylation were set as variable modifications. Carbamidomethylation was set as a fixed modification

Accession Numbers

Arabidopsis sequence data is available under the following AGI accession numbers: EDR1 (At1g08720), NAA50 (At5g11340), γ-TIP (At2g36830), NAA10 (AT5G13780), SDF2 (AT2G25110). RNA sequencing data is accessible through the NCBI GEO database (GSE145580).

Table 3-1. Primers used in this study.

Name	Description	Sequence	Citation
attb1-NAA50 F	NAA50 Gateway Cloning	GGGGACAAGTTTGTACAAAAAAGCAGGCTATGGGAGCTGGGAGA	
attb4-NAA50 R	NAA50 Gateway Cloning	GGGGACAACTTTGTATAGAAAAGTTGGGTGTTTGTTGGCTTCAGA	
attP1-NAA50 F	NAA50 Gateway Cloning	GGGGACAAGTTTGTACAAAAAAGCAGGCTTAATGGGAGCTGGGAGAGAAGT	
attP2-NAA50 R	NAA50 Gateway Cloning	GGGGACCACTTTGTACAAGAAAGCTGGGTTTCATTTGTTGGCTTCAGATT	
XHOI-NAA50 R	for PGADT7	CGCGCTCGAG TCATTTGTTGGCTTCAGA	
CLAI-NAA50 F	for PGADT7	GCGCATCGATAC ATGGGAGCTGGGAGAGAA	
T7 F	Sequencing	TAATACGACTCACTATAGGGC	
PGADT7 INS R	Sequencing	AGATGGTGCACGATGCACAG	
PGBKT7 INS R	Sequencing	TAGCTTGGCTGCAAGCGCGC	
pNAA50 KpnI R	For PMDC32 NAA50 Native Promoter	GCGCGGTACCCGCCGTCGAACAATCTAG	
pNAA50 HindIII F2	For PMDC32 NAA50 Native Promoter	GCTCAAGCTTAATGAAACCTCTGGGTGG	
LB3	Genotyping SAIL TDNA lines	GCATCTGAATTTCATAACCAATCTCGATACAC	
NAA50-1 TDNA F	Genotyping SAIL TDNA lines	TCACTGTGAATAAATGGCACG	
NAA50-1 TDNA R	Genotyping SAIL TDNA lines	TATTTCATTGCAGTTGCTTGG	
NAA50-2 TNDA F	Genotyping SAIL TDNA lines	TCACTTTTGTGAAACCCTTGG	
NAA50-2 TDNA R	Genotyping SAIL TDNA lines	CCAAACGAAAATGTCCAAAGCC	
SmaI-EDR1 F	EDR1 pgbkt7 cloning	GAGCCCGGGGATGAAGCATATTTTCAAGAAGC	
SalI-EDR1 R	EDR1 pgbkt7 cloning	ACCGGTCGACCTATTGTGGTGTAGGAAGTACA	
NAA50 ami1 I	NAA50 amiRNA cloning	gaTTATAAACTCGCATGGCGCCAtctctcttttgtattcc	
NAA50 ami1 II	NAA50 amiRNA cloning	gaTGGCGCCATGCGAGTTTATAAtcaaagagaatcaatga	
NAA50 ami1 III	NAA50 amiRNA cloning	gaTGACGCCATGCGACTTTATATtcacaggtcgtgatatg	
NAA50 ami1 IV	NAA50 amiRNA cloning	gaATATAAAGTCGCATGGCGTCAtctacatatatattcct	
NAA10 B1 F	Naa10 Gateway Cloning	GGGGACAAGTTTGTACAAAAAAGCAGGCTATGGTTTGCATCAGGC	
NAA10 B4R-2	Naa10 Gateway Cloning	GGGGACAACTTTGTATAGAAAAGTTGGGTGTTTGGAAACTGCTTTACC	
NAA50 I145A MF	PCR Mutagenesis	CATCAACGCTGAGCCAAGAGATTGCTACG	
NAA50 I145A MR	PCR Mutagenesis	CTTGGCTCAGCGTTGATGTAATAGTTTTG	
NAA50 P31A MF	PCR Mutagenesis	CTCAACACGGTTTTGTTCGCGGTTCGTTAC	
NAA50 P31A MR	PCR Mutagenesis	CTTGTCGTTGTAACGAACCGCGAACAAAACC	
NAA50 F30A MF	PCR Mutagenesis	GATACTCAACACGGTTTTGGCCCCGGTTCG	
NAA50 F30A MR	PCR Mutagenesis	GTCGTTGTAACGAACCGGGGCCAAAACCG	
NAA50 Y34A MF	PCR Mutagenesis	CCGGTTCGTGCCAACGACAAGTACTACGCC	
NAA50 Y34A MR	PCR Mutagenesis	CTTGTCGTTGGCACGAACCGGGAACAAAACCG	
ACTIN2 RTF	qPCR and RT PCR	AGTGGTCGTACAACCGGTATTGT	
ACTIN2 RTR	qPCR and RT PCR	GATGGCATGAGGAAGAGAGAAAC	
NAA50 RT F2	qPCR and RT PCR	GTGGGGCCATGCGAGTTTAT	
NAA50 RT R2	qPCR and RT PCR	TGCGTCTTCGTTGTTTGTCTG	
bZIP60F4	RT-PCR	GAAGGAGACGATGATGCTGTGGCT	Deng et al., 2011
bZ60UB1 R	RT-PCR	GCAGGGATTCCAACAAGAGCACAG	Deng et al., 2011
bZ60SB2 R	RT-PCR	AGCAGGGAACCCAACAGCAGACT	Deng et al., 2011
CNX1_qRT216f	qPCR	TGCTACTGTGACGATCAAACG	Kim et al., 2018
CNX1_qRT321r	qPCR	CATGCTTCCATACACCTTCG	Kim et al., 2018
SEC31A_qRT2142f	qPCR	GATTTCTCTGTATGCAGAACCTGA	Kim et al., 2018
SEC31A_qRT2231r	qPCR	GATTTCTCTTGATATGGATTGGAAA	Kim et al., 2018

Literature Cited

Aksnes, H., Van Damme, P., Goris, M., Starheim, Kristian K., Marie, M., Støve, Svein I., Hoel, C., Kalvik, Thomas V., Hole, K., Glomnes, N., Furnes, C., Ljostveit, S., Ziegler, M., Niere, M., Gevaert, K. and Arnesen, T. (2015) An organellar N-acetyltransferase, Naa60, acetylates cytosolic N termini of transmembrane proteins and maintains Golgi integrity. Cell Reports **10:** 1362-1374.

Aksnes, H., Drazic, A., Marie, M. and Arnesen, T. (2016) First things first: vital protein marks by N-terminal acetyltransferases. Trends in Biochemical Sciences **41:** 746-760.

Arnesen, T., Anderson, D., Torsvik, J., Halseth, H.B., Varhaug, J.E. and Lillehaug, J.R. (2006) Cloning and characterization of hNat5/hSan: an evolutionarily conserved component of the NatA protein N-α-acetyltransferase complex. Gene **371:** 291-295.

Arnesen, T., Van Damme, P., Polevoda, B., Helsens, K., Evjenth, R., Colaert, N., Varhaug, J.E., Vandekerckhove, J., Lillehaug, J.R., Sherman, F. and Gevaert, K. (2009) Proteomics analyses reveal the evolutionary conservation and divergence of N-terminal acetyltransferases from yeast and humans. Proceedings of the National Academy of Sciences **106:** 8157.

Arnesen, T., Starheim, K.K., Van Damme, P., Evjenth, R., Dinh, H., Betts, M.J., Ryningen, A., Vandekerckhove, J., Gevaert, K. and Anderson, D. (2010) The chaperone-like protein HYPK acts together with NatA in cotranslational N-terminal acetylation and prevention of Huntingtin aggregation. Molecular and Cellular Biology **30:** 1898-1909.

Arnesen, T. (2011) Towards a functional understanding of protein N-terminal acetylation. PLOS Biology **9:** e1001074.

Babicki, S., Arndt, D., Marcu, A., Liang, Y., Grant, J.R., Maciejewski, A. and Wishart, D.S. (2016) Heatmapper: web-enabled heat mapping for all. Nucleic acids research **44:** W147-W153.

Bao, Y. and Howell, S.H. (2017) The unfolded protein response supports plant development and defense as well as responses to abiotic stress. Frontiers in Plant Science **8**.

Bao, Y., Bassham, D.C. and Howell, S.H. (2019) A functional unfolded protein response is required for normal vegetative development. Plant Physiology **179:** 1834.

Bowling, S.A., Guo, A., Cao, H., Gordon, A.S., Klessig, D.F. and Dong, X. (1994) A mutation in Arabidopsis that leads to constitutive expression of systemic acquired resistance. The Plant Cell **6:** 1845-1857.

Brown, J.L. and Roberts, W.K. (1976) Evidence that approximately eighty per cent of the soluble proteins from Ehrlich ascites cells are Nalpha-acetylated. Journal of Biological Chemistry **251:** 1009-1014.

Cho, Y. and Kanehara, K. (2017) Endoplasmic reticulum stress response in Arabidopsis roots. Frontiers in Plant Science **8**.

Christiansen, K.M., Gu, Y., Rodibaugh, N. and Innes, R.W. (2011) Negative regulation of defence signalling pathways by the EDR1 protein kinase. Molecular Plant Pathology **12:** 746-758.

Clough, S.J. and Bent, A.F. (1998) Floral dip: a simplified method for Agrobacterium-mediated transformation of *Arabidopsis thaliana*. The Plant Journal **16:** 735-743.

Das, S. and Bhattacharyya, N.P. (2016) Huntingtin interacting protein HYPK is a negative regulator of heat shock response and is downregulated in models of Huntington's Disease. Experimental Cell Research **343:** 107-117.

Deng, Y., Humbert, S., Liu, J.-X., Srivastava, R., Rothstein, S.J. and Howell, S.H. (2011) Heat induces the splicing by IRE1 of a mRNA encoding a transcription factor involved in the unfolded protein response in Arabidopsis. Proceedings of the National Academy of Sciences of the United States of America **108:** 7247-7252.

Deng, Y., Srivastava, R. and Howell, S.H. (2013) Protein kinase and ribonuclease domains of IRE1 confer stress tolerance, vegetative growth, and reproductive development in Arabidopsis. Proceedings of the National Academy of Sciences **110:** 19633-19638.

Deng, Y., Srivastava, R., Quilichini, T.D., Dong, H., Bao, Y., Horner, H.T. and Howell, S.H. (2016) IRE1, a component of the unfolded protein response signaling pathway, protects pollen development in Arabidopsis from heat stress. The Plant Journal **88:** 193-204.

Dinh, T.V., Bienvenut, W.V., Linster, E., Feldman-Salit, A., Jung, V.A., Meinnel, T., Hell, R., Giglione, C. and Wirtz, M. (2015) Molecular identification and functional characterization of the first Nα-acetyltransferase in plastids by global acetylome profiling. PROTEOMICS **15:** 2426-2435.

Duan, Y., Zhang, W., Li, B., Wang, Y., Li, K., Sodmergen, Han, C., Zhang, Y. and Li, X. (2010) An endoplasmic reticulum response pathway mediates programmed cell death of root tip induced by water stress in Arabidopsis. New Phytologist **186:** 681-695.

Earley, K.W., Haag, J.R., Pontes, O., Opper, K., Juehne, T., Song, K. and Pikaard, C.S. (2006) Gateway-compatible vectors for plant functional genomics and proteomics. The Plant Journal **45:** 616-629.

Evjenth, R., Hole, K., Karlsen, O.A., Ziegler, M., Arnesen, T. and Lillehaug, J.R. (2009) Human Naa50p (Nat5/San) displays both protein Nα- and Nϵ-acetyltransferase activity. Journal of Biological Chemistry **284:** 31122-31129.

Feng, J., Li, R., Yu, J., Ma, S., Wu, C., Li, Y., Cao, Y. and Ma, L. (2016) Protein N-terminal acetylation is required for embryogenesis in Arabidopsis. Journal of Experimental Botany **67:** 4779-4789.

Ferrández-Ayela, A., Micol-Ponce, R., Sánchez-García, A.B., Alonso-Peral, M.M., Micol, J.L. and Ponce, M.R. (2013) Mutation of an Arabidopsis NatB N-alpha-terminal acetylation complex component causes pleiotropic developmental defects. PLOS ONE **8:** e80697.

Forte, G.M.A., Pool, M.R. and Stirling, C.J. (2011) N-terminal acetylation inhibits protein targeting to the endoplasmic reticulum. PLOS Biology **9:** e1001073.

Foyn, H., Thompson, P.R. and Arnesen, T. (2017) DTNB-based quantification of *in vitro* enzymatic N-terminal acetyltransferase activity. Protein Terminal Profiling: Methods in Molecular Biology **1574:** 9-15.

Frye, C.A. and Innes, R.W. (1998) An Arabidopsis mutant with enhanced resistance to powdery mildew. The Plant Cell **10:** 947-956.

Frye, C.A., Tang, D. and Innes, R.W. (2001) Negative regulation of defense responses in plants by a conserved MAPKK kinase. Proc Natl Acad Sci U S A. **98:** 373-378.

Gautschi, M., Just, S., Mun, A., Ross, S., Rücknagel, P., Dubaquié, Y., Ehrenhofer-Murray, A. and Rospert, S. (2003) The yeast Nα-acetyltransferase NatA is quantitatively anchored to the ribosome and interacts with nascent polypeptides. Molecular and Cellular Biology **23:** 7403-7414.

Gibbs, C.S. and Zoller, M.J. (1991) Rational scanning mutagenesis of a protein kinase identifies functional regions involved in catalysis and substrate interactions. J. Biol. Chem. **266:** 8923–8931.

Greenberg, J.T. and Yao, N. (2004) The role and regulation of programmed cell death in plant–pathogen interactions. Cellular Microbiology **6:** 201-211.

Gu, Y. and Innes, R.W. (2011) The KEEP ON GOING of Arabidopsis recruits the ENHANCED DISEASE RESISTANCE1 protein to trans-Golgi network/early endosome vesicles. Plant Physiology **155:** 1827-1838.

Gu, Y. and Innes, R.W. (2012) The KEEP ON GOING protein of Arabidopsis regulates intracellular protein trafficking and is degraded during fungal infection. The Plant Cell **24:** 4717-4730.

Hruz, T., Laule, O., Szabo, G., Wessendorp, F., Bleuler, S., Oertle, L., Widmayer, P., Gruissem, W. and Zimmermann, P. (2008) Genevestigator v3: a reference expression database for the meta-analysis of transcriptomes. Advances in Bioinformatics **2008:** 5.

Huber, M., Bienvenut, W.V., Linster, E., Stephan, I., Armbruster, L., Sticht, C., Layer, D.C., Lapouge, K., Meinnel, T., Sinning, I., Giglione, C., Hell, R. and Wirtz, M. (2019) Natb-mediated n-terminal acetylation affects growth and abiotic stress responses. Plant Physiology pp.00792.2019.

Hunter, T. (2007) The age of crosstalk: phosphorylation, ubiquitination, and beyond. Molecular cell **28:** 730-738.

Huot, B., Yao, J., Montgomery, B.L. and He, S.Y. (2014) Growth-defense tradeoffs in plants: a balancing act to optimize fitness. Molecular Plant **7:** 1267-1287.

Iwata, Y., Fedoroff, N.V. and Koizumi, N. (2008) Arabidopsis bZIP60 is a proteolysis-activated transcription factor involved in the endoplasmic reticulum stress response. The Plant Cell **20:** 3107-3121.

Iwata, Y., Iida, T., Matsunami, T., Yamada, Y., Mishiba, K.-i., Ogawa, T., Kurata, T. and Koizumi, N. (2018) Constitutive BIP protein accumulation in Arabidopsis mutants defective in a gene encoding chloroplast-resident stearoyl-acyl carrier protein desaturase. Genes to Cells **23:** 456-465.

Kachroo, P., Shanklin, J., Shah, J., Whittle, E.J. and Klessig, D.F. (2001) A fatty acid desaturase modulates the activation of defense signaling pathways in plants. Proceedings of the National Academy of Sciences **98:** 9448-9453.

Kim, J.-S., Yamaguchi-Shinozaki, K. and Shinozaki, K. (2018) ER-anchored transcription factors bZIP17 and bZIP28 regulate root elongation. Plant Physiology **176:** 2221.

Li, X., Clarke, J.D., Zhang, Y. and Dong, X. (2001) Activation of an EDS1-mediated R-gene pathway in the SNC1 mutant leads to constitutive, NPR1-independent pathogen resistance. Molecular Plant-Microbe Interactions **14:** 1131-1139.

Linster, E., Stephan, I., Bienvenut, W.V., Maple-Grødem, J., Myklebust, L.M., Huber, M., Reichelt, M., Sticht, C., Geir Møller, S., Meinnel, T., Arnesen, T., Giglione, C., Hell, R. and Wirtz, M. (2015) Downregulation of N-terminal acetylation triggers ABA-mediated drought responses in Arabidopsis. Nature Communications **6:** 7640.

Liszczak, G., Arnesen, T. and Marmorstein, R. (2011) Structure of a ternary Naa50p (Nat5/San) N-terminal acetyltransferase complex reveals the molecular basis for substrate-specific acetylation. Journal of Biological Chemistry **286:** 37002-37010.

Liu, J.-X. and Howell, S.H. (2010) Endoplasmic reticulum protein quality control and its relationship to environmental stress responses in plants. The Plant Cell **22:** 2930-2942.

Maere, S., Heymans, K. and Kuiper, M. (2005) BiNGO: a Cytoscape plugin to assess overrepresentation of gene ontology categories in biological networks. Bioinformatics **21:** 3448-3449.

Moreno, A.A., Mukhtar, M.S., Blanco, F., Boatwright, J.L., Moreno, I., Jordan, M.R., Chen, Y., Brandizzi, F., Dong, X., Orellana, A. and Pajerowska-Mukhtar, K.M. (2012) IRE1/bZIP60-mediated unfolded protein response plays distinct roles in plant immunity and abiotic stress responses. PLOS ONE **7:** e31944.

Nawrath, C. and Métraux, J.-P. (1999) Salicylic acid induction–deficient mutants of Arabidopsis express PR-2 and PR-5 and accumulate high levels of camalexin after pathogen inoculation. The Plant Cell **11:** 1393-1404.

Nekrasov, V., Li, J., Batoux, M., Roux, M., Chu, Z.-H., Lacombe, S., Rougon, A., Bittel, P., Kiss-Papp, M., Chinchilla, D., van Esse, H.P., Jorda, L., Schwessinger, B., Nicaise, V., Thomma, B.P.H.J., Molina, A., Jones, J.D.G. and Zipfel, C. (2009) Control of the pattern-recognition receptor EFR by an ER protein complex in plant immunity. The EMBO journal **28:** 3428-3438.

Nelson, B.K., Cai, X. and Nebenführ, A. (2007) A multicolored set of in vivo organelle markers for co-localization studies in Arabidopsis and other plants. The Plant Journal **51:** 1126-1136.

Pesaresi, P., Gardner, N.A., Masiero, S., Dietzmann, A., Eichacker, L., Wickner, R., Salamini, F. and Leister, D. (2003) Cytoplasmic N-terminal protein acetylation is required for efficient photosynthesis in Arabidopsis. The Plant Cell **15:** 1817.

Polevoda, B. and Sherman, F. (2003) Composition and function of the eukaryotic N-terminal acetyltransferase subunits. Biochemical and Biophysical Research Communications **308:** 1-11.

Polevoda, B., Arnesen, T. and Sherman, F. (2009) A synopsis of eukaryotic Nα-terminal acetyltransferases: nomenclature, subunits and substrates. BMC Proceedings **3:** S2.

Qi, D. and Scholthof, K.-B.G. (2008) A one-step PCR-based method for rapid and efficient site-directed fragment deletion, insertion, and substitution mutagenesis. Journal of Virological Methods **149:** 85-90.

Qi, Y. and Katagiri, F. (2009) Purification of low-abundance Arabidopsis plasma-membrane protein complexes and identification of candidate components. The Plant Journal **57:** 932-944.

Qi, D., DeYoung, B.J. and Innes, R.W. (2012) Structure-function analysis of the coiled-coil and leucine-rich repeat domains of the RPS5 disease resistance protein. Plant Physiology **158:** 1819-1832.

Qiang, X., Zechmann, B., Reitz, M.U., Kogel, K.-H. and Schäfer, P. (2012) The mutualistic fungus *Piriformospora indica* colonizes Arabidopsis roots by inducing an endoplasmic reticulum stress–triggered caspase-dependent cell death. The Plant Cell **24:** 794-809.

Raychaudhuri, S., Sinha, M., Mukhopadhyay, D. and Bhattacharyya, N.P. (2007) HYPK, a Huntingtin interacting protein, reduces aggregates and apoptosis induced by N-terminal Huntingtin with 40 glutamines in Neuro2a cells and exhibits chaperone-like activity. Human Molecular Genetics **17:** 240-255.

Reddi, R., Saddanapu, V., Chinthapalli, D.K., Sankoju, P., Sripadi, P. and Addlagatta, A. (2016) Human Naa50 protein displays broad substrate specificity for amino-terminal acetylation: detailed structural and biochemical analysis using tetrapeptide library. Journal of Biological Chemistry **291:** 20530-20538.

Reis, P.A.A., Rosado, G.L., Silva, L.A.C., Oliveira, L.C., Oliveira, L.B., Costa, M.D.L., Alvim, F.C. and Fontes, E.P.B. (2011) The binding protein BIP attenuates stress-induced cell death in soybean via modulation of the N-rich protein-mediated signaling pathway. Plant Physiology **157:** 1853-1865.

Richter, K., Haslbeck, M. and Buchner, J. (2010) The heat shock response: life on the verge of death. Molecular cell **40:** 253-266.

Schmittgen, T.D. and Livak, K.J. (2008) Analyzing real-time PCR data by the comparative C_T method. Nature Protocols **3:** 1101-1108.

Schwab, R., Ossowski, S., Riester, M., Warthmann, N. and Weigel, D. (2006) Highly specific gene silencing by artificial microRNAs in Arabidopsis. The Plant Cell **18:** 1121-1133.

Serrano, I., Gu, Y., Qi, D., Dubiella, U. and Innes, R.W. (2014) The Arabidopsis EDR1 protein kinase negatively regulates the ATL1 E3 ubiquitin Ligase to suppress cell death. The Plant Cell **26:** 4532.

Shao, F., Golstein, C., Ade, J., Stoutemyer, M., Dixon, J.E. and Innes, R.W. (2003) Cleavage of Arabidopsis PBS1 by a bacterial type III effector. Science **301:** 1230-1233.

Srivastava, R., Li, Z., Russo, G., Tang, J., Bi, R., Muppirala, U., Chudalayandi, S., Severin, A., He, M., Vaitkevicius, S.I., Lawrence-Dill, C.J., Liu, P., Stapleton, A.E., Bassham, D.C., Brandizzi, F. and Howell, S.H. (2018) Response to persistent ER stress in plants: a multiphasic process that transitions cells from prosurvival activities to cell death. The Plant Cell **30:** 1220.

Tang, D., Christiansen, K.M. and Innes, R.W. (2005) Regulation of plant disease resistance, stress responses, cell death, and ethylene signaling in Arabidopsis by the EDR1 protein kinase. Plant Physiology **138**.

Tintor, N. and Saijo, Y. (2014) ER-mediated control for abundance, quality, and signaling of transmembrane immune receptors in plants. Frontiers in Plant Science **5**.

Valente, M.A.S., Faria, J.A.Q.A., Soares-Ramos, J.R.L., Reis, P.A.B., Pinheiro, G.L., Piovesan, N.D., Morais, A.T., Menezes, C.C., Cano, M.A.O., Fietto, L.G., Loureiro, M.E., Aragão, F.J.L. and Fontes, E.P.B. (2008) The ER luminal binding protein (BIP) mediates an increase in drought tolerance in soybean and delays drought-induced leaf senescence in soybean and tobacco. Journal of Experimental Botany **60:** 533-546.

van Anken, E., Romijn, E.P., Maggioni, C., Mezghrani, A., Sitia, R., Braakman, I. and Heck, A.J.R. (2003) Sequential waves of functionally related proteins are expressed when B cells prepare for antibody secretion. Immunity **18:** 243-253.

Van Damme, P., Evjenth, R., Foyn, H., Demeyer, K., De Bock, P.-J., Lillehaug, J.R., Vandekerckhove, J., Arnesen, T. and Gevaert, K. (2011) Proteome-derived peptide libraries allow detailed analysis of the substrate specificities of Nα-acetyltransferases and point to hNaa10p as the post-translational actin Nα-acetyltransferase. Molecular & Cellular Proteomics **10:** M110.004580.

Vinatzer, B.A., Teitzel, G.M., Lee, M.-W., Jelenska, J., Hotton, S., Fairfax, K., Jenrette, J. and Greenberg, J.T. (2006) The type III effector repertoire of *Pseudomonas syringae* pv. *syringae* B728a and its role in survival and disease on host and non-host plants. Molecular Microbiology **62:** 26-44.

Vitale, A. and Boston, R.S. (2008) Endoplasmic reticulum quality control and the unfolded protein response: insights from plants. Traffic **9:** 1581-1588.

Walter, P. and Ron, D. (2011) The unfolded protein response: from stress pathway to homeostatic regulation. Science **334:** 1081.

Waterhouse, A.M., Procter, J.B., Martin, D.M.A., Clamp, M. and Barton, G.J. (2009) Jalview version 2—a multiple sequence alignment editor and analysis workbench. Bioinformatics **25:** 1189-1191.

Wawrzynska, A., Christiansen, K.M., Lan, Y., Rodibaugh, N.L. and Innes, R.W. (2008) Powdery mildew resistance conferred by loss of the ENHANCED DISEASE RESISTANCE1 protein kinase is suppressed by a missense mutation in *KEEP ON GOING*, a regulator of abscisic acid signaling. Plant Physiology **148:** 1510-1522.

Williams, B., Verchot, J. and Dickman, M.B. (2014) When supply does not meet demand-ER stress and plant programmed cell death. Frontiers in Plant Science **5:** 211-211.

Woehlbier, U. and Hetz, C. (2011) Modulating stress responses by the UPRosome: a matter of life and death. Trends in Biochemical Sciences **36:** 329-337.

Xu, F., Huang, Y., Li, L., Gannon, P., Linster, E., Huber, M., Kapos, P., Bienvenut, W., Polevoda, B., Meinnel, T., Hell, R., Giglione, C., Zhang, Y., Wirtz, M., Chen, S. and Li, X. (2015) Two N-terminal acetyltransferases antagonistically regulate the stability of a nod-like receptor in Arabidopsis. The Plant Cell **27:** 1547.

Zhang, L., Xin, Z., Yu, X., Ma, C., Liang, W., Zhu, M., Cheng, Q., Li, Z., Niu, Y., Ren, Y., Wang, Z. and Lin, T. (2017) Osmotic stress induced cell death in wheat is alleviated by tauroursodeoxycholic acid and involves endoplasmic reticulum stress–related gene expression. Frontiers in Plant Science **8**.

Appendix: Arabidopsis HYPK May Regulate Plant Development and Stress Responses

Introduction

Although there is mounting evidence that NTA plays an important role in regulating plant stress signaling and development, little is known about how NAT complexes function in plants. The NatA complex has been implicated in the regulation of plant stress signaling and development (Linster et al., 2015; Feng et al., 2016). It was recently demonstrated that loss of NatB results in dwarfism and altered osmotic stress responses (Huber et al., 2019). Furthermore, I have demonstrated a role for the NatE catalytic component NAA50 in regulating plant stress signaling and development (Chapter 3). Further investigation of NAT complexes may reveal additional roles in other aspects of plant development and stress signaling.

NAT complexes are comprised of enzymatic subunits and auxiliary subunits (Polevoda et al., 2009). The NatA complex associates with the Huntingtin yeast two-hybrid protein K (HYPK) (Arnesen et al., 2010). HYPK was initially identified as an interactor of Huntingtin protein in a yeast two-hybrid screen (Faber et al., 1998). Human HYPK physically interacts with NatA through a direct interaction with Naa10 and Naa15 (Arnesen et al., 2010; Gottlieb and Marmorstein, 2018). Association with HYPK may impact the activity of NatA and NatE. The N-terminus of HYPK has been shown to negatively impact NatA acetylation activity (Weyer et al., 2017). The inhibitory effect of HYPK on NatA activity is mediated by HYPK-dependent changes to the hNaa10 active site (Gottlieb and Marmorstein, 2018). Although HYPK may inhibit NatA activity, loss of

HYPK results in reduced accumulation of Naa10 and Naa15, indicating that it is essential for the formation of the NatA complex (Arnesen et al., 2010). HYPK may also be important for NatE-mediated NTA. The association of HYPK with NatA inhibits the association of hNaa50 with the complex (Gottlieb and Marmorstein, 2018). These studies demonstrate that HYPK is an important modulator of NTA mediated by the NatA and NatE complexes.

In addition to playing a role in the regulation of N-terminal acetylation, HYPK has been implicated as an inhibitor of protein aggregation. HYPK has been shown to display chaperone-like activity (Raychaudhuri et al., 2008). Loss of HYPK results in increased aggregation of Huntingtin protein as well as apoptosis and cell cycle arrest (Arnesen et al., 2010). Although HYPK displays chaperone-like activity, HYPK displays characteristics that distinguish it from other chaperones. For instance, HYPK localizes to ribosome-associated complexes, and does not co-localize with Huntingtin aggregates (Arnesen et al., 2010). This demonstrates that the chaperone-like activity of HYPK is likely required co-translationally.

Additional work investigating the roles of NAT complex components may yield insight into the function of NTA in regulating plant development and stress signaling. Here, I describe preliminary work exploring the role of HYPK in Arabidopsis. I have demonstrated that loss of *HYPK* results in altered plant development, enhanced drought resistance, and induced UPR signaling. These results suggest that Arabidopsis HYPK may function to repress ER stress in plants.

Results

HYPK is Conserved in Arabidopsis

Although HYPK has been characterized in humans, it has not been investigated in plants. A BLAST search using the human HYPK amino acid sequence returned a single hit in *Arabidopsis thaliana*, the protein encoded by At3G06610. Human and Arabidopsis HYPK share 36.94% identity (Figure 4-1). This demonstrates that HYPK is likely conserved in plants and indicates that Arabidopsis HYPK may function similarly to human and yeast HYPK.

Figure 4-1. HYPK is conserved in Arabidopsis. An amino acid alignment between the Arabidopsis and human HYPK proteins is displayed. This alignment was generated using Clustal Omega (https://www.ebi.ac.uk/Tools/msa/clustalo/) and visualized in Jalview (Waterhouse et al., 2009).

Arabidopsis HYPK Displays ER-Like Localization

I have shown that Arabidopsis NAA50 localizes primarily to the ER (Figure 3-1E). To test whether Arabidopsis HYPK displays a similar localization, we transiently expressed a sYFP-tagged HYPK in *N. benthamiana*. HYPK-sYFP displayed an ER-like localization pattern (Figure 4-2). This demonstrates that like other Arabidopsis NAT-associated proteins, HYPK may also localize to the ER. Furthermore, it suggests that Arabidopsis HYPK may associate with the ER-localized NAA10 and NAA50.

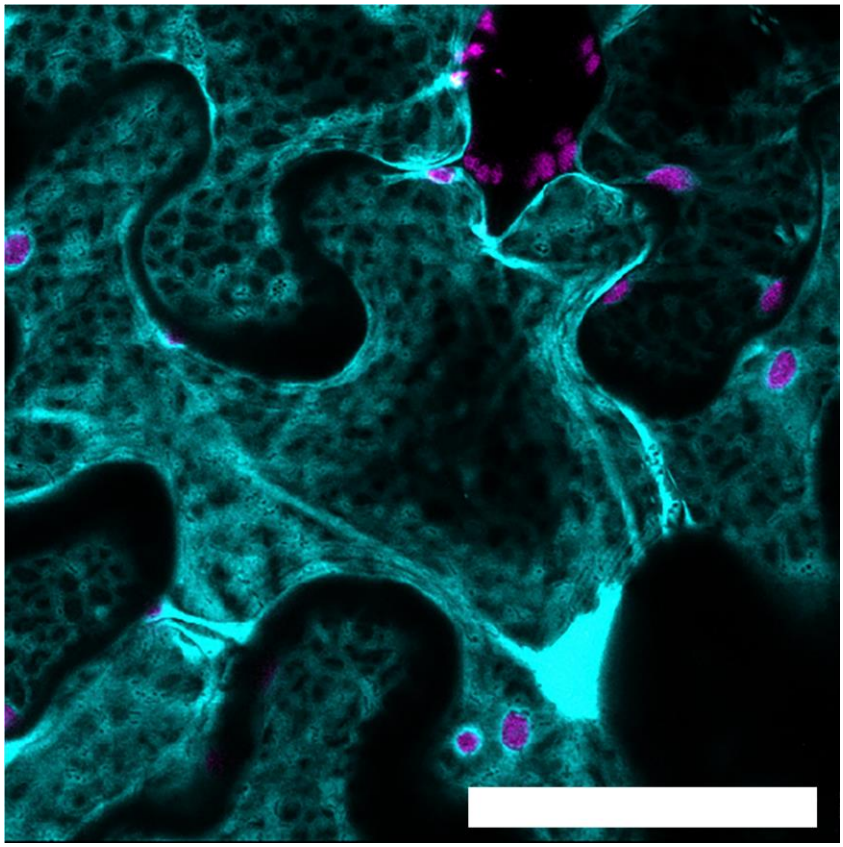

Figure 4-2. Arabidopsis HYPK displays ER-like localization. sYFP-tagged HYPK was transiently expressed in *N. benthamiana*. A z-stack image is displayed. The bar represents 50 microns.

Loss of *HYPK* Results in Developmental Defects

Given that *HYPK* is conserved (Figure 4-1), we hypothesized that *HYPK* may be essential for plant development or stress responses. To test this, we characterized a *HYPK* T-DNA insertion mutant, (SALK_080671; *hypk-1*). Adult homozygous *hypk-1* plants were dwarfed compared to wildtype and displayed altered leaf morphology (Figure 4-3). *hypk-1* plants were not sterile and produced viable seed.

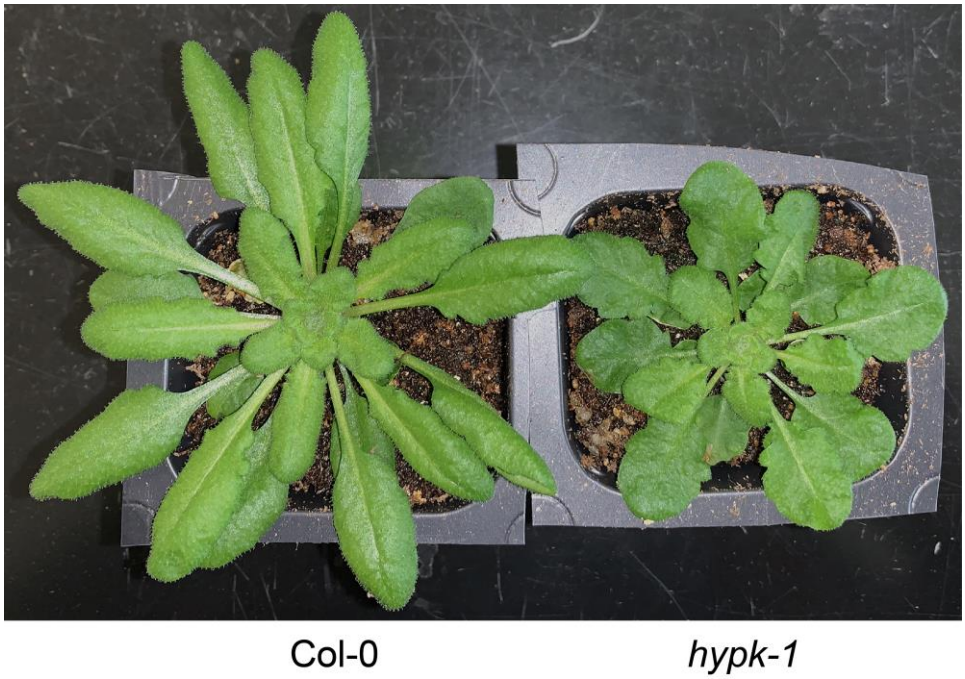

Figure 4-3. Loss of *HYPK* results in developmental defects. Representative five-week-old plants are displayed.

hypk-1 Plants Display Enhanced Drought Tolerance

Loss of the NatA components NAA10 and NAA15 has been shown to result in enhanced drought tolerance (Linster et al., 2015). Additionally, I have shown that constitutive knockdown of *NAA50* results in enhanced drought tolerance (Figure 3-5). We therefore hypothesized that loss of *HYPK* may alter plant drought tolerance. Indeed, we found that *hypk-1* plants displayed enhanced drought tolerance (Figure 4-4A). After extended periods of drought, *hypk-1* plants fared significantly better than wildtype plants and retained more fresh weight during drought treatment (Figure 4-4, B-C). That loss of *HYPK* results in enhanced drought tolerance indicates that *HYPK* may be a repressor of drought response signaling. Alternatively, loss of *HYPK* may induce a stress response that ultimately induces drought tolerance. This adds to previous observations that loss of NatA and NatE components results in enhanced drought tolerance.

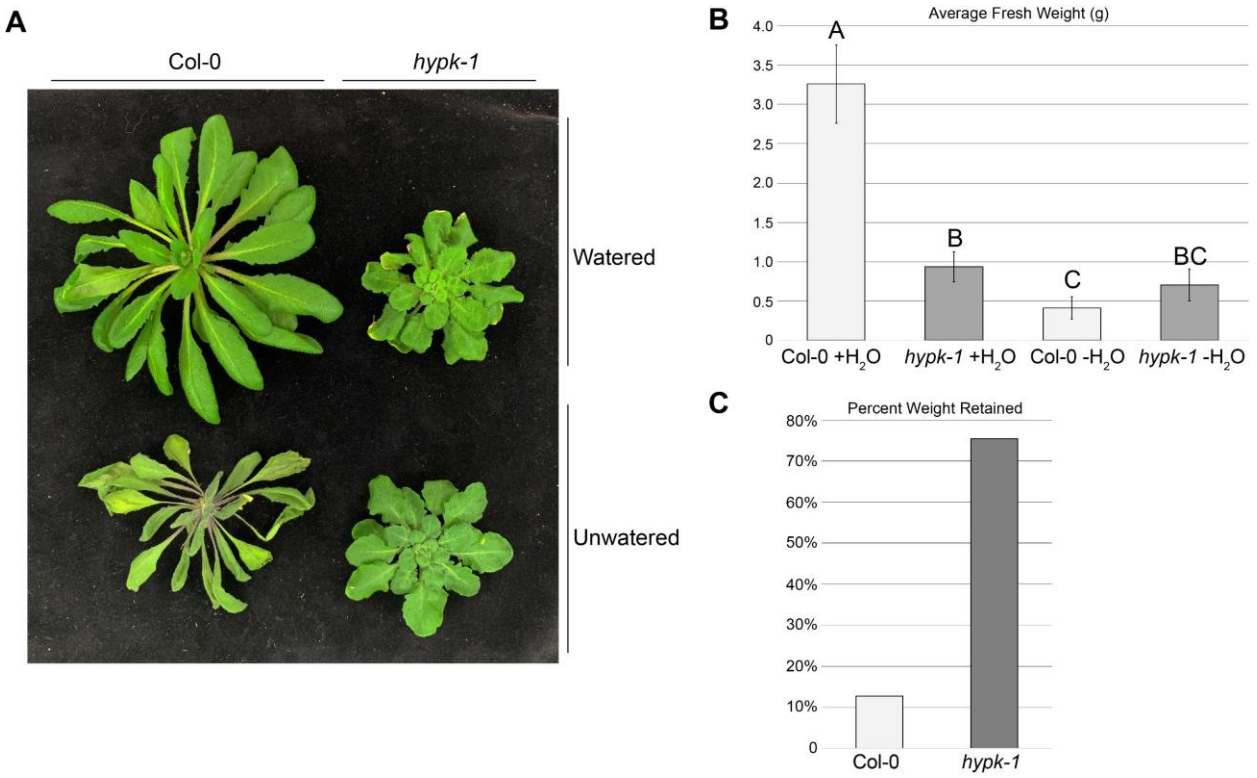

Figure 4-4. *hypk* mutants display enhanced drought tolerance. **A.** 5-week-old plants underwent a 4-day period of drought, or normal watering. Representative plants are shown. This experiment has been repeated three times with similar results. **B.** Fresh weight measurements were taken of rosettes from 5-week-old plants following a 4-day period of drought (-H2O), or normal watering (+H2O). Bars represent averages from 6 individual plants. Error bars represent standard deviation. Significance was determined using a Students t-test (P <0.05). **C.** Percent fresh weight retained was calculated based on the average fresh weight of watered and unwatered plants in B.

hypk-1 Plants Display ER Stress Tolerance and Constitutive UPR Signaling

I have demonstrated that loss of *NAA50* in Arabidopsis results in constitutive ER stress and the induction of the UPR (Figure 3-7). We therefore hypothesized that loss of *HYPK* may result in altered ER stress sensitivity. We investigated the ER stress sensitivity of *hypk-1* plants through treatment with tunicamycin (TM). Leaves of four-week-old plants were injected with TM and allowed to grow for 6 days. We found that *hypk-1* plants fared better than wildtype plants, displaying reduced senescence and tissue collapse (Figure 4-5A).

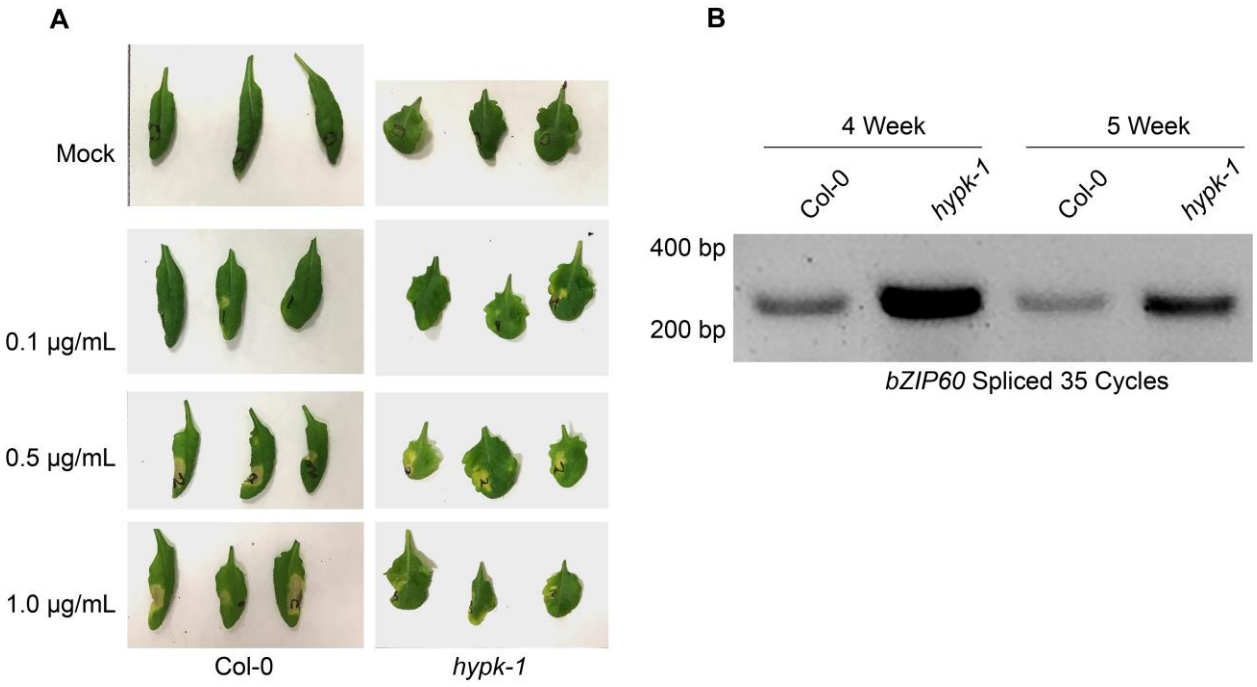

Figure 4-5. Loss of *HYPK* results in enhanced ER stress tolerance and constitutive UPR activation. **A.** 4-week-old Col-0 and *hypk-1* plants were injected with TM. Representative leaves are shown. Leaves were detached and images taken 6 days after injection with tunicamycin. This experiment was repeated twice with similar results. **B.** Spliced *bZIP60* was detected by performing RT-PCR on cDNA generated from 4- and 5-week-old Col-0 and *hypk-1* plants.

To test whether loss of *HYPK* induces constitutive ER stress, we utilized RT-PCR to measure *bZIP60* splicing in *hypk-1* plants. Indeed, we observed higher levels of spliced *bZIP60* in cDNA samples generated from 4- and 5-week-old *hypk-1* plants (Figure 4-5B). This result indicates that the UPR is activated in *hypk-1* plants in the absence of external stress or chemical induction of ER stress. The constitutive activation of the UPR in *hypk-1* plants may explain the enhanced ER stress tolerance of *hypk-1* plants. Activation of the UPR may prime *hypk-1* plants for response to ER stress. Furthermore, activation of the UPR may explain the morphological defects, dwarfism, and drought tolerance observed in *hypk-1* plants.

Discussion

Arabidopsis HYPK is Required for Development and Suppression of Stress Responses

We have demonstrated that the *HYPK* gene is conserved in Arabidopsis. As in humans, HYPK appears to play an important role in plants. Loss of *HYPK* results in altered development, indicating that HYPK may be essential for plant growth. This is similar to observations of plants lacking other NatA and NatE components. Knockdown of NatA and NatB complex components results in dwarfed plants (Linster et al., 2015; Huber et al., 2019). Similarly, I found that loss of *NAA50* results in altered rosette size and dwarfism (Figure 3-5B; Figure 3-2). That loss of *HYPK* results in a similar phenotype indicates that a similar process may be disrupted.

Our results suggest that HYPK may regulate ER stress signaling in plants. The *hypk-1* mutation results in enhanced resistance to ER stress and constitutive UPR signaling (Figure 4-5, B-C). This mirrors my findings demonstrating that loss of *NAA50* leads to constitutive UPR activation (Figure 3-7). Since human HYPK has been shown to have chaperone-like activity and to be involved in the regulation of protein aggregates (Raychaudhuri et al., 2008; Arnesen et al., 2010), it is possible that Arabidopsis HYPK fulfills a similar function. If true, loss of HYPK may therefore result in the formation of protein aggregates and induced ER stress. As discussed previously in Chapter 3, there is an established connection between ER stress and osmotic stress in plants. Given this connection, it is possible that ER stress induced by the loss of *HYPK* results in altered drought tolerance.

The observed developmental defects and altered stress responses of *hypk* plants may result directly from the loss of HYPK function, or from altered NatA or NatE activity. We have yet to demonstrate a molecular function for Arabidopsis HYPK. As in humans, it is possible that Arabidopsis HYPK functions as a chaperone protein and prevent the formation of protein aggregates. However, loss of HYPK may also influence the formation or activity of the NatA and NatE protein complexes, as has been observed in humans (Arnesen et al., 2010; Gottlieb and Marmorstein, 2018). Future work in Arabidopsis should aim to address whether the NatA and NatE complexes are intact and functional in *hypk-1* plants, as well as determine whether Arabidopsis HYPK displays chaperone-like activity.

Future work should aim to address questions surrounding HYPK function and conservation in eukaryotes. If HYPK does indeed function to repress protein aggregation,

it will be important to be able to detect the formation of protein aggregates in *hypk* mutants. Some attempts have been made at visualizing protein aggregate formation in Arabidopsis roots with fluorescent dyes (Cho and Kanehara, 2017). The use of similar techniques may prove useful in determining what effect the loss of *HYPK* has on plant cells. Most studies of HYPK have focused on characterizing human HYPK. The level to which HYPK function is conserved between plants and animals has yet to be investigated. Attempts to rescue the Arabidopsis *hypk-1* allele with the human *HYPK* gene may yield insight into the degree of functional conservation shared with Arabidopsis HYPK. The study of HYPK in Arabidopsis has the potential to shed light on the function of human HYPK and provide insight into the role of NatA- and NatE-mediated NTA.

Materials and Methods

Plant Material and Growth Conditions

Arabidopsis thaliana accession Col-0, and Col-0 mutants *hypk-1* (SALK_080671) were used in this study. For soil-grown plants, seed was directly sowed onto Pro-Mix PGX Biofungicide plug and germination mix supplemented with Osmocote 14-14-14 fertilizer (ICL Fertilizers). Flats were placed at 4^{o}C for 48 hours for stratification before being transferred to a growth room set to 23^{o}C and 12-hour light (150 µEm-2s-1)/12-hour dark cycle. For transient expression experiments, *Nicotiana benthamiana* was grown under the same growth room conditions as *A. thaliana*.

Plasmid Construction

HYPK was cloned into the gateway-compatible entry clone pDONRP1-P4 following amplification from Arabidopsis cDNA. HYPK-sYFP was generated in the cauliflower mosaic virus 35S promoter vector pEarleyGate100 (Earley et al., 2006) using a modified multisite Gateway recombination cloning system (Invitrogen) as described in (Qi et al., 2012). All primers used in this study are listed below (Table 4-1).

Fluorescence Microscopy

Confocal laser scanning microscopy was performed on a Leica TCS SP8 confocal microscope (Leica Microsystems) equipped with a 63X, 1.2-numerical aperture water objective lens and a White Light Laser. The sYFP fusion was excited at 514-nm and detected using a 522 to 545 nm band-pass emission filter.

ER Stress Assays

ER stress treatments were performed by injecting tunicamycin (Sigma) into the leaves of 4-week-old Arabidopsis plants using a needless syringe. Following injection, plants were allowed to grow under normal conditions for six days before leaves were detached and pictures were taken.

RT-PCR

For RT-PCR experiments, RNA was extracted using the Spectrum plant total RNA kit (Sigma-Aldrich) according to manufacturer's instructions. cDNA was produced from 1 µg total RNA using the Verso cDNA synthesis kit (Thermo Fisher Scientific). RT-PCR was

performed using MyTaq DNA polymerase (Bioline) according to manufacturer's instructions.

Table 4-1. Primers used in this study.

Name	Description	Sequence
hypk LP	For Genotyping	GAAGCTTTTCCTGGGAATTTG
hypk RP	For Genotyping	TTGTTGATCATTCTCGCTGTG
HYPK B1F	For Gateway Cloning	GGGGACAAGTTTGTACAAAAAAGCAGGCTATGGAGGGAGCAGAGGAAGC
HYPK B4R	For Gateway Cloning	GGGGACAACTTTGTATAGAAAAGTTGGGTGTAGAGGATATCGTGAAAGC
HYPK 34F	For RT-PCR	GCGGTTGATTCAAAGGACTTGC
HYPK 289R	For RT-PCR	CAACCGCATCACCTTTGTGCTC

Literature Cited

Arnesen, T., Starheim, K.K., Van Damme, P., Evjenth, R., Dinh, H., Betts, M.J., Ryningen, A., Vandekerckhove, J., Gevaert, K. and Anderson, D. (2010) The chaperone-like protein HYPK acts together with NatA in cotranslational N-terminal acetylation and prevention of Huntingtin aggregation. Molecular and cellular biology **30:** 1898-1909.

Cho, Y. and Kanehara, K. (2017) Endoplasmic reticulum stress response in Arabidopsis roots. Frontiers in Plant Science **8.**

Earley, K.W., Haag, J.R., Pontes, O., Opper, K., Juehne, T., Song, K. and Pikaard, C.S. (2006) Gateway-compatible vectors for plant functional genomics and proteomics. The Plant Journal **45:** 616-629.

Faber, P.W., Barnes, G.T., Srinidhi, J., Chen, J., Gusella, J.F. and MacDonald, M.E. (1998) Huntingtin interacts with a family of WW domain proteins. Human Molecular Genetics **7:** 1463-1474.

Feng, J., Li, R., Yu, J., Ma, S., Wu, C., Li, Y., Cao, Y. and Ma, L. (2016) Protein N-terminal acetylation is required for embryogenesis in Arabidopsis. Journal of Experimental Botany **67:** 4779-4789.

Gottlieb, L. and Marmorstein, R. (2018) Structure of human NatA and its regulation by the Huntingtin interacting protein HYPK. Structure **26:** 925-935.e8.

Huber, M., Bienvenut, W.V., Linster, E., Stephan, I., Armbruster, L., Sticht, C., Layer, D.C., Lapouge, K., Meinnel, T., Sinning, I., Giglione, C., Hell, R. and Wirtz, M. (2019) NatB-mediated N-terminal acetylation affects growth and abiotic stress responses. Plant Physiology pp.00792.2019.

Linster, E., Stephan, I., Bienvenut, W.V., Maple-Grødem, J., Myklebust, L.M., Huber, M., Reichelt, M., Sticht, C., Geir Møller, S., Meinnel, T., Arnesen, T., Giglione, C., Hell, R. and Wirtz, M. (2015) Downregulation of N-terminal acetylation triggers ABA-mediated drought responses in Arabidopsis. Nature Communications **6:** 7640.

Polevoda, B., Arnesen, T. and Sherman, F. (2009) A synopsis of eukaryotic Nα-terminal acetyltransferases: Nomenclature, subunits and substrates. BMC Proceedings **3:** S2.

Qi, D., DeYoung, B.J. and Innes, R.W. (2012) Structure-function analysis of the coiled-coil and leucine-rich repeat domains of the RPS5 disease resistance protein. Plant Physiology **158:** 1819-1832.

Raychaudhuri, S., Sinha, M., Mukhopadhyay, D. and Bhattacharyya, N.P. (2008) HYPK, a Huntingtin interacting protein, reduces aggregates and apoptosis induced by N-terminal Huntingtin with 40 glutamines in Neuro2a cells and exhibits chaperone-like activity. Human Molecular Genetics **17:** 240-255.

Waterhouse, A.M., Procter, J.B., Martin, D.M.A., Clamp, M. and Barton, G.J. (2009) Jalview version 2—a multiple sequence alignment editor and analysis workbench. Bioinformatics **25:** 1189-1191.

Weyer, F.A., Gumiero, A., Lapouge, K., Bange, G., Kopp, J. and Sinning, I. (2017) Structural basis of Hypk regulating N-terminal acetylation by the NatA complex. Nature Communications **8:** 15726.

Matthew Paul Neubauer, Ph.D.
Indiana University Department of Biology, Myers Hall 150
915 East Third Street, Bloomington, IN 47405
mattneub@iu.edu

EDUCATION

Indiana University (2013-2020)
Genome, Cell, and Developmental Biology Ph.D. Program
GPA: 3.984

Loyola University Chicago (2010-2013)
Bachelor of Science, Biology with Molecular Emphasis

RESEARCH

Indiana University (January 2014 – March 2020)
Graduate Student with Dr. Roger W. Innes

- ◊ Areas of focus include plant-pathogen interactions, plant abiotic stress responses, plant development, post-translational protein modification, and endomembrane trafficking.
- ◊ Studied an uncharacterized N-terminal acetyltransferase that is required for plant development.
  - Created and characterized transgenic plant lines to study an essential plant gene.
- ◊ Identified a link between EDR1 and the EDS1/PAD4 salicylic acid signaling network.
  - Utilized various protein-protein interaction assays and fluorescence microscopy to implicate EDR1 in the direct regulation of EDS1/PAD4.

Loyola University Chicago (January 2012 – May 2013)
Undergraduate Student with Dr. Fred Pickett

- ◊ Studied the role of cardiac troponin in the Frank-Starling mechanism of the heart.
- ◊ Created transgenic zebrafish to serve as models for drug discovery.

AWARDS

NIH Training Grant in Genetics, Cellular, and Molecular Sciences (Fall 2014 – Spring 2015), Miller Fellowship (Fall 2015), Cleland Plant & Fungal Science Travel Award (2016, 2017, 2018, 2019).

SKILLS and TECHNIQUES

- ◊ Proficient with cloning, protein expression, and protein purification.
- ◊ Protein isolation for mass spectrometry analysis.
- ◊ RNAseq data analysis.
- ◊ Fluorescence microscopy.
- ◊ *In vitro* enzyme assays.
- ◊ Generation and characterization of transgenic and mutant plants.
- ◊ Yeast-two hybrid, co-immunoprecipitation, bifluorescence complementation.

TEACHING

Assistant Instructor:

L319 Genetics Laboratory, Indiana University (January 2016 – May 2016; August 2016 – December 2016)

- ◊ Led weekly lab exercises.
- ◊ Maintained materials for lab exercises, such as drosophila and yeast strains.

L113 Biology Laboratory, Indiana University (January 2014 – May 2014)

- ◊ Designed and delivered weekly lectures, assignments, and quizzes.
- ◊ Instructed students in the design and completion of independent research projects

Mentoring:

STEM Summer Scholar Institute, Indiana University (Summer 2018)

- ◊ Mentored a student in a project focused on plant genetics and development.

Undergraduate Mentoring, Indiana University (Fall 2018 – Present)

- ◊ Mentor to an undergraduate working to characterize a plant gene involved in stress responses and development.

PRESENTATIONS

- ◊ **Poster Presentations** – MPMI 2016, ASPB Midwest 2017, ICAR 2017, ASPB-PB 2018, Missouri IPG 2019
- ◊ **Talk and Poster** – GCMS Training Grant Symposium, Indiana University, May 2014

PUBLICATIONS

Neubauer, M.P., Serrano, I., Rodibaugh, N., Bhandari, D. D., Bautor, J., Parker, J.E., Innes, R.W. 2019. Arabidopsis ENHANCED DISEASE RESISTANCE1 Protein Kinase Regulates the Association of ENHANCED DISEASE SUSCEPTIBILITY1 and PHYTOALEXIN DEFICIENT4 to Inhibit Cell Death. *Molecular Plant-Microbe Interactions*. Manuscript accepted for publication.

Neubauer, M.P., Innes, R.W. 2020. The Arabidopsis N-terminal Acetyltransferase NAA50 Regulates Plant Growth and Defense. *Manuscript submitted for publication*.